The Thesis Committee for Robert Patton Fortenberry
Certifies that this is the approved version of the following thesis:

Experimental Demonstration and Improvement of Chemical EOR
Techniques in Heavy Oils

APPROVED BY

SUPERVISING COMMITTEE:

Supervisor:

Gary A. Pope

Upali Weerasooriya

Experimental Demonstration and Improvement of Chemical EOR Techniques in Heavy Oils

by

Robert Patton Fortenberry, B.S.

Thesis

Presented to the Faculty of the Graduate School of

The University of Texas at Austin

in Partial Fulfillment

of the Requirements

for the Degree of

Master of Science in Engineering

The University of Texas at Austin

May 2013

Dedication

To my family and my friends.

Acknowledgements

My educational experience at University of Texas Petroleum Engineering Department was overwhelmingly positive, and I owe thanks to many who made my work and leisure in Austin so pleasant and productive. Firstly I would like to acknowledge Dr. Gary A. Pope, who offered me this great opportunity. He spent many hours over the course of two years helping me improve my engineering skills and was generous with personal advice. Dr. Do Hoon Kim mentored me in the lab and in the value of work-life balance. Chris Britton taught me how to solve problems, on the job and otherwise. Stephanie Adkins demonstrated daily how to manage challenges with grace. Dr. Upali Weerasooriya led by example in his technical abilities and relationship skills.

The laboratory staff was helpful and friendly to me over the last few years, without them this would have been impossible. In particular Erandi Kularwardina, Suneth Rajapaksha, Dharmika Lansakara, Nadeeka and Pradeep Upamali, Gayani Kennedy and Gayani Pinnawala helped me build skills and confidence. Jith Liyanage and Sophie Dofur were coworkers inside the lab and friends outside of it. Undergraduate students were also involved over the years; Brian Connolly, Ethan Jones and Adrian Adame contributed many hours of their significant talents. Pearson Suniga and Richard Hernandez lent me their experience often. Bob McNeil has a wealth of knowledge to which I often turned.

The Administrative staff played a large role in the completion of this thesis. In particular Leilani Swafford and Heather Felauer helped me day-to-day with needs, requests and their general positive dispositions. Esther Barrientes and Frankie Hart were crucial in my success as a student. Joanna Castillo kept myself and others in line and supported.

Perhaps more than anyone else, the other graduate students at the University of Texas welcomed me and made me feel at home. Mac Pedlow is great friend and climbing

partner. Nabi Nizamidin's hard work and camaraderie were constant. Jun Lu, Vincent Lee and Mike Unomah brought great energy inside and outside the lab. Heesong Koh, Leonard Chang and Jiajia Cai made the office a place I liked to return to. The graduate students before me paved the path and deserve mention, especially Sriram Solairaj, Dustin Walker, Matt Dean, Mohsen Taghavifar and Matthew Winters.

Abstract

Experimental Demonstration and Improvement of Chemical EOR Techniques in Heavy Oils

Robert Patton Fortenberry, M.S.E.

The University of Texas at Austin, 2013

Supervisor: Gary A. Pope

Heavy oil resources are huge and are currently produced largely with steam-driven technology. The purpose of this research was to evaluate an alternative to steam flooding in heavy oils: chemical EOR.

Acidic components abundant in heavy crude oils can be converted to soaps at high pH with alkali, reducing the interfacial tension (IFT) between oil and water to ultra-low levels. In an attempt to harness this property, engineers developed alkaline and alkaline-polymer (AP) flooding EOR processes, which met limited success. The primary problem with AP flooding was the soap is usually too hydrophobic, its optimum salinity is low and the ultra-low IFT salinity range narrow (Nelson 1983). Adding a hydrophilic co-surfactant to the process solved the problem, and is known as ASP flooding. AP floods also form persistent, unpredictable and often highly viscous emulsions, which result in high pressure gradients and low injection rates. Addition of co-solvents such as a light alcohol (typically 1 wt %) improves the performance of AP floods; researchers at the University of Texas at Austin have coined the term ACP (Alkaline Co-solvent Polymer) for this new process.

ACP has significant advantages relative to other chemical flooding modes in recovering heavy oils. It is less costly than using surfactant, and has none of the design challenges associated with surfactant. It shows the benefit of nearly 100% displacement sweep efficiency in core floods when properly implemented, as heavy oils tend to produce significant IFT-reducing soaps (Nelson, Lawson, Thigpen, & Stegemeier, 1984). The use of polymer for mobility control ensures good sweep efficiency is also achieved.

Since heavy oils can be extremely viscous at reservoir temperature, moderate reservoir heating to reduce oil viscosity is beneficial. In a series of core flood experiments, moderately elevated temperatures (25-75°C) were used in evaluating ACP flooding in heavy oils. The experiments used only small amounts of inexpensive co-solvents while recovering >90% of remaining heavy oil in a core, without need for any surfactant. The most successful experiments showed that a small increase in temperature (25°) can have very positive impacts on core flood performance. These results are very encouraging for heavy oil recovery with chemical EOR.

Table of Contents

List of Tables

List of Figures

Chapter 1: Introduction

1.1 MOTIVATION

With 90 million barrels of oil consumed worldwide daily, conventional oil reserves are being drawn down rapidly. New sources of hydrocarbon are required to supplement the decline of traditionally produced light crudes with low viscosity. Alternative sources of hydrocarbon energy include coal, shale production of oil and gas, heavy oils and oil shale. This work is concerned with the production of heavy oils, which is normally defined as oil having API gravity < 20°. This arbitrary definition encompasses oils that are relatively mobile and light to completely immobile bitumens, which can be heavier than water.

Heavy oils have been traditionally produced initially with primary production followed by waterflood, hot water flood, steam flood, cyclic steam (CCS), or steam assisted gravity drainage (SAGD). The primary premise of this work is that enhanced recovery of heavy oils with chemicals deserves evaluation along with more traditional waterflood and thermal recovery techniques.

1.2 MICELLAR-POLYMER FLOODING IN HEAVY OILS

Traditional primary and waterflood recovery techniques in reservoirs leave significant fractions of oil in the reservoir unrecovered. Even the thermal processes described above will abandon significant fractions of oil as residual; this residual oil is held immobile by capillary forces. The ratio of these trapping capillary to viscous forces which mobilize oil is defined in the dimensionless capillary number as (Lake, 1989):

$$N_c = \frac{|k * \nabla \Phi|}{\gamma}$$

Equation defining capillary number as ratio of mobilizing viscous force (numerator) and capillary force (denominator)

Where k is the permeability tensor, $\nabla\Phi$ the potential gradient (gravitational and pressure forces) and γ the interfacial tension (IFT) between two fluids. This simplified force balance will be addressed in more detail in 0. In order to mobilize significant amounts of residual oil, the capillary number needs to be increased by four orders of magnitude, which is only practically achievable by decreasing the IFT term.

Surface active molecules that contain both hydrophilic and hydrophobic groups are suitable for lowering the IFT between water and oil to the drastic extent needed to mobilize the residual oil. There are natural and manmade species of these molecules; manmade molecules are called surfactants, while natural surfactants derived from the crude itself are soaps. These soaps form via deprotonation of carboxylic acids and saponification of esters found in crude oils in high pH (10 and above) environments (Jennings, 1975). A significant advantage in micellar-polymer flooding in heavy oils is their predisposition to forming large amounts of such soaps; their presence can diminish or eliminate the need for more expensive manmade surfactants in a chemical flood.

Heavy oils have other potential advantages as targets for EOR processes. A study of 120 clastic heavy-oil reservoirs showed they had high average permeability (1500 mD), porosity (30%), and initial oil saturation (60-80%) (Lu X. , 2010). The high permeability value is particularly important; these viscous oils require high viscosity injection fluids to ensure proper mobility control in the reservoir is achieved. Without high permeability, injection of significant amounts of viscous polymer along with a chemical slug may not be practical.

As the particular oils used in this study are extremely viscous at reservoir temperature (5,000-30,000 cP), reservoir heating was assumed to be needed. Initial experiments were conducted at 100 °C and the temperature was steadily dropped as a control variable to find the limitation of the technology. A second important aspect was minimizing use of costly surfactant and polymers in these chemical floods. For a coreflood to be considered a technical success, it needed to demonstrate not only high tertiary oil recovery, but recovery at a sustainable pressure drop in the field and with a feasible amount of chemical injected.

Chapter 2: Heavy Oil Recovery

2.1 RESOURCE SUMMARY

The world resource base of heavy oils (<20º) API has been estimated to be as much as 70% of all non-gas petroleum types. This corresponds to a resource endowment of ~ 3.5 trillion barrels of oil. Of this, approximately 15% of the world total is between 10-20º API and has reservoir viscosity < 20,000 cP (Dusseault M. , 2001); these particular oils were the subject of investigation in this work. If only 10% of the heavy oil and bitumen in Canada were produced, it would amount to reserves the size of Saudi Arabia's (Energy Information Agency, 2012).

2.2 GEOCHEMISTRY AND SARA ANALYSIS

Heavy oils have much lower saturates fractions relative to conventional oils, and are enriched in aromatics, resins and asphaltenes. A quantitative analysis of these four components is called SARA analysis, and is used to help in understanding chemistry of the oils. The saturates fraction includes all alkanes, saturated cyclic groups and branched groups, and is fully non-polar. Aromatics contain one or more aromatic ring structures, and have slightly polar character. Resins contain polar constituents, but are still fully soluble in pure pentane. Asphaltenes are similar to resins, but are more polar and insoluble in pentane (Fuhr, Holloway, & Reichert, 1986). Enrichment in aromatics, resins and asphaltenes increase the viscosity of a crude oil (Dusseault M. , 2001).

These oils are rich in heteroatoms (oxygen, nitrogen, sulfur, vanadium, nickel), which helps explain their more polar character. These heteroatoms are concentrated in the large asphaltene molecules (Asomaning, 1997).

Heavy oils also tend to be very reactive with alkali, due to a moderate correlation between increasing acid number with decrease in API gravity (Fan & Buckley, 2007).

Though the relationship remains obscure, high acid number crudes do generally show lower IFT at high pH than low acid number crudes (Buckley & Fan, 2007). This relationship is not reflected in all datasets, for example in a study of 10 Saskatchewan pipeline oils (Parker & Chung, 1986). Inconsistency in measurement techniques is mentioned in virtually every work involving heavy oil and acid number, and is a major obstacle in comparing data between researchers.

2.3 ORIGIN

Typical heavy oils once were chemically similar to conventional oils; the process of kerogen deposition and maturation has been demonstrated in many heavy oil reservoirs. It was primarily after maturation that several secondary factors contributed to the sometimes extreme increase in viscosity found in heavy oils. This process has been confirmed by units of altered and unaltered crudes in close proximity of the Mannville unit in Alberta (Deroo, 1979).

Biodegradation is considered the primary mechanism for viscosity increase in heavy oils. These shallow, extremely high permeability reservoirs were in contact with freshwater aquifers, which often would be cycled with surface water. Anaerobic bacteria exposed to the oil steadily consumed light alkanes in their metabolism, then move on to heavier alkanes and isoprenoids (olefins). A secondary result of their metabolism is enrichment of multi-cyclic ring compounds (asphaltenes and resins, see below), corresponding to steroid-based organic molecules (Deroo, 1979).

Other processes leading to heavy oil formation include migration of mobile components, which probably occurs over geologic timescales in such large and permeable formations. Viscosity profiles in the Athabasca basin demonstrate this phenomenon; lowest in the reservoir are the densest oils most fully stripped of light hydrocarbons, while

5

the oils at the top of the formation are less viscous and relatively rich in light ends (Fustic, 2006). Much of this migration probably results in total loss from the reservoir. Additionally, oxidation from surface waters consumes some light ends.

Finally, the shallow depth of these reservoirs may prevent them from reaching true thermal maturity as crudes. Especially in shallower reservoirs, this can be shown to be the case (Deroo, 1979).

2.4 CURRENT HEAVY OIL PRODUCTION SCHEMES

Heavy oil production currently is produced via primary drainage, secondary recovery and EOR techniques (Alvarado, 2010).

Primary Production and CHOPS

Traditional primary production is quite poor in heavy oil reservoirs, essentially always below 15% recovery, and in Alberta typically 2%. In unconsolidated sand reservoirs, Cold Heavy Oil Production with Sand (CHOPS) has been demonstrated to be economic in Alberta since 2000. CHOPS schemes intentionally produce reservoir sands and significantly surpass primary recovery; the Alberta Energy Ministry reports up to 20% recovery is possible with CHOPS. The formation of wormholes is proposed as the primary recovery mechanism. This scheme has been described as alternately damaging and enhancing to the formation involved (Dusseault M. , 2002).

Waterflood Performance

Waterflood performance in heavy oils is complex and dependent on many factors. Of great import is mobility ratio between water and oil, the presence of mobile water at the start of waterflooding and zones of significant reservoir heterogeneity (thief zones or impermeable layers). In the extensive literature review undertaken by Kumar *et. al.* in

6

2005, waterflood recoveries in heavy oil are reported as low as 1% to 20% of OOIP (Kumar, 2008). Virtually all these projects were in Saskatchewan, and all produced significant water very early in the flood due to the adverse mobility ratio between the water and oil. Though lower viscosity oils tended to have better recovery, there was significant variation. Additionally, extremely poor waterflood performance is not usually reported, meaning waterflood recoveries published are better than average.

Thermal EOR Techniques in Heavy Oils

Current EOR techniques used to recover heavy oils are almost exclusively thermal. Cyclic Steam Stimulation (CSS aka huff-and-puff) involves injecting steam into a reservoir, shutting it in to allow it to heat the formation, and afterwards producing from the same well. CSS suffers from limited impact (only the near wellbore region is treated) and decreasing recovery with subsequent steam cycles, leading to low oil recovery factors (Shandrygin et. al., 2010).

Steam flooding (or steam drives) involves injecting steam into a viscous oil reservoir to reduce oil viscosity and improve its mobility, displacing it to a production well. Steam drives are the most successful EOR method to date, with very high oil recoveries seen in some of the projects. However, to be economical the technology is limited to shallow reservoirs with high permeability, porosity and thickness.

Steam-Assisted Gravity Drainage (SAGD) is useful for producing extremely viscous oils and bitumens in-situ, and has found primary application in the Athabasca Basin in Alberta. Horizontal wells are drilled across the top and bottom of a formation. The upper well is flooded with steam, developing an upper steam chamber. The hot oil and water drain with gravity toward the lower horizontal. SAGD has proven to be economic in Alberta, where recoveries of over 50% OOIP have been reported (Dusseault M. , 2002).

Despite good performance, SAGD isn't applicable in thin-pay layers and areas with low vertical permeability. Additionally, steam generation is quite expensive (Dusseault M. , 2002). Alberta in 2009 produced 664,000 bbl./day of heavy oil using SAGD (Alberta Energy Ministry, 2009).

In-situ combustion is applicable to heavy oil production, but is currently not contributing significantly to rates.

Mobility Ratio

Fluid displacements of oil with water in porous medium are usefully defined by the concept of fluid mobility, defined as:

$$M_f = \frac{\bar{k} k_{rf}}{\mu_f}$$

M_f is the mobility of the fluid,
$\bar{k}$ is the single phase permeability (usually defined with respect to brine),
k_{rf} is the relative permeability of the fluid,
μ_f is the viscosity of the fluid,
The ratio of displacing fluid mobility to displaced fluid mobility is called mobility ratio,

Dake (1978) defined the shock-front mobility ratio where water displaces oil as:

$$M_s = \frac{k_{oil}/\mu_{oil} + k_w/\mu_w}{k_{oil}/\mu_{oil}} \text{, where}$$

M_s = Mobility of the shock front

This definition is well suited for waterflood (Dake, 1978). The displaced phase (denominator) contains only oil, while the displacing phase includes water and oil. If the value of M_s is unity or below, the displacement is said to be viscously stable and will result in efficient sweep. If it is greater than one, the flood may exhibit instability in the form of

viscous fingering. The resulting water fingers propagate through the porous medium rapidly and early water breakthrough will be seen as a result (Kumar, 2008).

Chapter 3: Chemical EOR Literature Review

This chapter will begin with a literature review in chemical EOR (CEOR). After the literature review, the specific flooding techniques will be explored individually in terms of physics and applicability to various geologies.

3.1 LITERATURE REVIEW

Trapping Number, Capillary Number and Desaturation of Residual Oil

Waterflooding of oil reservoirs is known to abandon significant fractions of oil in the reservoir, even in well-contacted zones. This oil is described variously as 'immobile' or 'residual' oil. The presence of residual oil is required when application of immiscible two-phase flow theory is understood. A droplet of oil in a waterflood feels opposing forces; viscous forces of the displacing water phase to dislodge the droplet, and capillary forces which trap the droplet and are proportional to the interfacial tension between the water and oil. The ratio of the viscous force and gravitational force to the capillary force is known as the trapping number, defined below:

$$N_t = \frac{|\bar{\bar{k}} \cdot (\nabla \Phi_{l'} + g \Delta \rho \nabla D)|}{\gamma_{ll'}}$$

Where N_t is the trapping number, $\bar{\bar{k}}$ is the permeability tensor, $\nabla \Phi_{l'}$ is the potential gradient across fluid l', $g\Delta\rho\nabla D$ is the buoyancy term accounting for the density difference between the fluids, and $\sigma_{ll'}$ is the interfacial tension between the fluids of interest. It buoyant force is negligible compared to the pressure gradient force (often), trapping number is represented by capillary number, below.

10

$$N_c = \frac{|\bar{\bar{k}} \cdot (\nabla \Phi_{l'})|}{\gamma_{ll'}}$$

The figure 3.1 below demonstrates that trapping number controls this residual saturation, i.e. as the trapping number increases and viscous forces dominate capillary ones, residual oil trapped in pores will be mobilized and oil saturation will decrease. Note that there is no throughput term, so no amount of increasing throughput will increase oil production at a given trapping number (Lake, 1989).
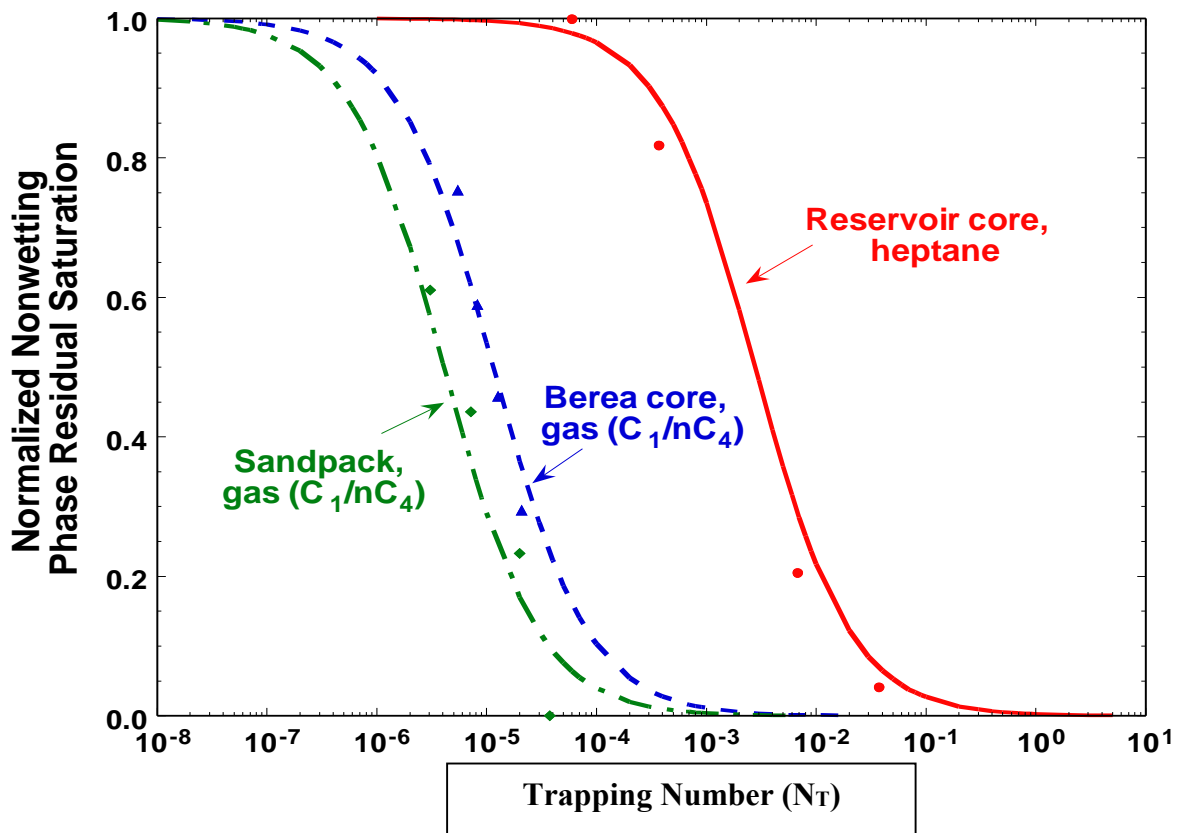
Figure 3.1 Capillary Desaturation in Sandstones, from Pope et. al. 2000

In a typical reservoir environment with pressure gradients around 1 psi/ft, the capillary/trapping number is approximately 10^{-8} (Pope et. a. 2000, Kamath et. al. 2001). In

11

order to reduce residual oil saturation to near-zero values, the IFT must be reduced by four orders of magnitude. While increasing pressure drop in a lab core flood can desaturate more oil, the pressure gradient limitations of a reservoir prevent this. Decreasing the IFT between the oil and water is therefore the only practical way to achieve trapping numbers high enough to desaturate oil (Lake, 1989; Stegemeier, 1977). This can be achieved via the use of highly-surface active chemicals called surfactants.

Surfactant Basics

Surfactants are surface active molecules which will naturally tend to accumulate at fluid interfaces. Commonly, they will contain a polar 'head' group and a non-polar 'tail' group, which have greatly variable affinity for polar and non-polar solutions (Green & Willhite, 1998). When concentration of surfactant passes some threshold value (known as the critical micelle concentration, or CMC), micelles begin to form. In an aqueous-continuous solution, polar head groups would face outwards while the non-polar tail groups would be isolated from the excess phase inside the micelle; if oil were present these non-polar tail groups would solubilize a certain amount of oil within the micelles. The scientific field of study of such three (or more) component systems is called microemulsion phase behavior.

Overview of Flood Schemes

The chemical EOR methods evaluated in the work are named based on their constituent chemicals, and include polymer flooding (PF), Surfactant-Polymer Flooding (SP), Alkali-Surfactant-Polymer flooding (ASP) and the newly-developed Alkali-Cosolvent-Polymer flooding (ACP).

In PF, polymer is added to water to increase its viscosity. This will result in improved areal and vertical sweep, allowing more of the reservoir to be contacted. Higher pressure drop in high-permeability sections will divert polymer into lower-permeability zones, helping overcome heterogeneity. Fractional flow theory demonstrates that increasing aqueous viscosity will result in lower water cut and less volume of injection water per volume of oil produced. If the fluid viscosity is high enough a stable piston-like displacement may occur, where all mobile oil is swept from the reservoir within 1 pore volume. Polymer flooding is simple compared to the other chemical flooding technologies and is much more mature, with many examples of successful field implementations. Typically chemical floods require the use of polymer for mobility control, though there are exceptions; without it surfactant and chemicals can propagate rapidly through the reservoir as the most wetting phase, and show extremely early breakthrough (Hirasaki, van Domeselaar, & Nelson, 1983). China's large Daqing polymer flood has been very successful, while the Britnell polymer pilot in the Pelican Lake Basin, Alberta, has demonstrated good recovery of viscous oil (>5000 cP).

Surfactant-Polymer (SP) flooding uses polymer for the mobility control. It also includes surfactants to lower IFT and sweep virtually all the oil from contacted zones in the reservoir. The ability to produce residual oil can result in an oil target 50-100% larger than in water or polymer floods if the flood is executed properly. SP floods often include the use of cosolvents (detailed below) to assist in breaking up viscous emulsions and phases, though they have major secondary benefits as well.

Alkali-Surfactant-Polymer (ASP) flooding obeys the same physics as SP flooding, but involves addition of alkali to generate soaps from the crude oil to lower IFT, as well as

decrease adsorption of surfactant onto the rock (Falls, et al., 1994). Alkali is shown to have other benefits such as stabilizing certain surfactants and polymers.

Polymer floods may involve the continuous injection of polymer, or a polymer slug followed by a water chase. Low-IFT SP and ASP floods start with a slug containing chemical (typically 0.25-0.4 PV), followed by a polymer drive (PD) to maintain mobility control. The polymer drive is essential to success; without it, chase water will finger through the surfactant/AS/AC bank and the flood may fail entirely. These floods may be performed as secondary or tertiary production methods.

Microemulsion Phase Behavior

Winsor in 1954 described the behavior of surfactants in the presence of oil and brine. He observed the presence of thermodynamically stable phases, so-called microemulsions (Winsor, 1954). These are distinct from traditionally defined emulsions or macroemulsions, which are unstable thermodynamically, though they may persist for very long periods.

Mixtures of oil, brine and surfactant are typically described using pseudo-ternary diagrams, see, for example, (Lake, 1989) or *Microemulsions and Related Systems* (1988) by Bourrel and Schechter. Most such experiments also involve a multiple surfactant species as well as a cosolvent (usually an alcohol) to improve equilibration time and decrease viscosity of the microemulsion. Altering any intensive variable (temperature, pressure, salinity) will alter the behavior of a microemulsion (Winsor, 1954), but the parameter of most practical interest is brine salinity.

In a typical experiment, brine containing electrolyte, surfactant and oil are mixed in a pipette. At low salinity, a Windsor Type 1 microemulsion will form. This microemulsion will be continuous in the aqueous phase, with surfactant micelles forming

14

in the brine and solubilizing in their interior droplets of oil. These microemulsions are known as 'oil-in-water' (O/W) microemulsions, as brine is the continuous phase with oil contained in micelles. Above the type 1 microemulsion will be a pure oil phase, with negligible amounts of surfactant. At sufficiently high surfactant concentrations, the system will be a single-phase microemulsion (see ternary diagrams in above reference for image).

As the salinity (electrolyte concentration) of the brine phase is increased (all other variables remain constant), the dissolved salts start competing with the polar 'head' group of the surfactant for interactions with the water molecules. At sufficiently high salinity, the surfactant will be pushed completely out of the brine and into the oil phase, forming a Windsor type 2 or water-in-oil (W/O) microemulsion. This microemulsion will be oil continuous, with water solubilized inside reverse surfactant micelles, whose polar groups now point inward. The brine phase below will be virtually free of surfactant.

At salinities between the extremes of the type 1 and type 2 microemulsions, a Windsor type 3 microemulsion will form. This state occurs when surfactant is roughly equally favored thermodynamically in the oil phase and the brine phase, and is demonstrated by the appearance of a third 'middle' phase between lower phase brine and upper phase oil. The internal geometry of the type 3 microemulsion is less well understood than that of types 1 and 2. However they may be well visualized from Scriven's work on equilibrium interfaces, as:

> *... [A] continuous, orientable surface of positive genus, without intersection. This divides the volume into two multiply connected, interpenetrating subvolumes, each of them physically continuous (mathematically connected) ... for example sandstone. (Scriven, 1976).*

From the mass balance, it is simple to calculate the volume of brine and oil which are dissolved in the type 3 emulsion. A salinity where equal proportions of oil and water

15

are solubilized by the microemulsion is defined as the 'optimum' salinity; optimum salinity often exhibits ultralow IFT.

Interfacial Tension and Solubilization Ratio

The development of Winsor classifications for microemulsions is important due to its relationship with interfacial tension and therefore capillary desaturation. In 1974, Healy and Reed developed relationships between interfacial tension and microemulsion types (Healy & Reed, 1974). In 1979, Chun Huh derived a relationship relating the solubilization ratio at optimum salinity to interfacial tension. A simple yet generally valid form of his equation is:

$$\gamma = \frac{C}{\sigma^2}$$

Where C is well approximated as a constant ~ 0.3 dynes/cm, and σ is the solubilization ratio, defined for oil or water as:

$$\sigma_l = \frac{v_l}{v_s}$$

Where σ_l is the solubilization ratio, v_l is the volume of oil or water solubilized and v_s is the volume of surfactant. This breakthrough allowed IFT to be calculated quite accurately and simply from phase behavior scans. The region of lowest IFT corresponds approximately to optimum salinity.

3.2 CHEMICALS USED IN MICELLAR-POLYMER FLOODING

A Note on Aqueous Stability

In most modern varieties of chemical floods, chemicals of interest must be mixed in an aqueous solution, though emulsion injection (consisting of ampiphile, brine and

hydrocarbon) does receive attention as well (Fu & Mamora, 2010). This implies that surfactant, polymer, and cosolvent must be completely soluble in brine at or near the optimum salinity. This can be a challenging criterion, as many surfactants in the past used to be close to insoluble in water at the salinities of injection fluid.

To ensure a chemical formulation fulfills the solubility criteria, an aqueous stability test is performed. All the injected chemicals are mixed in a vial, which is blanketed with argon, sealed and heated to reservoir temperature. After mixing it is observed for any cloudiness or decrease in clarity that would result in a failed test. Not passing the aqueous stability test usually disqualifies a chemical formulation.

Polymer

Water-soluble polymer is a fundamental component in almost all chemical floods. It performs the essential role of increasing the viscosity of the injection fluid, to ensure that oil is stably displaced. Indeed, typical surfactant slugs are relatively low volume and cannot tolerate viscous fingering (Hirasaki, van Domeselaar, & Nelson, 1983). Without polymer, surfactant floods are much less efficient unless stabilized by gravity (Lu et. al. 2013). For proper mobility control, the polymer viscosity in chemical floods and drive should be equal to the inverse of the minimum total mobility of the oil bank.

Polymers (Lu, Pope, & Weerasooriya, 2013) evaluated for EOR include hydrolyzed polyacrylamide (HPAM), polyacrylamide, acrylamido-2-methylpropane sulfonate (AMPS), hydroxyelthylcellulose (HEC), xanthan gum and scleroglucan. Currently HPAM is much more prevalent than other polymers, but has certain limitations. Other polymers are more robust to extreme salinities and temperatures (Kulawardana et. al., 2012). Levitt *et. al.* in 2008 developed screening criterion to assist in selecting appropriate polymer for various reservoir conditions (Levitt, 2008).

HPAM molecules include acrylamide monomers, some of which are hydrolyzed. The polymer solution rheology is non-Newtonian, and shows a Newtonian viscosity plateau at low shear rates, a power-law region of shear thinning in intermediate shear rates, and finally a plateau at high shear rates. At extreme shear rates, polymer can degrade due to shearing effects. This shear-thinning character is advantageous in a reservoir, where it is of lower viscosity at high rates near a wellbore and higher viscosity where more mobility control is needed; this characteristic is seen in various degrees in all polymers.

Surfactants

Surfactant molecules used in EOR have two basic requirements; they must interact with both polar and non-polar molecules equally, and must do so strongly. There are many such molecules manufactured commercially, which are generally divided based on the character of their polar head group into four classes: anionic, cationic, non-ionic and zwitterionic. Anionic surfactants receive the most attention as chemical EOR surfactants, as they demonstrate low adsorption on negatively charged rock facies, which are especially prevalent at high pH (Hirasaki et. al. 2011).

Surfactant chemistry has improved significantly over the last several decades. Older surfactants included molecules such as Alkyl Benzene Sulfonate (ABS), a sulfonated head group attached to benzene with a hydrophobic tail of various lengths. Though effective in lowering IFT, ABS demonstrated poor aqueous stability and lack of calcium tolerance. Other surfactants such as Internal Olefin Sulfonates (IOS), Alcohol Ethoxy Sulfates, and Ether Sulfonates have shown excellent performance in corefloods (Levitt et. al., 2008).

New surfactants including Guerbet alkoxy sulfates have high performance and low cost (Adkins et. al, 2010). They contain a large-branched Guerbet alcohol-based

hydrophobic tail, followed by propylene oxide groups (PO), then ethylene oxide groups (EO) and finally an anionic sulfate. The molecule therefore shows a continuous variation from hydrophobic (tail) to moderately hydrophobic (PO group) to moderately hydrophilic (EO) to hydrophilic (anionic head). The branched Guerbet anionic tail confers many advantages to the molecule: they are inexpensively synthesized branched tails reduce formation of viscous gels and liquid crystals (Abe et. al., 1986) and can be size-customed to best match the oil of interest (Solairaj et. al., 2012). The addition of Ethoxy (EO) and Propoxy (PO) groups increases tolerance to divalent ions. Increasing the number of EO groups in a molecule tends to increase its hydrophilicity and therefore optimum salinity and aqueous stability. Increasing the number of PO groups tends to have an opposite effect (Bourell & Schechter, 1988, Flaaten et. al, 2009).

Despite mostly excellent performance, these Guerbet alkoxy sulfates as with any other ether sulfates hydrolyze at temperatures above 60°C unless the pH is increased to around pH 10-11. Lu *et. al.* demonstrated that Guerbet alkoxy carboxylates have many of the same performance advantage as the sulfate molecules, and are thermally stable up to at least 120°C (2012). These carboxylate molecules have demonstrated excellent performance in corefloods.

Surfactant formulations often include two or more surfactants. Blending diverse surfactants increases disorder around the interface, breaking up problematic surfactant structures (Hirasaki, Miller, & Puerto, 2011; Levitt et. al., 2008; Abe, Schechter, Wade, Weerasooriya, & Yiv, 1986). This will reduce microemulsion viscosity, pressure drop in corefloods and generally increase robustness. These advantages can also be conferred by cosolvent molecules.

Cosolvent

Cosolvent molecules range from small, pure alcohols such as IBA to ethoxylated alcohols with hydrophobic tails as long as C6. The most important distinction from surfactants is that cosolvent molecules tend to increase IFT, while surfactants reduce it.

Cosolvents serve several major roles in chemical EOR processes. They help break up viscous emulsions formed in microemulsion phases; these viscous emulsions are associated with high surfactant retention, which can retard the propagation of the flood. Viscous emulsions can also create significant reservoir engineering issues, as they are unpredictable and unstable, as well as extremely non-Newtonian in rheology (Walker et. al., 2012). Cosolvents achieve this positive effect on microemulsions in ways similar to multiple, branched surfactants; they increase disorder at the interface and help destroy viscous phases (Salter, 1977). In addition to breaking up emulsions, cosolvents decrease the time microemulsions take to equilibrate, and significantly reduce the absolute viscosity of these microemulsions (Bourrel & Schechter, 1988). Finally, cosolvents are hydrophilic molecules that can be used to manipulate optimum salinity and aqueous stability parameters (Sahni, et. al., 2012).

Cosolvents have drawbacks that must be managed in virtually every design scenario. The added cost can make flood economics much less appealing. Additionally, cosolvent increases the IFT and decreases the solubilization ratio (Hirasaki, Miller, & Puerto, 2011; Salter, 1977). Despite these drawbacks, cosolvent is often necessary for good performance.

Alkali

The addition of alkali can benefit the robustness and economics of a chemical flood immensely. Alkali can generate soaps from reactive crude oils, whose activity is quantified

by titration with a strong base such as KOH in a total-acid-number measurement (TAN) (Jennings, 1975). TAN unfortunately is only weakly correlated to production of useful IFT reducing soaps (Buckley & Fan, 2007). The mechanism for the formation of soaps is saponification of esters and carboxylic acids in crude oils, and forming carboxylate soaps with large hydrophobes. These soaps tend to be quite hydrophobic so a hydrophilic surfactant or cosolvent is needed to balance the soaps. Soaps are extremely effective at reducing IFT, and can sometimes do so sufficiently to eliminate the requirement for added surfactants entirely.

In addition to creating soaps, increasing the pH with alkali has been shown to significantly decrease adsorption of surfactant to the rock facies, often by over an order of magnitude (Hirasaki, Miller & Puerto 2011). This will allow the flood to propagate rapidly (less surfactant retardation) and require less surfactant. As alkali is inexpensive relative to surfactant, this is enough of an advantage that even non-active oils can benefit from alkali.

Alkali is very reactive with reservoir minerals. Sodium hydroxide (NaOH, pH 14) is too reactive for most applications. Sodium Carbonate (Na_2CO_3 pH ~11) is preferred due to its low cost and moderate pH and buffering capacity, but cannot be used if the formation contains anhydrite or gypsum.

Chapter 4: Experimental Methods and Equipment

4.1 FLUID PREPARATION

Brine Preparation

Brines used in the research all soft, consisting of NaCl and Na_2CO_3. Concentrated brine stock was made using deionized water from Barnstead water deionizer. Deionized water was added to a 4L container with a stir bar. Typically salt was added to generate 4 x stocks, i.e. the brine would be diluted with other chemicals in a ratio of 4:1. After salt was added, a large stir bar was inserted and the brine was allowed to mix at least 20 minutes on a stir plate before being used. As the DI water used was often somewhat acidic, 1M NaOH was added to raise the pH to 7-8.

In some experiments, it was necessary to remove oxygen from the brine injected into the core. This was done to maintain the reduced state of the core; natural in a reservoir environment. Typically, the brine was bubbled with argon for a minimum of 30 minutes. An injection column was evacuated, and the oxygen free brine was then allowed to fill the column. Sodium dithionite (generally 1000-2000 ppm) was used to scavenge remaining oxygen and lower the redox potential (ORP), converting soluble iron to the less harmful Fe 2+ state .

Surfactant Stock

Surfactant stocks were made at 4x final concentration. Liquid surfactant (with activity from 5% up to 100%) was carefully pipetted into DI water in a glass mixing jar. Electrolyte was added if needed. As with brine, the pH was adjusted to be approximately neutral after mixing.

Injected surfactant slugs also needed to be reduced and deoxygenated in some experiments. As these slugs contained polymer and surfactant, bubbling argon is a challenging but necessary step. Low flow rates are needed so the argon doesn't simply bubble the slug away. The slugs were allowed to bubble with argon for 2 hours minimum; afterwards concentrated sodium dithionite was added to obtain 1,000 ppm final concentration. An evacuated column was then filled with the slug for injection.

Polymer Stock & Filtration Ratio

HPAM 3630s polymer stocks were made with very concentration of polymer (7,000-10,000 ppm). Careful quality control is very important with polymer: thorough mixing is required, and exposure to oxygen can degrade it. The following procedure was therefore carefully followed:

Approximately 500 ml of DI water was massed in a 750 ml plastic mixing jar. Electrolytes were then added, along with a large stir bar. Using a properly-sized stir bar is critical for adequate mixing of the polymer stock (the bar should be 75% the diameter of the mixing vessel). The resulting brine was mixed at about 300 rpm, or fast enough that the vortex barely touched the stir bar.

Argon was blanketed over the vortex. Solid polymer stock was removed from an oxygen scavenging container and the required amount was massed. This solid polymer was then slowly added over 2-3 minutes to the shoulder of the vortex. The stock was allowed to mix at this high rate until the stirrer was unable to continue mixing. Afterwards it was turned down to 80-100 rpm and allowed to mix for 3-4 days, a requirement for homogeneity in high concentration polymer. Several times during this period, the stock container was inverted vigorously for more mixing.

Polymer stocks and injection slugs need to be homogenous. Heterogeneity can lead to core plugging as well as unpredictability in mobility control. All polymer solutions must pass a filtration ratio test before they are injected.

To measure filtration ratio, ~250 ml of stock or slug is poured into a 90 mm filter bell. The filter paper used in the test is 1.2 micron multipore cellulose acetate. The solution is filtered through the bell under 15 psi of argon pressure; Time elapsed for each 20 ml of filtered fluid is recorded. The filtration ratio (F.R.) is defined as

$$F.R. = \frac{t\ 80\ ml - t\ 60\ ml}{t\ 200\ ml - t\ 180\ ml}$$ Where,

t is elapsed time at volume indicated. If the filtration ratio is below 1.2, the solution is acceptable. If the filtration ratio is above 1.2, the solution can be mixed longer, filtered at a larger diameter filter size and re-filtered, or simply re-filtered at 1.2 microns if the F.R. is close to passing.

Oil Dilution

Crude S dead oil was diluted with decalin according to the EACN calculations detailed in Chapter 6. To do this, ~600 ml dead oil was poured from a large container into 1 L glass jars. The glass jar was then placed in a water bath at 68°C for 30-60 min with a loosely attached lid. A large stir bar was placed in the jar and rotated at ~80-100 rpm. The stochastically calculated mass of decalin was added in intervals of 2-6 ml, with ample stirring between intervals with a glass stirring rod used to assist the stir bar. The final concentration of decalin added was 13.1 wt.%. It is important to add decalin slowly, as the high asphaltene content of the crude S used could result in precipitation if a large amount were suddenly added. After all the decalin was added, the oil was stirred by hand for 5 minutes and finally inverted several times. Any time the 1L vessel was used, the jar was first inverted several times to ensure the sample was well-mixed.

4.2 PHASE BEHAVIOR SCANS

Phase behavior scans were designed to help understand the microemulsion phase behavior described in chapter 2. Pipette repeaters were used to add brine stock, DI water and finally surfactant stock to sealed borosilicate pipettes in desired amounts. The pipettes are arranged in order from low salinity to high salinity to easily observe the effects of salinity on microemulsion phase behavior and the evolution of type I-III-II microemulsions. After all the aqueous fluids were added, the pipettes were gently tapped on a hard surface to dislodge air bubbles from the tips. The levels of aqueous phase were then measured; this step allows for calculation of solubilization ratio for surfactants and also indicates if there are obvious problems with pipetting.

Polymer is typically not added to phase behavior pipettes. Polymer has been shown to have little effect on the phase behavior of fluids involved, see for example Pope et al, who describes among other phenomena the limited impact of polymer on optimum salinity (1982).

After the aqueous phase is added and measured, the pipettes were put in a hot oven for 2-3 minutes (generally 68°C) to allow them to heat up. The diluted viscous oil must heat for 10-12 minutes for it to be easily pipettes into the narrow borosilicate tubes. Even after heating, the oil is several hundred cP and requires care and skill to pipette accurately. The required 0.4-2.0 ml of oil was added depending on the water-oil ratio (W.O.R.) needed.

Argon was used to displace volatile gasses in the tube, which was then sealed with a flame torch and put in the oven at temperature of interest. The tubes are then arranged by order of increasing salinity in the rack. They were mixed after several minutes, and over the next 3-4 days were mixed often, every 1-2 hours on average.

25

4.3 AQUEOUS STABILITY TEST

Any formulation containing surfactant, brine and polymer needs to pass the aqueous stability test, as the fluids need to be injected as a clear aqueous phase. Any solution to be injected in the subsurface must be completely clear, i.e. entirely water soluble; any solid precipitation at all is unacceptable in a reservoir injection scheme.

To test this solubility criterion, chemicals used in the phase behavior test above (including polymer) are combined in a salinity scan called an aqueous stability test. Glass vials are arranged and labeled according to salinity. Brine, DI, polymer and surfactant stocks are then added to the vials to represent a final chemical mixture. The vials are blanketed with argon and then sealed with a torch.

At lower values of salinity, the solution should be perfectly clear. At some higher value of salinity, the solution will begin to become cloudy. At this salinity, salt has successfully pushed the surfactant out of the aqueous phase and forced it to precipitate, a phenomenon known as 'salting-out'. It is important that this 'salting-out' salinity or aqueous stability be safely higher than the injection salinity for the chemical formulation. Polymer can affect aqueous stability and is therefore required in the vials.

Chapter 5: Heavy Oil Characterization

One crude oil was primarily used in experiments in the study, and will be called crude S. Crude S is the oil used in all ASP formulations, corefloods, and many of the ACP formulations. Crude S will be the primary focus of the following chapters, other crudes used will be mentioned as needed. Characterizing the oil is an important first step in any phase-behavior based experimentation.

5.1 LIVE AND DEAD OIL VISCOSITY

An Ares LS-1 viscometer was used to measure the viscosity of the dead oil at temperatures up to 95 °C, after which the crude reaches its bubble point. Initially, a transient rate test was run to ensure normal behavior of oil viscosity. Afterward, the crude was heated in intervals of 5-10°C and the viscosity was measured. The results of the surrogate oil viscosity and the dead oil viscosity are seen in Figure 5.1 Viscosity of Crude S and Surrogate Oil. The extremely strong dependence of oil viscosity on temperature is highly advantageous in heavy oil EOR. Increasing the reservoir temperature just 30°C will decrease the surrogate oil viscosity an order of magnitude.
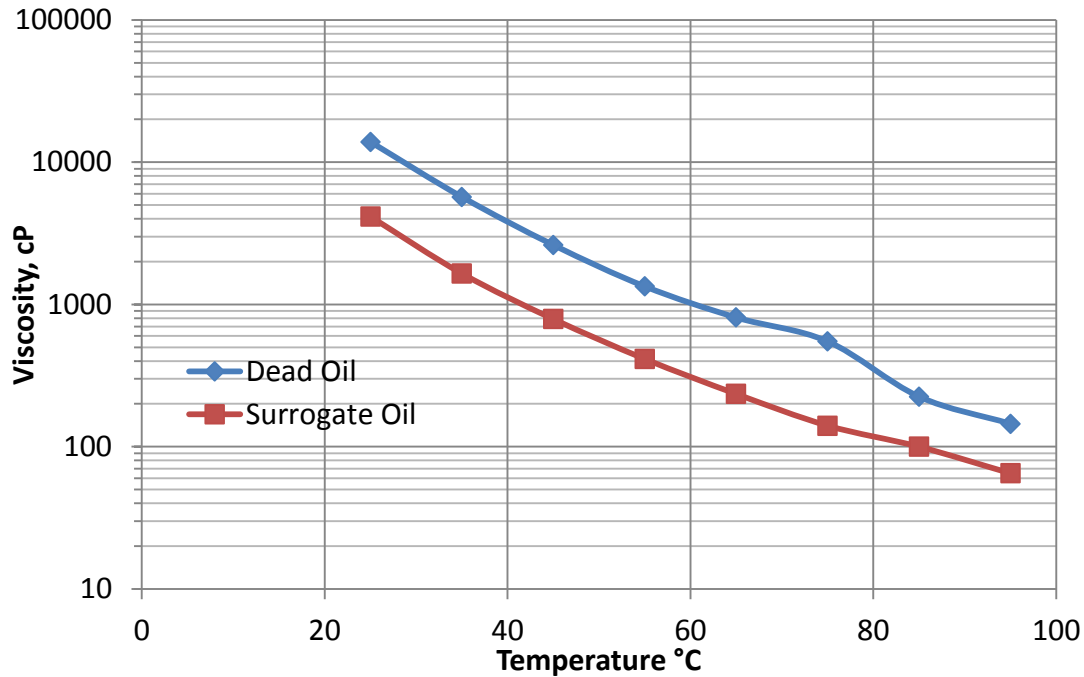
Figure 5.1 Viscosity of Crude S and Surrogate Oil

5.2 EACN AND SURROGATE OIL

Dead oil is not representative of oil in the subsurface; light ends have escaped from the oil, increasing its viscosity and increasing its equivalent alkane carbon number (EACN). EACN expresses the concept that varying hydrocarbon groups predictably change the optimum salinity of microemulsion phase behavior. A mole-weighted average of the EACN of each molecule results in an overall EACN of the mixture; in this case a heavy crude oil. Though EACN is impossible to directly calculate for a crude oil due to sheer complexity, its value can be measured as described below and in the literature (Cayias, Schechter, & Wade, 1976; Solairaj et. al., 2012).

28

To calculate EACN in the absence of a PVT report containing live oil composition, gas-oil-ratio (GOR) is needed (85 SCF/BBL for Crude S) along with molecular weight of gas (assumed pure methane; = 16 g/mol) and molecular weight of oil (500 g/mol based on correlation from molecular weight and room temperature viscosity).

A good phase behavior formulation is needed to measure EACN. The optimum salinity for Crude S was determined using the ASP formulation F-1, 0.15% C-28-25PO-55EO-carboxylate, 0.15% IOS 19-23 with 1% IBA-5EO. As this oil was active, it is important to use multiple different hydrocarbon dilutants at the same oil concentration, rather than using one dilutant at multiple concentrations (changing the oil concentration changes the amount of produced soaps and therefore the optimum salinity shifts). Alkane dilutants ranging from C8 to C20 were used, and the optimum salinity was recorded. Dead oil EACN was determined by iteratively altering the dead oil EACN until the log of optimum salinity vs. EACN of the oil (crude + dilutants) fell on a straight line. Dead oil EACN was determined to be 17.0.
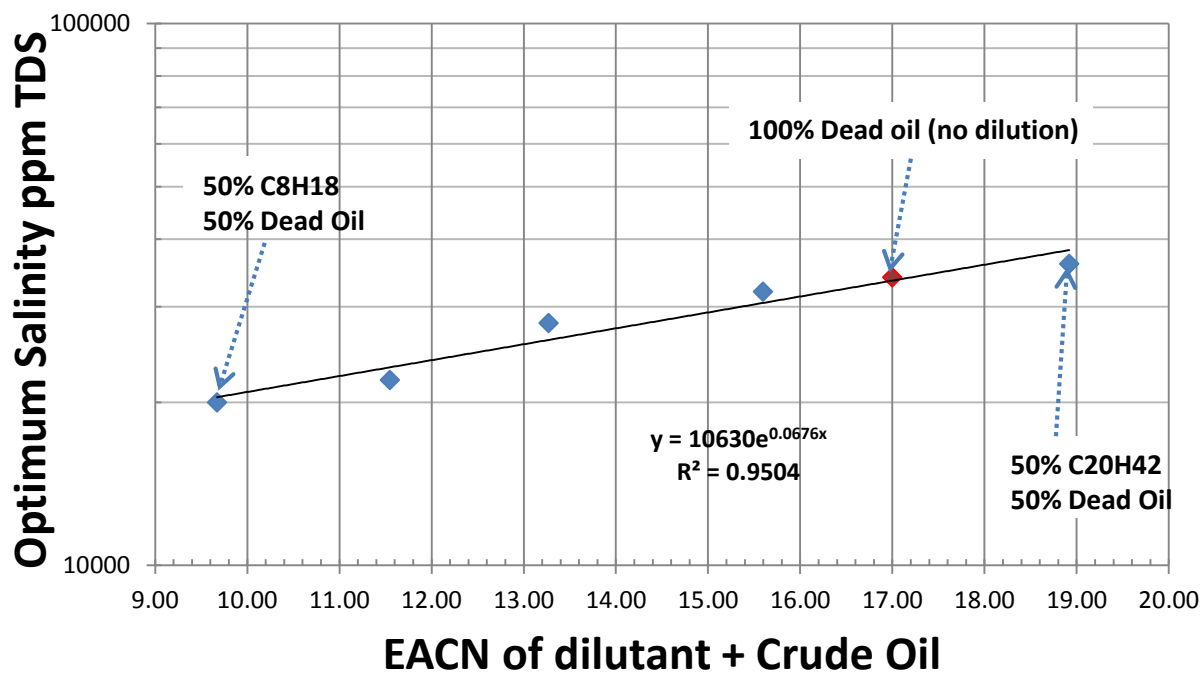
Figure 5.2 Optimum salinity vs. EACN of dilution for crude oil S

The tight relationship above between optimum salinity and EACN shows the strength of the correlation using a dead oil EACN of 17; the sound basis for EACN is demonstrated in many similar datasets (Cayias, Schechter, & Wade, 1976; Bourrel & Schechter, 1988).

5.3 PROPERTIES OF THE CRUDE S

IFT was measured between oil and water using a ring tensiometer. The average value was 26 dynes/cm. Total acid number is approximately 3-4 mg KOH/ g Oil.

Chapter 6: ASP Phase Behavior Experiments

As mentioned in Chapter 1, heavy oil resources are very vast and largely untapped. In this section, the applicability of ASP flooding was evaluated for heavy oils at elevated temperatures (100°C). The surrogate oil viscosity at this temperature was ~71 cP, a significant decrease from the viscosity in the reservoir of about 5000 cP.

6.1 ASP PHASE BEHAVIOR

Initial Phase Behavior Tests

ASP phase behavior studies were carried out for many combinations of surfactants, cosurfactants and cosolvents. Sodium carbonate was the only alkali investigated, though other alkali species has shown promise in ASP coreflood applications. Attempts were made to find an alkali-free SP formulation, but finding a formulation with suitable microemulsion characteristics and ultra-low IFT were unsuccessful.

Initial experiments were conducted primarily with Tristyryl Phenol (TSP) alkoxy carboxylate surfactants with IOS co-surfactants in dead heavy oil. These experiments were conducted at 100°C. Initial scans demonstrated very high viscosity of microemulsion, which could have been unfeasible to propagate through a core though these scans often demonstrated ultra-low IFT. In order to mitigate these viscous phases, later formulations contained high concentrations of cosolvent, in particular Ethoxylated 2 wt. % Isobutanol (IBA-xEO) and TriEthylene Glycol Butyl Ether (TEGBE). This is higher cosolvent concentration than desired since co-solvent increases IFT.

As an alternative to increasing the concentration of cosolvent, the temperature of many formulations were raised to 120°C, to decrease the formation of viscous phases without increasing the cosolvent requirements in the formulation. Though this was largely

successful, the difficulties of working at 120°C precluded any corefloods being done at that temperature.

After unsuccessfully attempting many formulations for the dead oil, the decision was made to create surrogate oil from the crude as described in 5.2 EACN and Surrogate Oil sections. To do this, certain information about the oil was required, especially solution-gas ratio and oil molecular weight. The latter was obtained from a relationship relating oil molecular weight to room temperature viscosity (Closmann & Seba, 1990). Dilution with 13.1% decalin was appropriate in terms of EACN, final oil viscosity and showed no evidence of asphaltene precipitation.

Aqueous stability was almost always higher than optimum salinity for these formulations, as the surfactants used tended to be quite hydrophilic to compliment the highly hydrophobic soaps.

Successful Phase Behavior Test

After diluting the oil, phase behavior studies showed greatly improved microemulsion phase behavior, but TSP surfactants didn't demonstrate adequately low IFT. Phase behavior using large-hydrophobe alkoxy carboxylate surfactants showed low microemulsion viscosity as well as ultra-low IFT. Other tests using older, smaller-hydrophobe (13 carbon) TDA-xPO-Sulfate also demonstrated much promise, despite thoughts that the larger hydrophobe surfactants should perform better with the large EACN heavy oils (Solairaj et. al., 2012).

Lowering cosolvent concentration to 1% IBA-5EO and surfactant concentration to 0.3% (1:1 ratio of primary surfactant to cosurfactant) showed ultralow IFT, moderate microemulsion viscosity, absence of gel phases and appropriate activity map behavior. Details on two leading ASP candidates are described below.

F-1 ASP Formulation

The formulation F-1, 0.15% C-28 25PO 55EO carboxylate, 0.15% IOS 19-23 with 1% IBA-5EO was considered a good candidate for testing in an ASP coreflood. It showed ultralow interfacial tension at all oil concentrations, an appropriate activity map favorable for coreflooding, low microemulsion viscosity, aqueous stability and no gels or liquid crystals. Additionally, the carboxylate surfactant used as a primary surfactant is stable at elevated temperature (Adkins, et. al., 2010). An activity map for the flood is shown below.
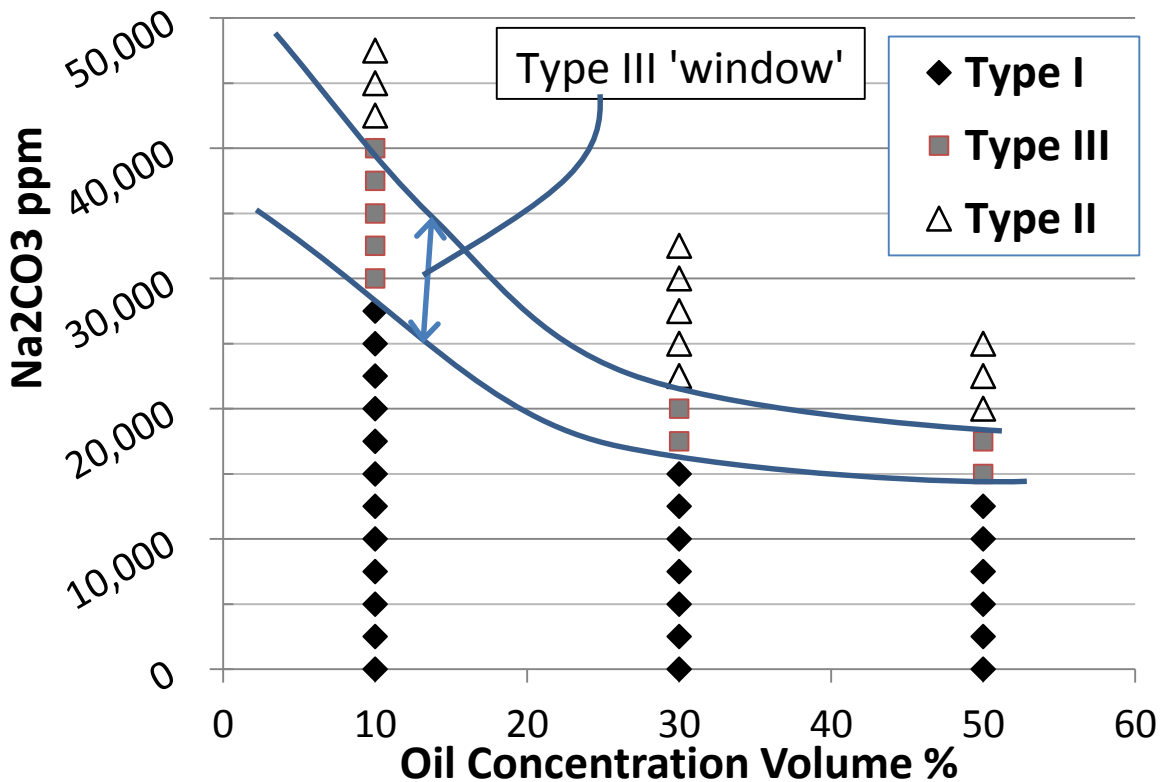
Figure 6.1.1: Activity map of F-1 formulation at 100°C.

The activity map shows typical behavior for ASP formulations in oils generating in-situ soaps. The alkali scans above show the low oil percentage (10% oil = water oil ratio

(WOR) of 9) region has higher optimum salinity, as proportionally less hydrophobic soap is generated. As the oil fraction increases, the in-situ soaps dominate the microemulsion behavior and the optimum salinity decreases, until it levels-off around 50% oil concentration (WOR = 1). The gradient depicted above is somewhat steep, with the 10% oil optimum salinity (35,000 ppm) almost twice that of the 30% oil optimum. Decreasing the hydrophilicity of the surfactants would have the effect of changing the ratio of hydrophobic to hydrophilic molecules between the surfactant and the soap, and would make the slope of the activity map flatter. The type III 'window' corresponds to microemulsion phase behaviors showing a distinct middle phase, and usually corresponds to the lowest IFT. A broader type III region can lead to a more robust design, more tolerant to local variations in salinity, oil composition or other unknowns in a reservoir. The above scan has an acceptably large type III window of 5,000-10,000 ppm TDS.

Figure 5.2 depicts solubilization ratios for 10% oil (WOR = 9). IFT can be estimated using the Chun Huh equation.
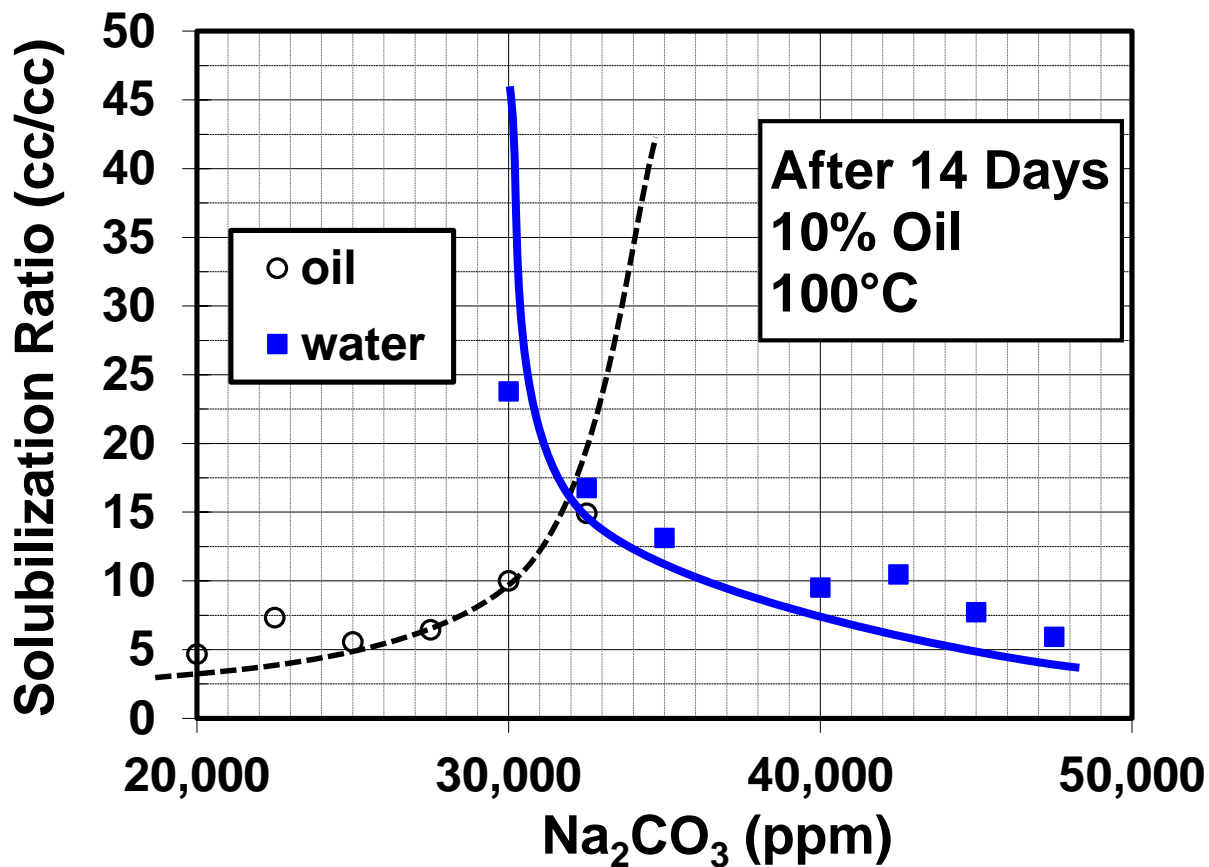
Figure 6.1.2: Solubilization ratios in 10% oil for formulation F-1.

As described earlier in the section Interfacial Tension and Solubilization Ratio, a solubilization ratio greater than 10 corresponds to ultra-low IFT from the Chun-Huh equation, and is adequate to reduce oil saturation to nearly zero in most cores. Note here that the area with solubilization ratio >10 is rather small. This is due to the fact that at 10% oil, there is little help from the in-situ generated soaps in lowering IFT; the surfactant barely manages to lower IFT to ultralow level. The results at 30% oil (WOR = 3/7) are shown below:
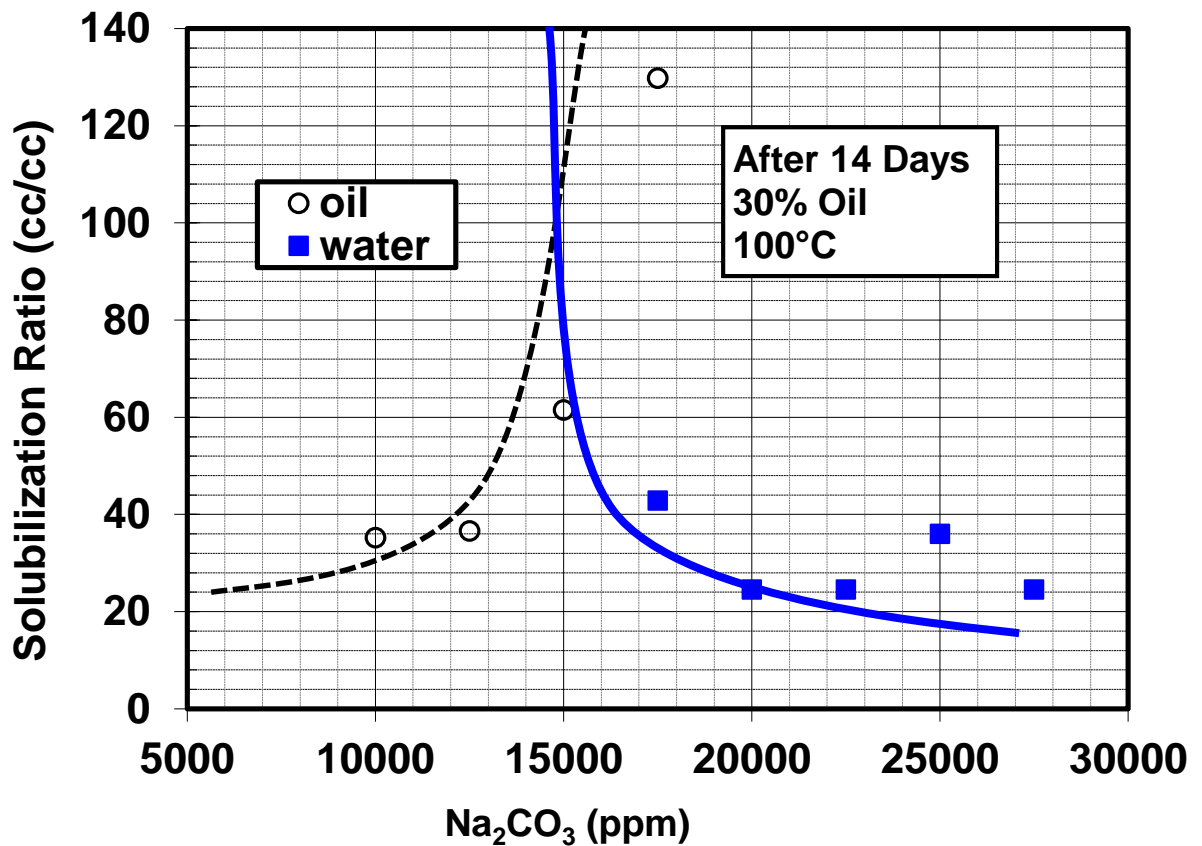
Figure 6.1.3: Solubilization ratios in 30% oil in formulation F-1.

The formulation above demonstrates the significance of soaps in lowering IFT. While the solubilization ratio at 10% oil is not much above 10, we see here that solubilization ratio is much higher at 30% oil. This is not because the surfactant becomes more effective at greater oil concentrations, but because the soaps generated by alkali acting synergistically with the added surfactants are extremely effective in lowering interfacial tension. As the amount of soap generated is difficult to measure, it is not included in the 'solubilization ratio' shown in these figures.

F-2 ASP Formulation

   Though the F-1 formulation was a good candidate for coreflooding, it was desired to find a formulation which performed slightly better at low oil fractions (high WOR). A formulation F-2 containing 0.15% TDA-13PO Sulfate, 0.15% IOS 19-23, 1% IBA-5EO demonstrated similarly good characteristics as F-1, with the added benefit of performing better at high WOR. A potential problem is the formulation used sulfate surfactants, which are unstable at high temperatures. This problem is mostly alleviated by the use of high pH, which stabilizes the sulfates even at 100°C.
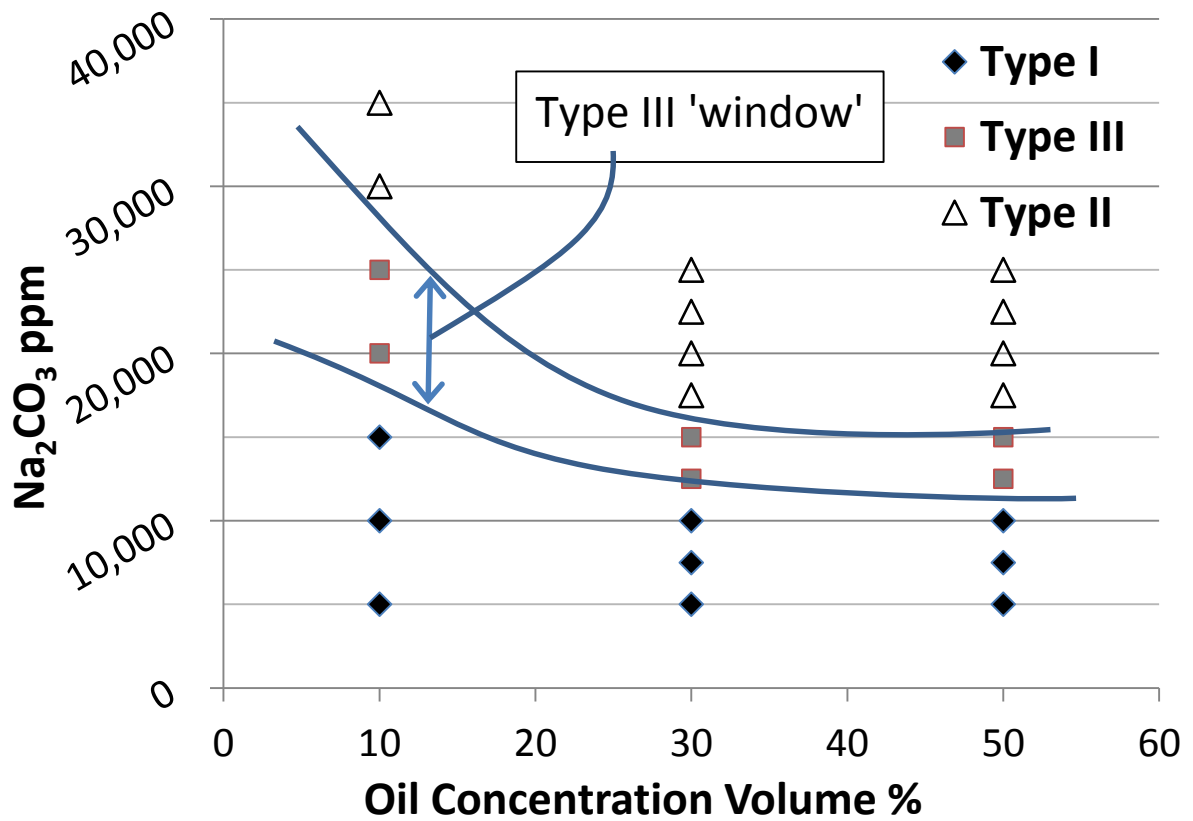
Figure 6.1.4: Activity map for F-2 formulation

The F-2 formulation is less hydrophilic, resulting in a flatter activity map. Note that at 50% oil, F-1 and F-2 have the same optimum salinity (15,000 ppm), due to the strong influence of the soap on phase behavior. The solubilization ratio curves for F-2 use volume % of oil as the above figure.
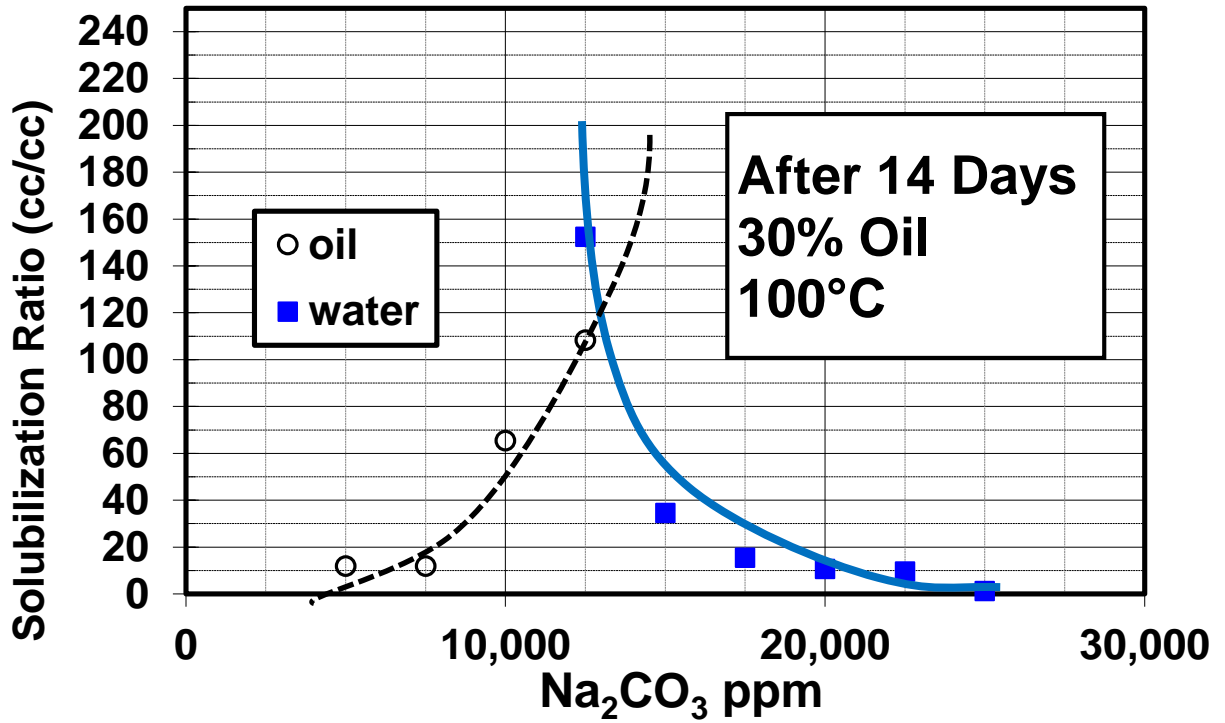
Figure 6.1.5: F-2 ASP formulation solubilization ratio for 30% oil.
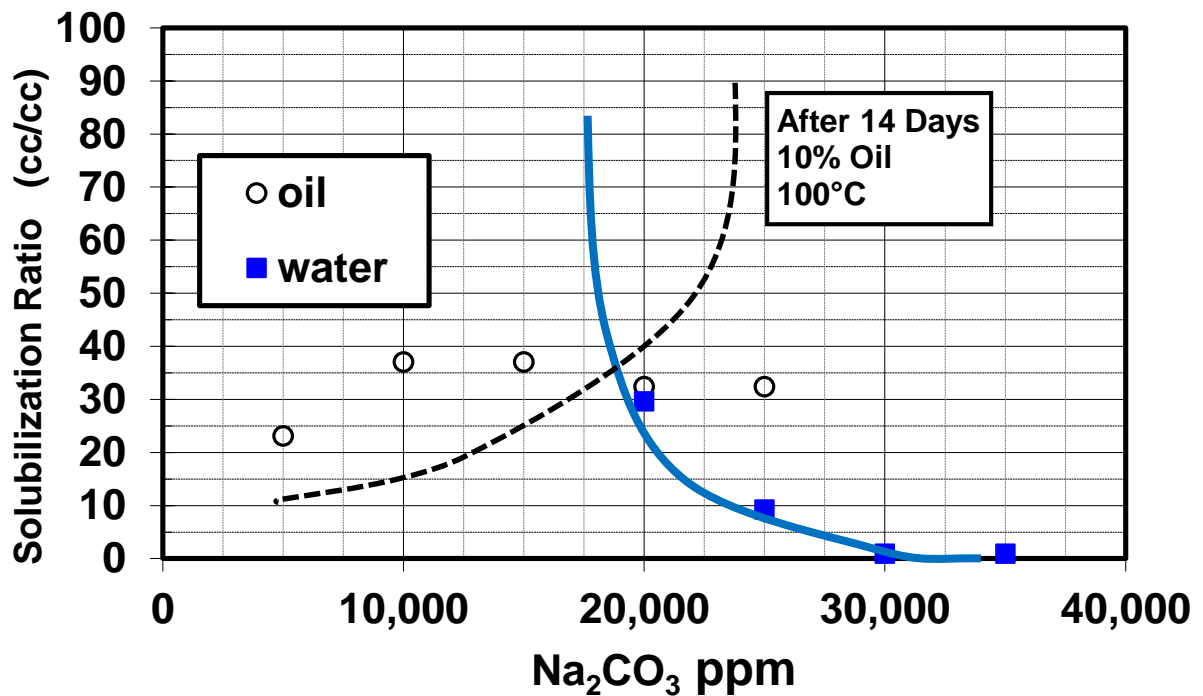
Figure 6.1.6: F-2 ASP formulation solubilization ratio for 10% oil.

Note the significantly higher solubilization ratios for F-2 vs. F-1, especially in the region of 10 vol.% oil. The improvement in IFT at high WOR was the basis for selecting F-2 as the formulation of interest for the corefloods ASP-1 and ASP-2.

6.2 ASP-1 COREFLOOD

ASP-1 Coreflood Objective

ASP-1 coreflood was designed to evaluate the performance of ASP flooding in heavy oils at temperatures above their reservoir temperature. Increasing the reservoir temperature will improve the feasibility of a chemical flood by reducing the oil viscosity, therefore increasing oil recovery and decreasing pressure drop. Additionally, lowering the

viscosity of the viscous oil will increase injectivity and therefore throughput rates in the field. The ASP core floods were conducted in Berea sandstone due to its relative homogeneity, high permeability (100's of mD) and lack of clay content.

ASP-1 Core Properties

The properties of the Berea core used in ASP-1 flood follow in table 6.2.1.

Core ASP-1		
Outcrop	Berea	
Mass	1021	g
Porosity	0.197	
Length	11.52	in
Diameter	1.84	in
Area	2.63	in^2
Temp	100	°C
Brine Perm	246	mD
PV	101	ml

Table 6.2.1: ASP-1 Core Properties

ASP-1 Coreflood Setup

The core was first measured in dimensions and mass. Afterwards it was placed inside a 2 inch ID steel-jacketed core holder. Confining pressure of 1000 psi was applied to the outside of the core with an ISCO syringe pump. Pressure taps were drilled into the core at fixed intervals of 2.9 inches, to allow monitoring of pressure across different sections of the core. Dead volume in the core was to 2 ml.

After securing the core in the core holder, a vacuum was applied to the core for 30 minutes. After this time, the core was saturated with filtered 10,000 ppm NaCl brine. The volume of brine was measured and converted to pore volume of the core, approximately 102 ml. 10,000 ppm NaCl brine was assumed to have a density of 1g/ml.

ASP-1 Tracer Test and Brine Flood

After obtaining a volumetric measurement of pore volume, a tracer test was done with 40,000 ppm NaCl brine. This was the same resident brine used in the coreflood. The initially saturated 25,000 ppm brine was displaced with the resident brine at 5 ml/minute, while samples were collected every 3 ml (~ 36 seconds). Salinities were measured using a refractometer (reads refractive index, calibrated to NaCl) and recorded. The curve in Figure 6.2.1: ASP-1 tracer data resulted from the test.
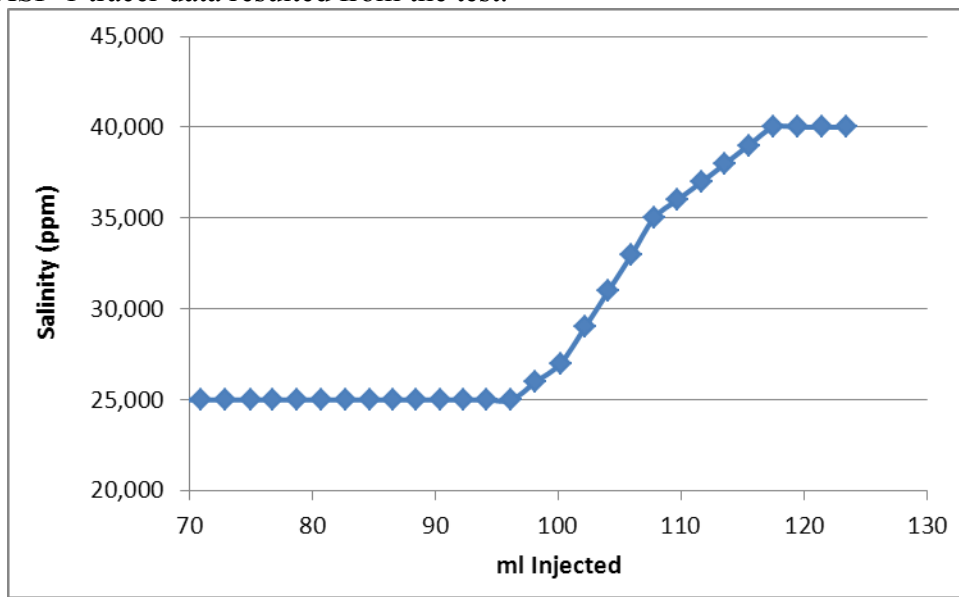
Figure 6.2.1: ASP-1 tracer data used to calculate pore volume

Integrating the area above the curve gives the pore volume of the core; the result was 101 ml, in close agreement with the volumetric values of 102 ml.

After completing the tracer test, flow rate of brine was increased to 10 ml/min. Pressure drops for the brine flood were monitored, and Darcy's law was applied to calculate brine permeability. This permeability was calculated at room temperature and later at 100°C.

41

Table 6.2.2: Brine flood performance @10 ml/min & 25°C in ASP-1 coreflood

Section	ΔP_{Brine}, psi	k_{Brine}, mD
1	1.28	228
2	1.18	246
3	1.04	281
4	1.08	262
Whole core	4.65	249

After completion of the brine flood, the core was placed in a 100°C oven. Confining pressure was maintained at a constant 1000 psi by an ISCO syringe pump, while brine was occasionally bled from the effluent lines on the core.

ASP-1 Oil Flood

Unfiltered surrogate crude oil was heated to 100°C over 3 hours. Pressure was released every 10 minutes to ensure safety of equipment and experimenters. The oil flood was conducted at constant rate of 8.1 ml/min (100 ft/day) to ensure high pressure drop and desaturation of resident brine.

It was apparent from the pressure drop data, which steadily increased with injection volume, that the unfiltered crude oil was plugging the face of the core. To test this hypothesis, the flow direction was reversed, and the plugging was removed from the initial inlet and replaced with plugging at the outlet. Initially it was thought that filtering the viscous oil might have an undesirable effect on phase behavior, therefore it remained unfiltered. It became an obvious necessity, and was filtered sequentially through 5, 3 and 1.2 micron filters in an 85°C oven. Phase behavior changed slightly with filtration, as loss of light ends increased the optimum salinity 2500 ppm in 10 and 30 vol. % oil. It remained constant at 50 vol. % oil at about 15,000 ppm.

Filtered crude was injected in a second oil flood, whose results are below. Pressure drops were recorded after they reached a steady state value. The k_{ro} for the entire core was 0.97, see table 6.2.3.

Table 6.2.3: Filtered oil flood #2 performance @ 100°C in coreflood ASP-1

Section	$\Delta P_{Oil\ flood}$, psi	k_{Oil}, mD	k_{ro}
1	19.5	235	1.034
2	16.0	287	1.181
3	14.3	321	1.143
4	23.7	188	0.718
Whole core	75.5	241	0.97

Relative permeability > 1 is somewhat common in water-wet rocks with viscous oil, as Odeh showed in the late 1950's (Downie & Crane, 1961). The low permeability in the last core is attributed to face plugging mentioned earlier; it wasn't possible to entirely remove the plugging on both faces exposed to the unfiltered crude. Initial oil saturation S_{oi} was 75%.

ASP-1 Water Flood ASP-1

After oil flooding, SB-1 brine was pumped through the core at 0.7 ml/min or 9.68 ft/day. A back pressure regulator set to 32 psi was attached to the core to prevent vaporization of brine and light ends. After pressure drop reached steady state, k_{rw}^o was calculated to be 0.038 for the core, though this value is artificially low due to the face plugging at the outlet. Relative permeability values for each section are shown below in table 6.2.4.

Table 6.2.4: Waterflood performance @100°C and 9.68 ft/day in ASP-1 Coreflood

Section	$\Delta P_{waterflood}$, psi	K_w, mD	K_{rw}^o
1	1.98	10	0.045
2	1.75	12	0.048
3	1.85	11	0.039
4	3.00	7	0.025
Whole core	8.60	9	0.038

Residual oil saturation S_{orw} after waterflood was 41.4%.

ASP-1 Mobility Control Requirements

The ASP-1 coreflood was designed to be a stable displacement. Figure 6.2.2 shows the apparent viscosity and total relative mobility required to displace the oil bank.
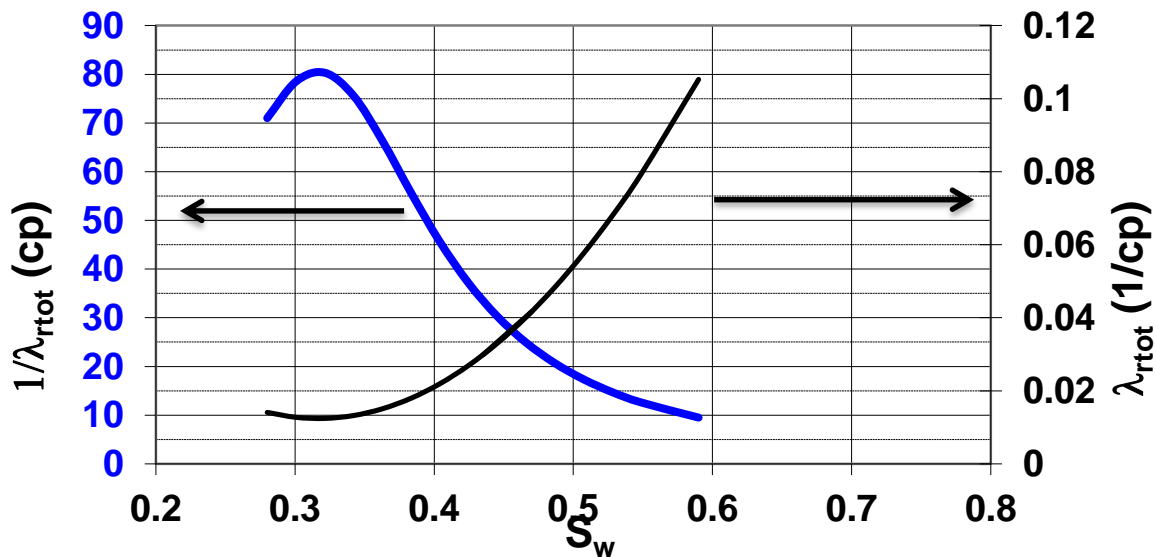
Figure 6.2.2: Apparent viscosity and total relative mobility of oil bank in ASP-1

The parameters used in the calculations are as follows:

Table 6.2.5: Mobility control requirement parameters

Parameter	Definition	Value	Justification
k_{rw}^o	End point water relative permeability	0.04	Obtained from water flood
k_{ro}^o	End point oil rel. perm	1	Obtained from oil flood
n_w	Fractional flow exponent water	2	Assumed for water wet
n_o	Fractional flow exponent oil	2	Assumed for water wet
S_{wr}	Residual water saturation to oil	0.28	Calculated from mass balance
S_{or}	Residual oil saturation to water	0.46	Calculated from mass balance
μ_w	Water Viscosity	0.38 cP	Known value
μ_o	Oil Viscosity	71 cP	Measured in rheometer

From the above total mobility calculations, it is apparent the minimum viscosity for a stable displacement fluid is ~82 cP. Polymer solutions are extremely shear-thinning, and shear rate is difficult to determine with certainty in a core flood due to combined effects of oil saturation, distribution and relative permeability. With this in mind it is important to design a robust formulation for mobility control. In the case of ASP-1, 100 cP at a shear rate of 10 sec^{-1} (the approximate shear rate in the core) was determined to be appropriate. HPAM FP 3630s was used as the mobility control polymer in these experiments due to its high molecular weight.

ASP-1 Salinity Gradient Design

Another critical design parameter in a successful coreflood is the salinity gradient. As constant-salinity floods suffer various disadvantages, it is critical to reduce the salinity in steps from over-optimum to below optimum. This has the net effect of ensuring every

region in the core experiences the ultralow IFT in the type III microemulsion region corresponding to the optimum salinity.
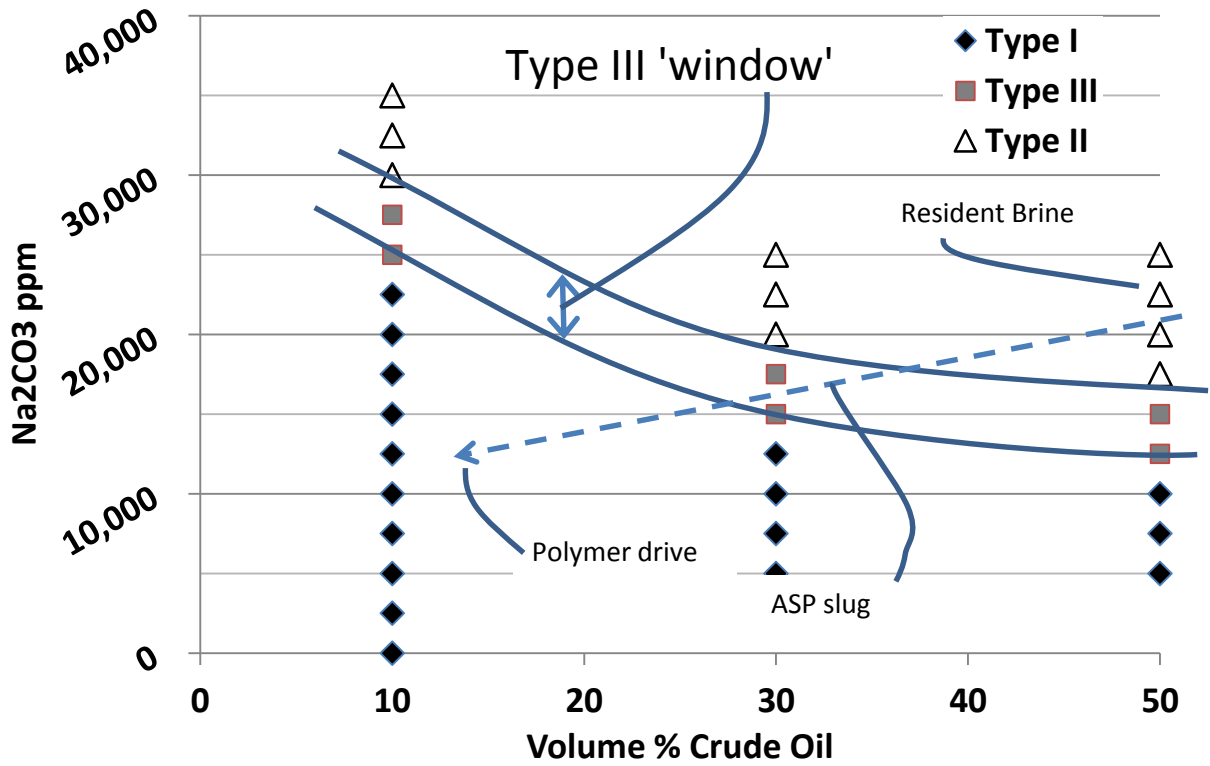
Figure 6.2.3 : ASP-01 salinity gradient design. The dotted line represents the salinity gradient.

Pope and Nelson (1978) showed the salinity gradient will retard the surfactant bank from an early breakthrough by the formation higher-salinity type II microemulsion in the front. The lower salinity behind it ensures all swept areas pass through the zone of ultralow IFT in type III, and the final lowest salinity brings the emulsion to type I, where capillary desaturation of aqueous phase should desaturate all trapped surfactant.

ASP-1 Chemical Flood

The final injection ASP slug and polymer drive had the following composition, based on the design criterion described above and methods described in the experimental methods section. Before injecting the ASP slug, a sample tube of crude in the core and ASP slug were mixed together to ensure IFT was ultra-low. This last step ensures that no mistakes have been made in the slug and drive by checking the mixture for low IFT. Additionally, a refractometer can be used to check the total dissolved wt.% in the slug and drive (electrolyte, surfactant, cosolvent, and polymer) as a second test of quality control in the slug and drive.

Table 6.2.3: ASP-1 Slug and drive composition

Slug Component	ASP Slug	Polymer Drive
PV injected	0.5	2
[HPAM 3630s] ppm	3,750	4,000
PV_{inj} *[Surf #1 + #2]	15	---
[Surf #1], wt.%	0.15% TDA-13 PO SO_4^-	---
[Surf #2], wt.%	0.15% IOS 19-23	---
[Cosolvent], wt.%	1% IBA-5EO	---
ppm Na_2CO_3	15,000	10,000
TDS ppm	15,000	10,000
Frontal velocity ft/day	1.08	1.08
Viscosity at 10/s & 100°C, cP	70	101

Filtration Ratio F.R.	1.12	1.16
pH	10.8	10.5

Coreflood recovery was 97.4% of tertiary oil saturation. This demonstrated excellent performance of the ASP/PD design in elevated temperature environments for heavy oils. The coreflood result and recovery are below.
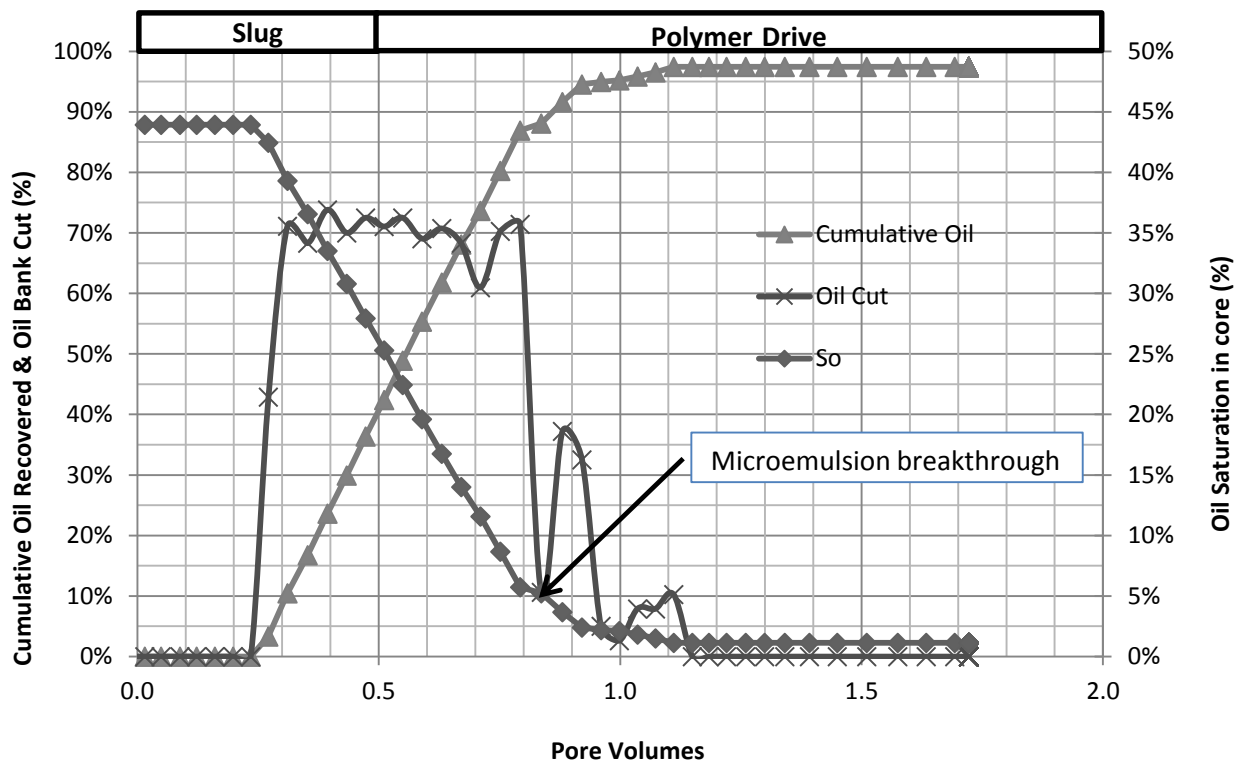
Figure 6.2.4: ASP-1 oil recovery, oil cut and oil saturation

The data in Figure 6.2.7 shows the oil bank breaks through at 0.25 PV of throughput, and rapidly increases to ~ 72% oil cut. This high oil cut is maintained until over 90% of oil is recovered. The microemulsion breakthrough is approximately 0.85 PV, slightly earlier than expected but still indicative of a stable displacement.   After

microemulsion breakthrough, oil cut continued to drop until it was negligible 1.12 PV. Pressure drops in the core in the Figure 6.2.8.
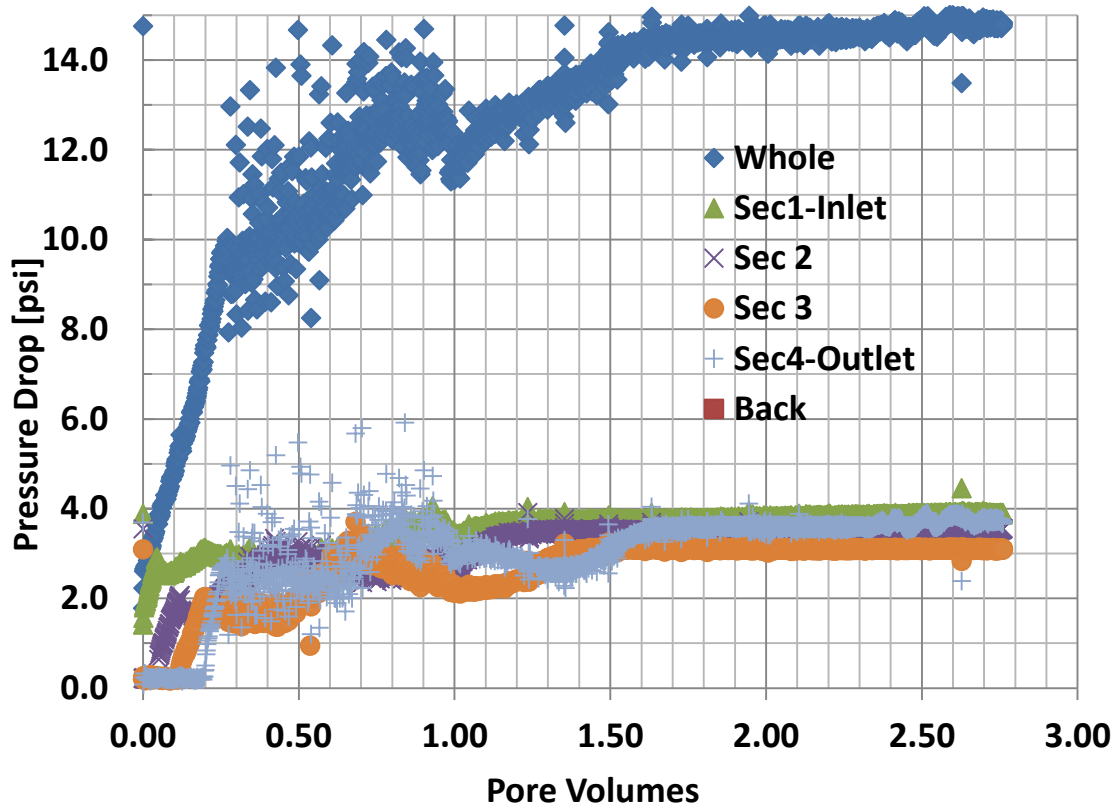
Figure 6.2.5: ASP-1 Chemical flood pressure drops

From the pressure drop data, the oil bank buildup, microemulsion and polymer drive are all clear to see. The total pressure drop is 14.8 psi/ft, which would be unsustainable in the field; however most rock containing heavy oils is permeable on the order of 1-5 Darcy; a corresponding pressure drop in such a rock would be 2-0.5 psi/ft.

ASP-1 Effluent Analysis

Effluent analysis of the ASP-1 coreflood was limited to salinity measurements and pH measurements. Both showed salinity and pH propagated well with the chemical slug. After breakthrough of the microemulsion at 0.85 PV, the pH steadily increased to the steady state slug value of 10.85 at ~1.15 PV. Proper pH propagation is critical to a successful ASP coreflood, as the generated soaps provide most of the IFT-lowering micelles. Chromatographic separation of surfactant and alkali is highly undesireable.

Salinity also showed proper propagation within the core. The salinity was measured using a refractometer, which captures all dissolved components, including surfactant, co-solvent and oil solubilized in micelles, if present. The total salinity of the surfactant slug is 32,000 ppm. The slug salinity measured from the refractometer reads a higher value than this at steady state (38,000), but is consistent with the initial measurement of the slug.
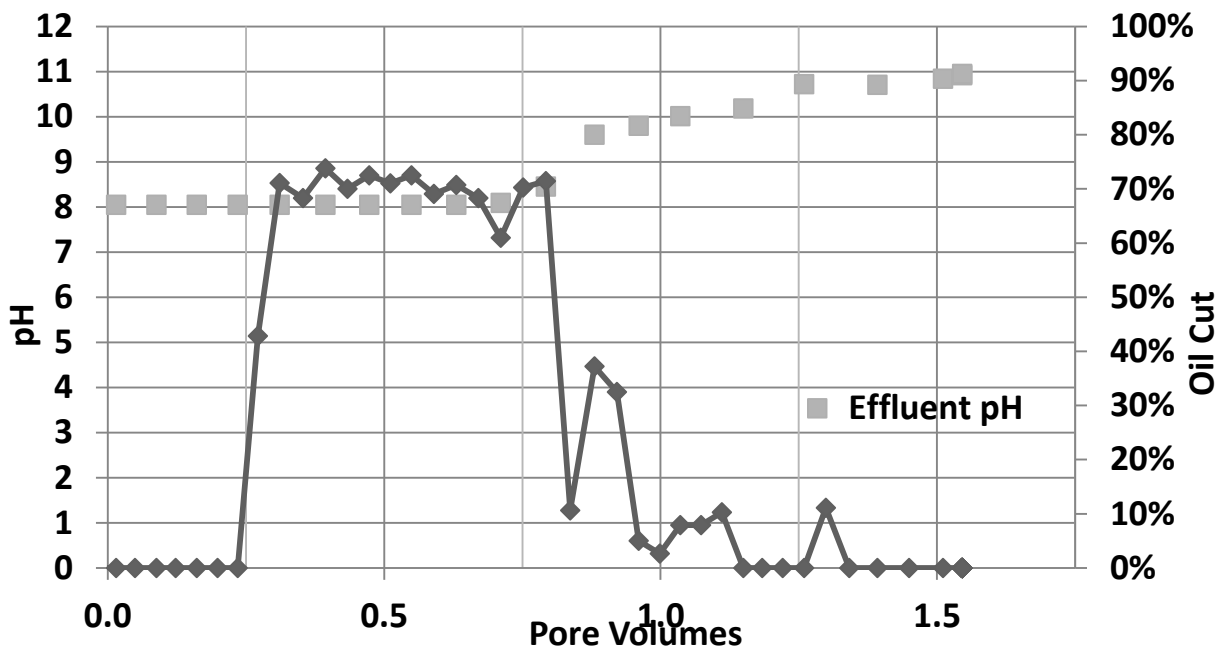
Figure 6.2.6: ASP-1 pH propagation with coreflood
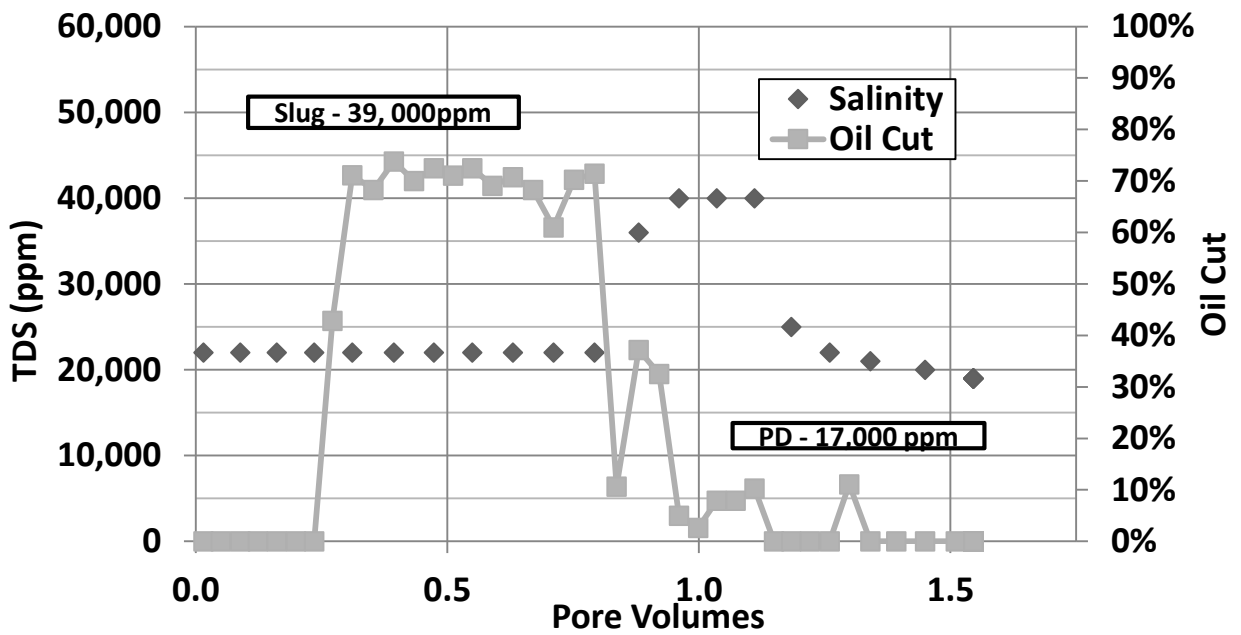
Figure 6.2.7: ASP-1 salinity propagation. This result corresponds well to slug breaking through and the ensuing polymer drive

51

6.3 ASP-2 COREFLOOD

ASP-2 Coreflood Justification

As the ASP-1 coreflood was a success, a more challenging design was selected for ASP-2. Though the ASP-1 coreflood had low surfactant concentration, the total ASP slug was large at 0.5 PV. The design for ASP-2 was identical to that of ASP-1, with the ASP slug designed to be only 0.25 PV. Such a low PV*C can significantly improve the economics of a surfactant flood.

ASP-2 Core Properties

As in ASP-1, the core material used in the flood was Berea sandstone, chosen for its relatively high permeability, low clay content and availability. The properties of the core used in ASP-2 flood follow.

Table 6.3.1: Core Properties of ASP-2 rock

Core ASP-2		
Outcrop	Berea	
Mass	1068	g
Porosity	0.205	
Length	11.44	in
Diameter	1.85	in
Area	2.63	in^2
Temp	100	C
Brine Perm	253	mD
PV	102	ml

The core overall is quite similar in character to that of ASP-1 core.

ASP-2 Coreflood Setup

The coreflood setup was identical to ASP-1. See table 6.2.1.

52

ASP-2 Brine Flood and Tracer Test

The tracer test was conducted at room temperature, as was the initial brine flood. The pore volume from the tracer and volumetrically was 102 ml. After the room temperature tests were completed, the core was placed into a 100°C oven. Confining pressure was maintained with an ISCO pump on the mineral oil jacket. Meanwhile, injection fluids were heated in the same oven. Both the brine column and the core were vented often to prevent an unsafe buildup of pressure.

After allowing the core to equilibrate overnight, a second tracer test was run at 100°C, to compare with the room temperature value and to ensure the core remained undamaged. The permeability to brine of different sections is tabulated below.

Table 6.3.2: Single phase brine permeability in ASP-2. 100°C, 5 ml/ min flow rate.

Section	ΔP_{Brine}, psi	K_{Brine}, mD
1	0.67	220
2	0.57	258
3	0.48	307
4	0.47	296
Whole core	2.30	253

ASP-2 Oil Flood

After the plugging issues experienced with ASP-1, oil was filtered immediately for use in this experiment. The final filter size was 1.2 μm under 20 psi filter pressure. An oil column was made in a steel vessel and allowed to equilibrate in the oven for 3 hours; a 50 psi back pressure regulator on the column allowed it to vent without loss of light ends as it heated.

Oil was flooded in the core from the bottom (this high density oil doesn't experience much gravitational instability) at high rates of 14 ft/day until pressure drops

were steady and oil cut was 100%. Mass balance calculations revealed the S_{oi} to be 77%. Permeability to oil flood was measured and recorded below.

Table 6.3.3: Pressure drops in oil flood, ASP-2 coreflood.

Section	$\Delta P_{Oil\ flood}$, psi	k_{Oil}, mD	k_{ro}
1	23.90	264	1.201
2	21.24	297	1.150
3	19.73	320	1.043
4	18.92	315	1.065
Whole core	87.0	286	1.133

The more uniform permeability distribution to oil perm in ASP-2 vs. ASP-1 is likely due to the lack of plugging seen in ASP-1.

ASP-2 Waterflood

After reaching S_{oi} the core was waterflooded at 9.68 ft/day (0.7 ml/min) until the oil cut was <1% and pressure drops were steady across the core. Heavy oils are expected to have poor waterflood performance; this means low sweep efficiency, early water breakthrough and high residual oil saturations. After 2 PV of water were injected, S_{orw} was 0.46, confirming expectations of poor performance. Waterflood permeability in various sections is Table 6.3.4.

Table 6.3.4: ASP-2 waterflood relative permeability

Section	$\Delta P_{waterflood}$, psi	k_w, mD	k_{rw}^o
1	2.75	8	0.034
2	1.52	14	0.053
3	1.40	15	0.048
4	1.60	12	0.041
Whole core	17.10	11	0.042

ASP-2 Design Requirements

Design requirements for ASP-2 are identical to those of ASP-1; the altered variable
is ASP slug size. To ensure good performance with the lower chemical concentration used,
viscosity of the slug was increased slightly. To accomplish this polymer concentration was
raised to 4,000 ppm in both the slug and drive. Viscosity curves for ASP slug and polymer
drive are below.
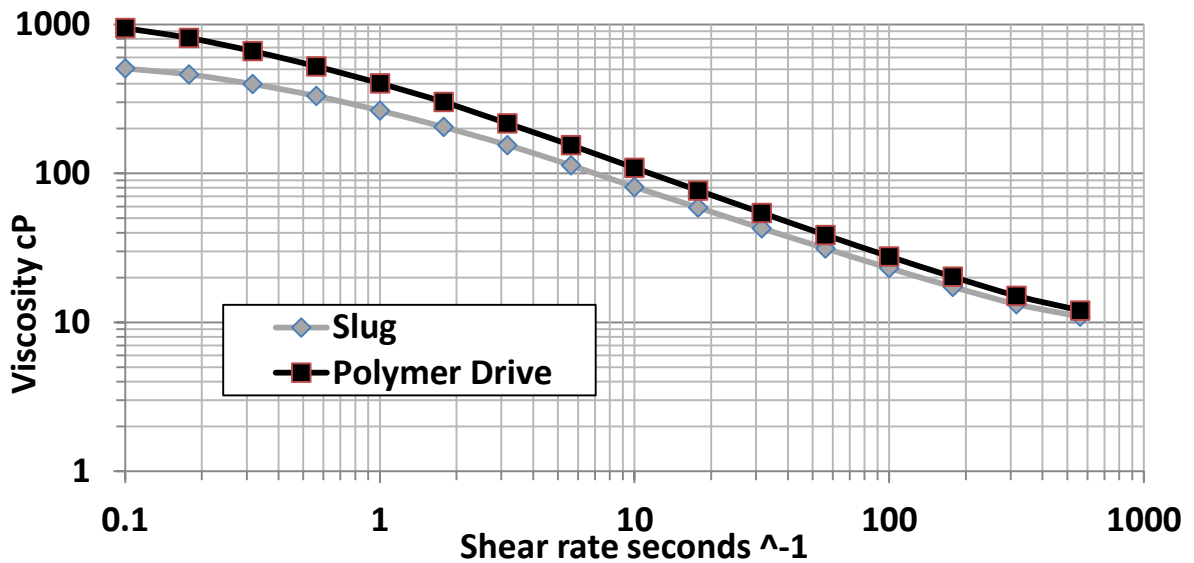
Figure 6.3.1: ASP-2 Slug & drive viscosity.

ASP-2 Chemical Flood

The ASP-2 chemical slugs injected are below. They are virtually identical to those
in ASP-1, with half the pore volume and slightly higher polymer concentration in the ASP
slug vs. ASP-1. Differences are in bold.

Table 6.3.5: ASP-2 ASP slug and polymer drive composition

Slug Component	ASP Slug	Polymer Drive
PV injected	**0.25**	2
[HPAM 3630s] ppm	**4,000**	4,000
PV_{inj} *[Surf #1 + #2]	**7.5**	---
[Surf #1], wt.%	0.15% TDA-13 PO SO_4^-	---
[Surf #2], wt.%	0.15% IOS 19-23	---
[Cosolvent], wt.%	1% IBA-5EO	---
ppm Na_2CO_3	15,000	10,000
TDS ppm	15,000	10,000
Frontal velocity ft/day	1.08	1.08
Viscosity at 10/s & 100°C, cP	**81**	**108**
Filtration Ratio F.R.	1.11	1.15
pH	10.5	10.6

The flood was very effective at recovering tertiary oil; 97.6% of residual oil was removed from the core and final oil saturation was 1.23%.
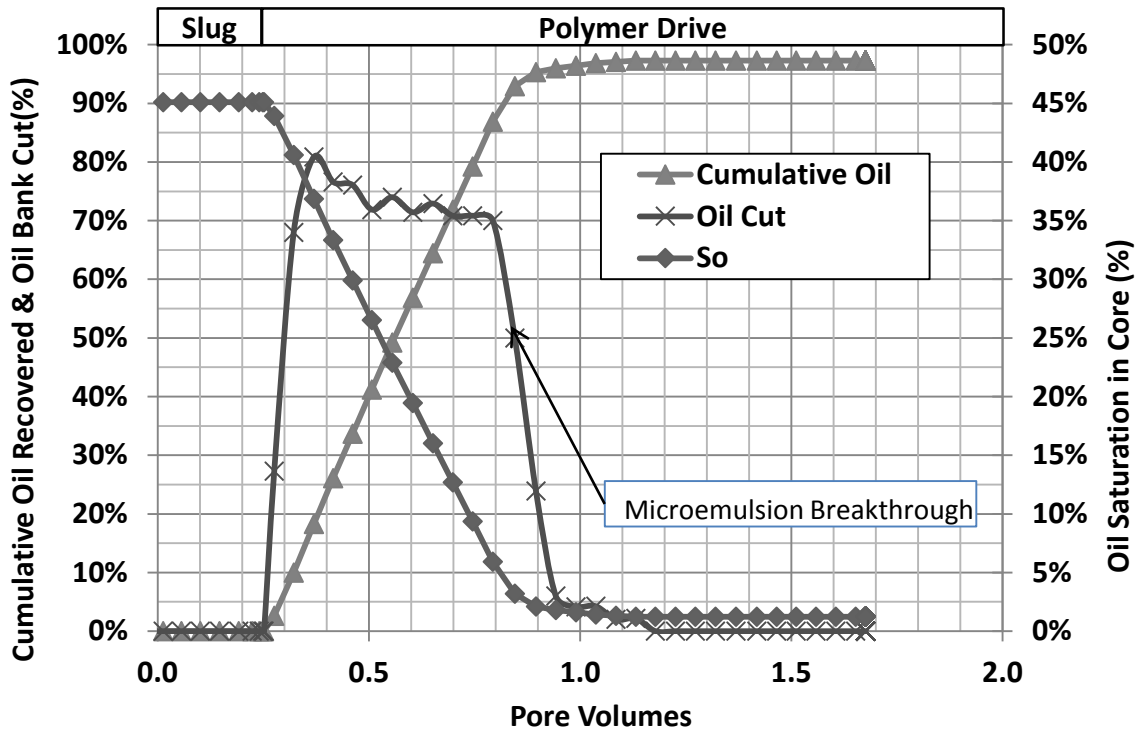
Figure 6.3.2: ASP-2 coreflood recovery, oil cut and oil saturation in the core vs. PV of chemicals injected.

The flood performance was equivalent to that of ASP-1; they both recoverd over 97% of the oil in the core. ASP-2 produced 93% of the oil before microemulsion breakthrough, vs. 88% in ASP-1, and produces all the oil before 1 PV, vs. 1.1 PV in ASP-1. This is probably due to the slightly greater mobility control used in ASP-2, which removed the small amount of viscous instability seen in ASP-1.

Pressure drops during the flood were as anticipated. Total pressure drop for the core at steady state was 17.2 psi/ft. Though this value is high for a reservoir, the rock used is significantly less permeable than many suitable heavy oil reservoirs, and the expected

pressure would be manageable for an oil of this viscosity in a multi-Darcy sand. Pressure

drop data for the chemical flood are shown in Figure 6.3.6.
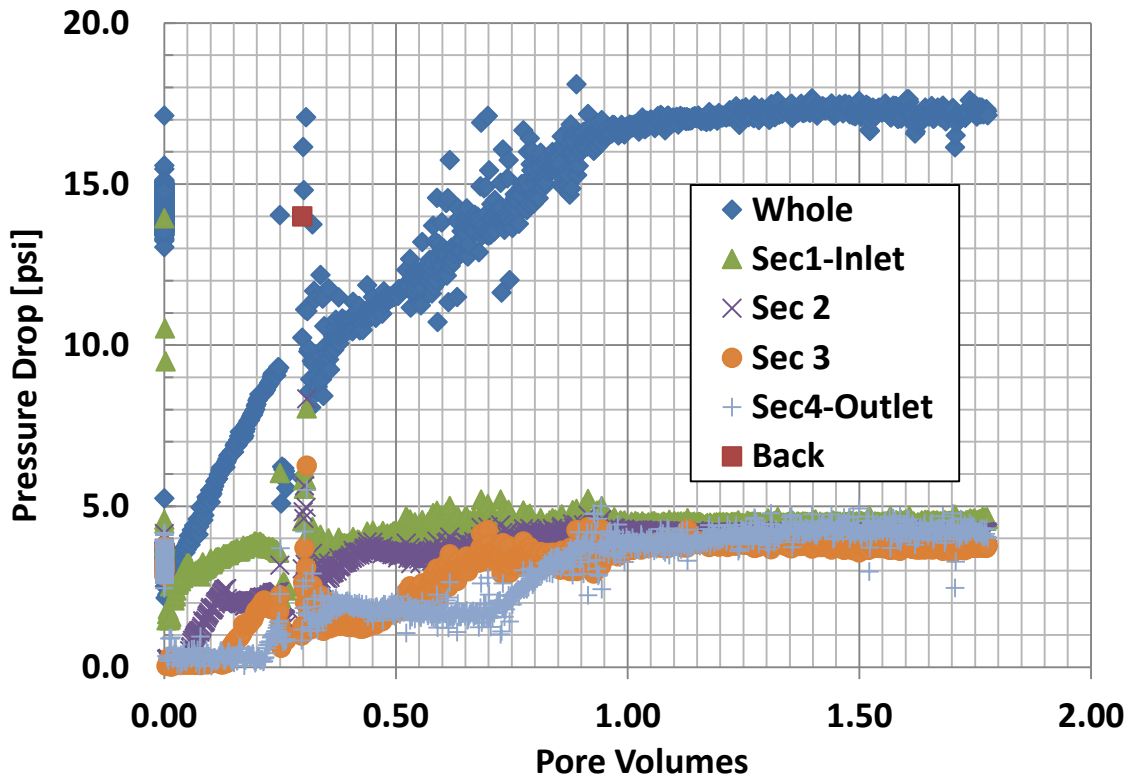
Figure 6.3.4: ASP-2 chemical flood pressure drops

The gap at 0.25 PV occurred when the column containing the polymer drive leaked.

Data wasn't written during a brief period when a replacement column was put online.

ASP-2 Effluent Analysis

ASP-2 was subject to the same effluent analysis as ASP-1. Salinity and pH were

both measured in effluent to confirm propagation of slug chemicals and are below:
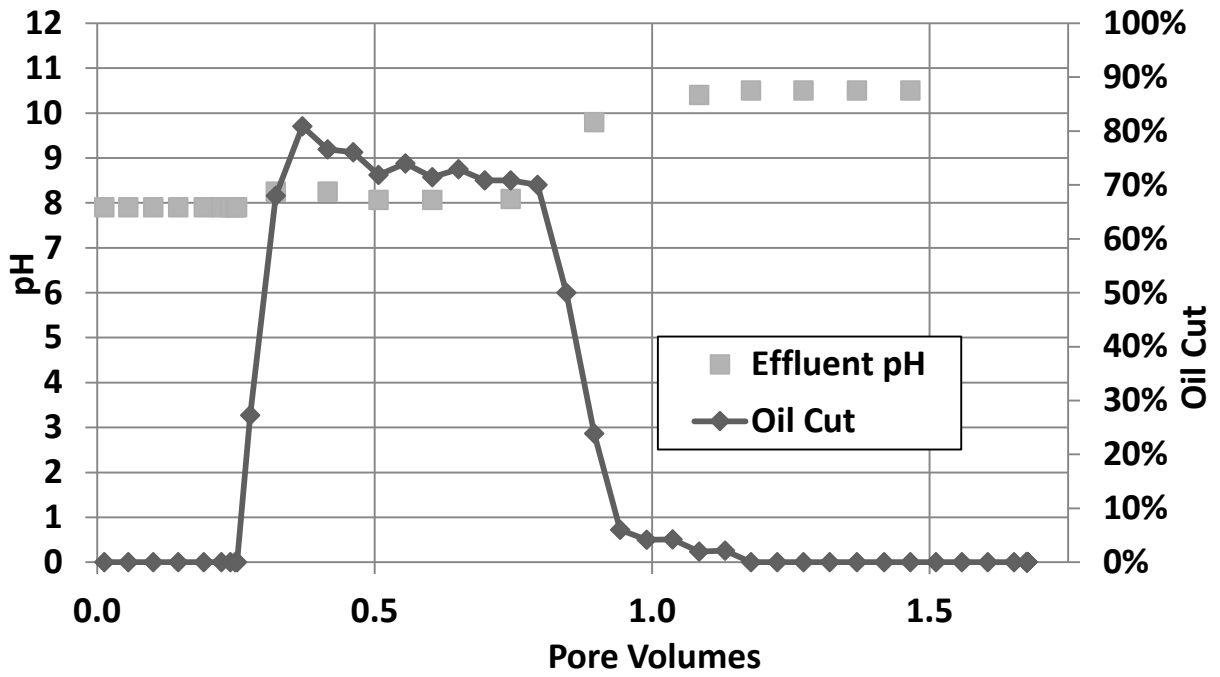
Figure 6.3.5: ASP-2 pH versus PV throughput
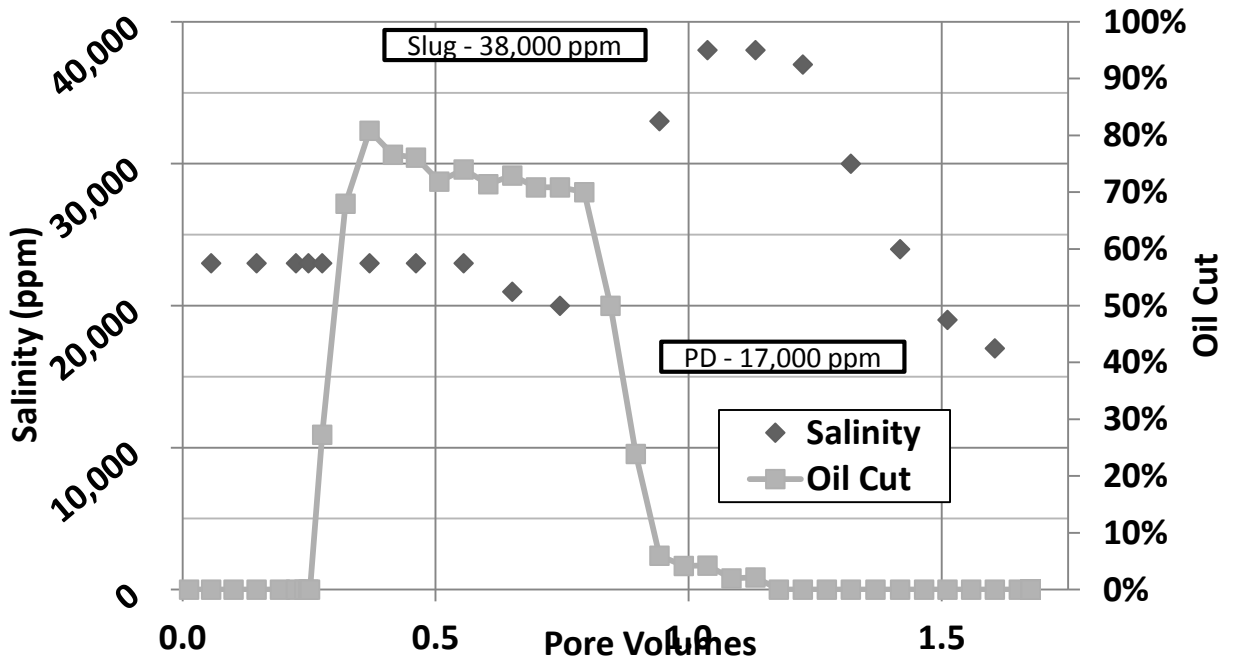
Figure 6.3.6: ASP-2 Salinity vs. throughput

59

ASP Flooding Conclusions

The ASP 1 & 2 floods demonstrated the applicability of the ASP technology to heavy oils in under elevated temperature conditions. Though work has been done with CEOR in heavy oils before, these have generally been in viscously unstable environments and without reservoir heating. This work demonstrates that heavy oil responds extremely well to ASP flooding when heated, and could potentially remove virtually 100% of the oil in contacted zones of a reservoir. Though there are certainly issues with heating a reservoir, the potential benefits of applying hybrid thermal-CEOR to heavy oil fields seem significant.

Additionally, only very small amounts of surfactant (PV * C = 7.5) are needed to successfully execute such a flood. Multiplying the % pore volume b surfactant concentration yields a numerical value, PV*C. The PV*C value for the ASP 2 core flood was only 7.5, a low value (% PV = 25, C = 0.3). This is likely due to low surfactant adsorption in a high pH environment and the contribution of in-situ generated soaps in reducing IFT to ultralow levels. Such low concentrations of surfactant would have significant impacts on the economics of a chemical flood.

Chapter 7: ACP Experiments

7.1 HISTORY OF ALKALINE FLOODING

Alkaline flooding has a long history; though it has received somewhat less attention recently than surfactant-based processes, it too was a subject of technological development with varying success. Very long ago, researchers like Thom (1926) realized that the presence of sodium carbonate (high pH) in formation brines resulted in better performing water-drives and the formation of emulsions. These observations led to a development of high-pH technology in the 1920s, when waterflooding was a new process. In 1925, Nutting published some of the earliest related work, calling the technology the 'soda processes'; he alludes to the earliest known alkaline flood in the same year, which was a failure (1925). An H. Atkinson in 1927 obtained a patent for the use of sodium hydroxide in waterflooding, though no record of its field implementation exists.

These early researchers grasped many of the fundamental concepts critical in alkaline flooding, though they were limited by the analytical techniques available at the time. They identified emulsification and entrainment (crude oil transported with emulsion, via lowered IFT), wettability reversal (generally oil- to water-wet) and emulsification and entrapment (plugging of emulsion to improve volumetric sweep) as mechanisms primarily responsible for producing residual oil (Johnson, 1976). By 1942 researchers such as Subkow had grasped the concept of in-situ soap formation via deprotonation of carboxylic acids (Subkow, 1942). These mechanisms were established based on their understanding of the O/W (oil in water) emulsion, where water forms a continuous phase with oil solubilized. Though such emulsions can exhibit ultralow IFT and cause wettability alteration, their behavior is challenging to predict; especially when compared to a

thermodynamically stable microemulsions. This was a critical issue in the lack of successful alkaline floods, as detailed below.

Understanding of the physics involved in surfactant process (for example, Windsor) helped improve the technology of alkaline flooding, and in the 1960's interest in the technology reemerged. The first 'modern' caustic flood was an attempt at wettability alteration from oil-wet to water-wet in the Harrisburg Field in Nebraska (Leach, Wagner, Wood, & Harpke, 1962). Though one watered-out well produced some oil, the test was not considered successful due to the large slug used. A second wettability alteration test in the Singleton field produced 2.3% PV of incremental oil from 1966-1970, another discouraging result. Both these tests involved small slugs of high-concentration sodium hydroxide to alter wettability in an originally oil-wet environment (Emery, Mungan, & R.W., 1970).

An attempt to use the other useful properties of the alkaline flood was made in 1964 at the Whittier field, where researchers hoped to use the viscous emulsion to divert flow in a reservoir to unswept zones. A targeted area had been waterflooded for 2.5 years prior to alkaline injection, and was in severe decline. The 60 acre pattern of interest was flooded in 1966 with a 23% PV slug of 2000 ppm sodium hydroxide, which corresponded to ultralow IFT. The rate turned around, almost immediately, and the test produced 350,000-470,000 barrels of incremental oil (Graue & Johnson, 1974). Johnson's 1973 report 'Status of Caustic and Emulsion methods' is a good overview of the period (Johnson, 1976).

Understanding improved over the next decade, and alkaline flooding (often called caustic flooding in this era) enjoyed a heyday in the late 1970's and early 1980's. A report by Mayer reveals the extent to which knowledge had improved in the area; researchers show better understanding of alkaline displacement mechanisms, including complexities

62

of emulsions and their failure to consistently produce oil via the emulsification and entrapment mechanism (aka plug and divert), challenges of relying on wettability alteration and the emulsification mechanisms. Impact of salinity on emulsion behavior is given attention. Understanding of the true chemistry of acidic components in oil (asphaltenes, resins) is revealed. The importance of sequestering divalent cations with the alkaline agent is mentioned, and even viewed as positive in terms of flow diversion. Much more detail is given to alkali consumption form various minerals, including clays and gypsum (Mayer, Berg, Carmichael, & Weinbrandt, 1983).

Two works from this period highlight the major leaps in understanding the process of alkaline flooding over the two prior decades: Burk's 1987 report on various alkaline agents and TIORCO's report on an Alkaline-Polymer flood. The TIORCO report is the first published account of alkaline flooding with polymer (AP) for conformance control, and took place in the Isenhour Unit, WY. This constituted a major breakthrough in the field; polymer to this point had been limited to surfactant-based or pure conformance applications, while alkaline floods were viewed as lower-tech, lower recovery technology. The Isenhour unit was a definitive success, despite its low permeability (21 mD) and fully emphasized the importance of conformance control, which had been addressed almost exclusively through the emulsification and entrapment mechanism to this point (Doll, 1988). The other report, 'comparison of Sodium Carbonate, Sodium Hydroxide and Sodium Orthosilicate for EOR' from TIORCO clearly shows improved understanding of the effects of alkali on rocks and with oil, with solid coreflood designs, often boasting 90% tertiary recovery when various polymers were used. This paper clearly endorsed the moderately lower pH buffering properties of sodium carbonate over the strong-base sodium hydroxide, a position now well established in the industry (Burk, 1987).

63

Despite the improved understanding of the time, alkaline floods continued to fail with regularity. The Mayer report shows that 12 alkaline floods (from the likes of Exxon, Amoco, Shell, Gulf and Union, among others) recovered between 0-8% PV of incremental oil, and typically were <1% PV (Mayer, Berg, Carmichael, & Weinbrandt, 1983). Even the 8% PV saturation reduction in Gulf's Estes, TX flood, while promising, is no show-stopper for an EOR technique. These failures, in the opinion of the author, stem from two main issues in design: the first is a total lack of mobility control, rooted in the hope that emulsions will divert a significant fraction of injection water and improve volumetric sweep. The other failure is related to the first; a lack of understanding of emulsion/microemulsion phase behavior and the way such emulsions will behave in the field. This lack of understanding led to field test implementation of alkaline floods hoping the plug-and-divert mechanism would produce significant incremental oil. Additionally, researchers failed to adapt the techniques advocated by surfactant researchers (Reed and Healy, 1976) for interpretation of microemulsion phase behavior.

In the 1990's and 2000's, alkaline flooding, like other chemical methods, received very little attention. Efforts were focused on heavy oil, primarily in Chinese and Canadian reservoir sands. The late 2000-2010's have seen resurgence in papers produced at the University of Calgary and in China. These papers emphasize the role of pressure buildup corresponding to ultimate recovery, effects of single-slug salinity and simulation matching. They still fail to take into account proper phase behavior studies, emulsion characterization, best practices like the salinity gradient and any mention of mobility control outside of polymer. See, for example (Pei, Zhang, Ge, Ding, Tang, & Zheng, 2012; Arhuoma, Dong, & Idem, 2009).

7.2 ARGUMENT FOR THE DEVELOPMENT OF ACP PROCESSES

In reviewing the literature, an argument for development of a new chemical flooding process emerges. Though alkaline flooding has shown potential over its decades of research, it has suffered from two looming problems. The first is lack of reliable mobility control: studies have repeatedly shown that even in a coreflood the emulsion is insufficient to provide good volumetric sweep. The second problem is the emulsions formed are challenging to interpret and harder to predict; unlike the microemulsions produced in surfactant based processes.

To address these two issues, low-cost cosolvents were added to the alkaline flooding process to significantly improve performance and robustness of design. Water-soluble polymer, specifically hydrolyzed polyacrylamide (HPAM), was added for mobility control; as demonstrated in earlier literature it is essential in high-performance design. Additionally, research at the University of Texas has shown the addition of cosolvent to a chemical formulation significantly improves the predictability, rheological properties and phase behavior of microemulsions. This new process, with alkali, cosolvent and polymer (ACP) constitutes a major breakthrough in chemical enhanced oil recovery; for suitable oils it promises to produce excellent volumetric and displacement sweep efficiency, at lower cost than surfactant-based processes. ACP technology also boasts less complexity, greater robustness and no issues with aqueous stability. The chemicals involved are ecologically benign: polymers, alcohols and salt, important in the highly-regulated industrial climate.

7.3 ACP-01 COREFLOOD

After crude S showed definite promise in ASP corefloods at 100°C, the decision was made to remove surfactant from the formulation entirely. The ACP corefloods

involving crude oil S comprise the first evaluation of the ACP process to recover truly heavy oils (API° <20). The objective in the flood design was to find practical limitations in oil viscosity and chemical concentrations. The flood design follows the best practices outlined in the ASP section above. The ACP-1 coreflood showed excellent performance and was a strong endorsement of the ACP technology in heavy oils, with over 90% tertiary oil recovery at reasonable pressure drop.

ACP-01 Phase Behavior

The crude oil S shows high activity and good phase behavior when alkali and cosolvent are added to the brine. A formulation with only 1% IBA-5EO in Na_2CO_3 showed promise in terms of coreflooding. It has an acceptable region of ultralow-IFT (though narrower than an equivalent ASP formulation), and a relatively flat activity profile, which is beneficial in salinity gradient design. Equally important is the fluidity of the microemulsion; the phase behavior at 100°C showed no viscous phases or gels. The activity map below shows the relationship between salinity and microemulsion class present. The dotted line represents the salinty gradient selected for the coreflood ACP-1.
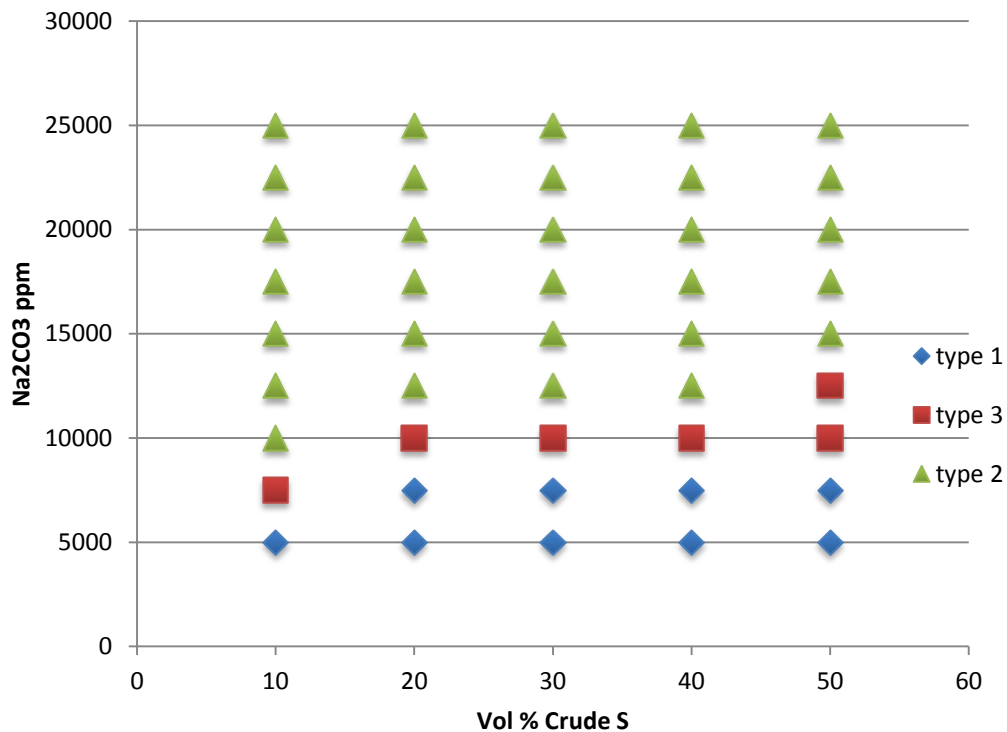
Figure 7.3.1: ACP-1 Activity Map

ACP-01 Core Properties

ACP-1 was another Berea Sandstone outcrop coreflood, run at 100°C. Like the previous ASP floods at this temperature, it was confined at 1000 PSI in a steel core holder, evacuated and saturated with 20,000 ppm NaCl connate brine. The pore volume was estimated from a tracer data, and single phase brine was pumped through the core to measure brine permeability. Filtered crude S displaced water at 1 ml/min, and final pressure drops were sufficiently high at ~85 psi/ft to ensure water was reduced to near-residual values. The core was then waterflooded with 20,000 ppm NaCl brine for several pore

volumes. Details of these processes can be found in the ASP section 6.2 – ASP-01 coreflood setup. Below are charts detailing the performance of the brine, oil and water-floods, as well as the essential core properties.

Table 7.3.1: ACP-1 Core Properties

Core ACP-1		
Outcrop	Berea	
Mass	1069	g
Porosity	0.205	
Length	11.44	in
Diameter	1.85	in
Area	2.63	in^2
Temp	100	C
Brine Perm	253	mD
PV	102	ml
S_{oi}	0.75	
S_{orw}	0.45	
K_{ro}	1.13	
K_{rw}	0.041	

Table 7.3.2: ACP-1 Flood data by section

Section	ΔP_{Brine} (psi)	k_{Brine} (mD)	k_{oil} (mD)	k_{ro}	k_{wf} (mD)	k_{rw}
1	0.23	211	276	1.31	10	0.049
2	0.24	280	297	1.06	11	0.041
3	0.20	337	360	1.07	12	0.036
4	0.23	276	299	1.08	10	0.037
whole core	0.99	268	304	1.13	11	0.040

ACP-1 Chemical Flood Design

Design of an ACP chemical slug follows the same requirements as an ASP slug. It needs to demonstrate adequate mobility control, a favorable salinity gradient, passing filtration ratio and aqueous stability. Figures 7.3.2 & 7.3.3 below show the salinity gradient

design and a total mobility curve. Chemical slugs were designed for mobility control to ensure stable displacement in the ACP flood; they were somewhat more viscous than the slugs in the ASP-2 flood. The excess mobility control contributed to higher pressure drop in the core during the ACP coreflood.
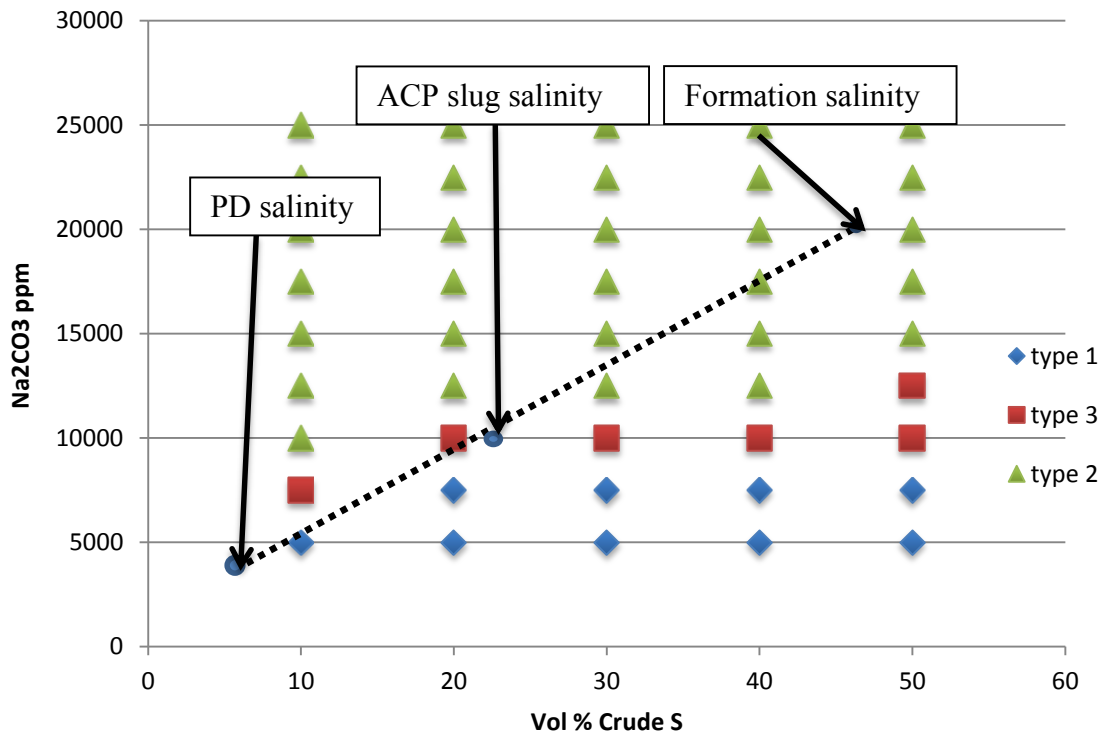
Figure 7.3.2: Salinity Gradient Design for ACP-1
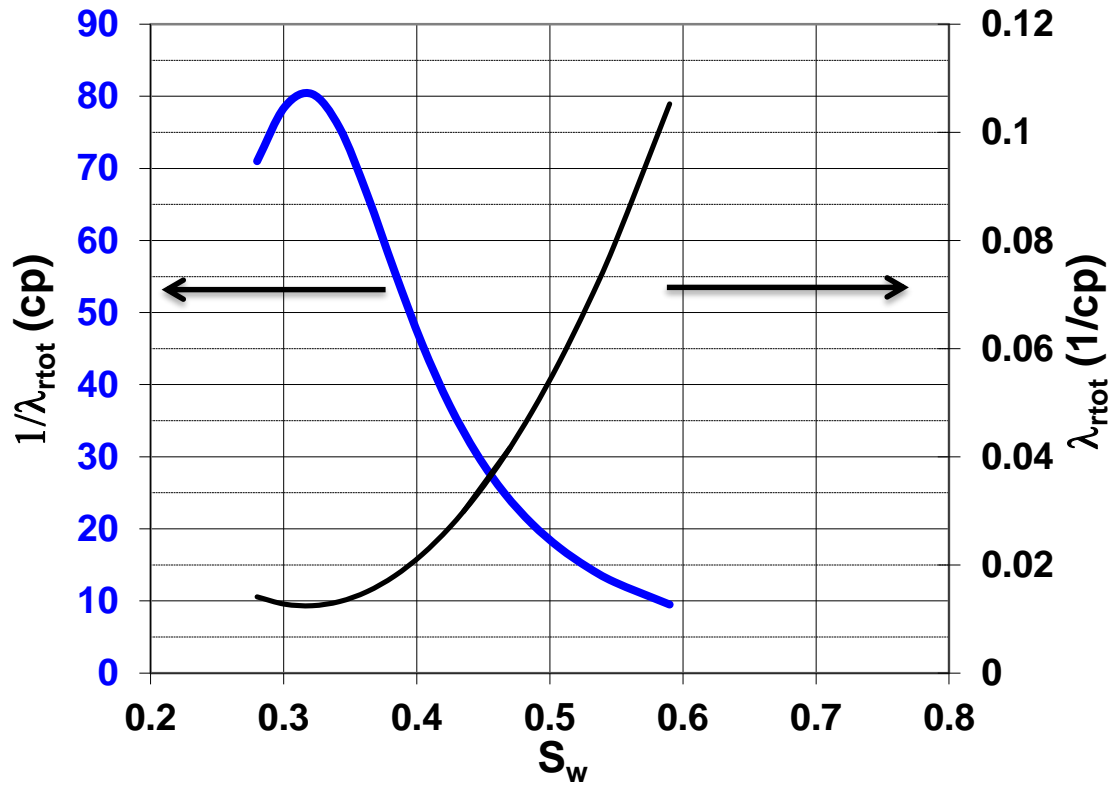
Figure 7.3.3: ACP-1Apparent viscosity and total relative mobility curves

The following chemical formulations were designed according to the principles above.

Table 7.3.3: ACP-01 chemical formulation

Slug Component	ACP Slug	Polymer Drive
PV injected	0.25	2
[HPAM 3630s] ppm	4,000	4,000
PV_{inj} *[Surf #1 + #2]	**0.0**	---
[Surf #1], wt.%	**None**	---
[Cosolvent], wt.%	1% IBA-5EO	---
ppm Na_2CO_3	**10,000**	**5,000**
TDS ppm	**10,000**	**5,000**
Frontal velocity ft/day	1.08	1.08
Viscosity at 10/s & 100°C, cP	**89**	**135**
Filtration Ratio F.R.	1.05	1.10
pH	10.5	10.6

These slugs were mixed for 4 hours, filtered and filtration ratio was measured. Afterwards, their viscosity was measured.
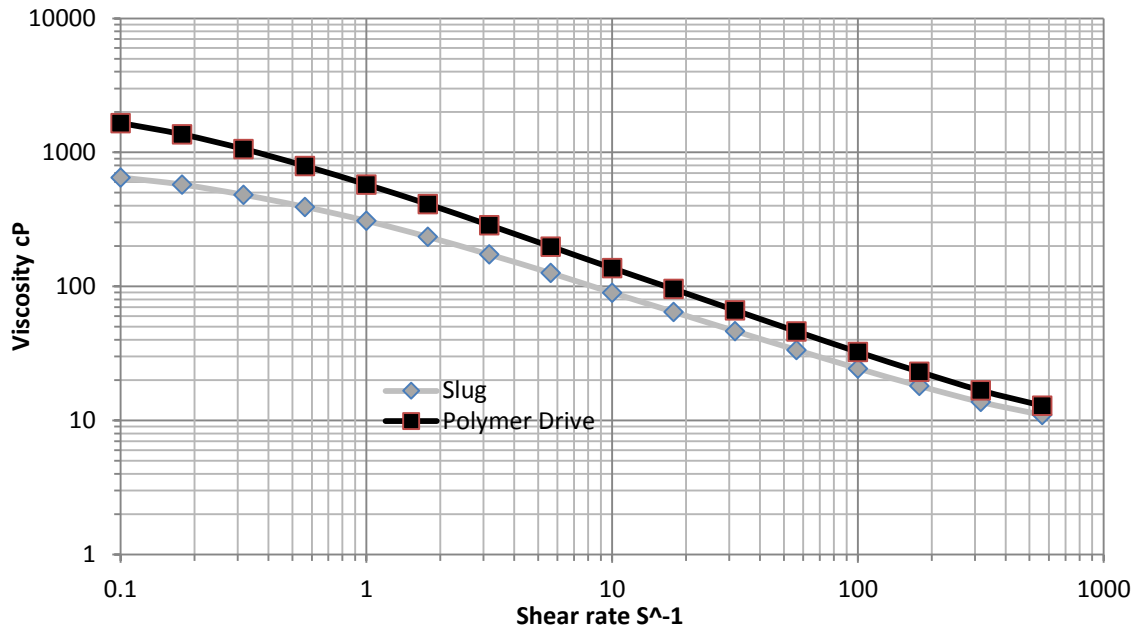
Figure 7.3.4: ACP-01 slug and drive rheological behavior

ACP-01 Results

The ACP-1 chemical flood was a clear success. The coreflood recovered 97.3% of the tertiary oil, and over 95% of this was produced at 0.95 PV. The oil bank broke through at 0.25 PV, as predicted by fractional flow theory. The oil bank was extremely consistent and clean, and microemulsion didn't break through until 0.90 PV, when almost all the oil had been recovered. Pressure drops reached a maximum of 21.5 PSI at the end of the flood due to the polymer drive. This Berea rock's low permeability means that this flood would likely see a sustainable field pressure drop of 1-4 PSI in high perm sand (1-5D) associated with heavy oil.
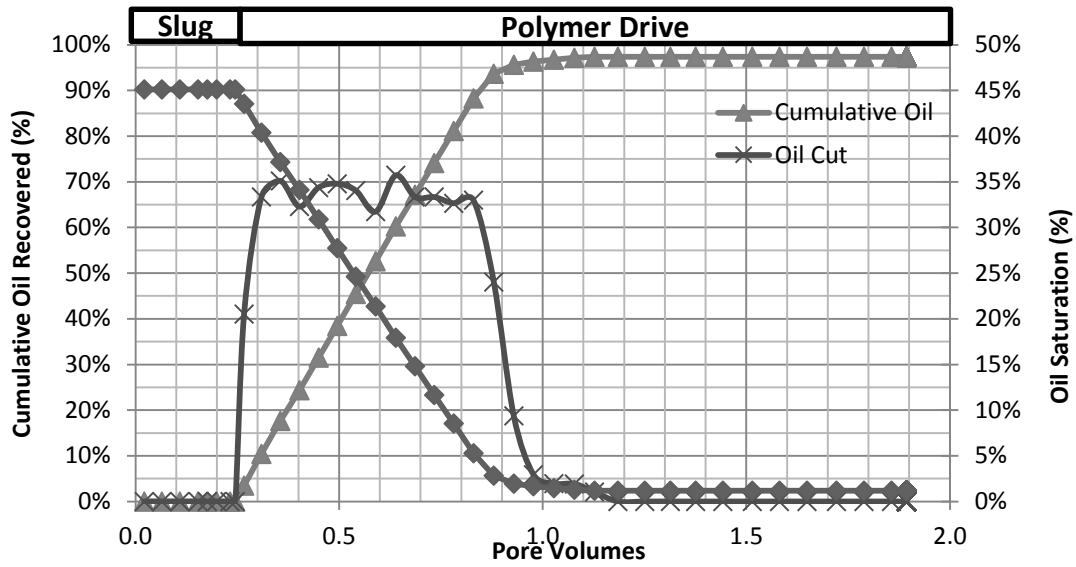
Figure 7.3.5: ACP-01 oil recovery
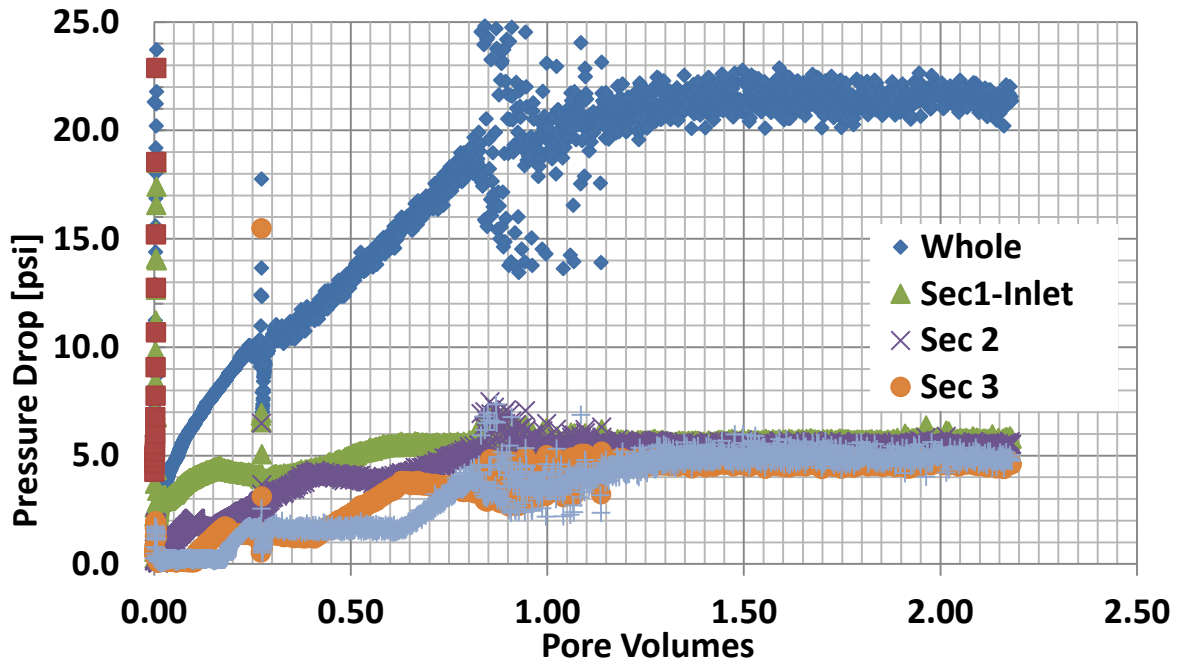
Figure 7.3.6: ACP-01 pressure drop data

73

The ACP-1 flood was clearly as successful as earlier ASP floods, demonstrating similar recovery, pressure drops and emulsion breakthroughs. This demonstrates the potential for ACP flooding in heavy oils when the reservoir is heated to reduce oil viscosity; The ACP process is cheaper, simpler and more robust than ASP designs.

ACP-01 Effluent analysis

Effluent analysis was done on the ACP-01 samples, and included salinity and pH. Curves for both measurements are below.
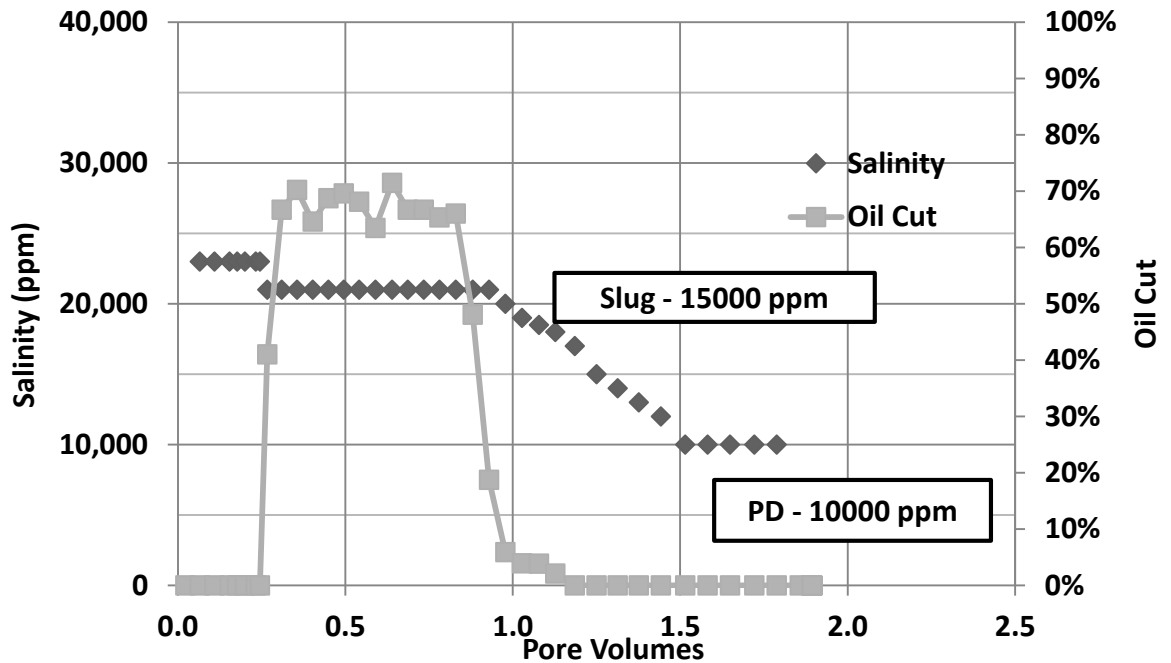
Figure 7.3.7: ACP-01 salinity propagation
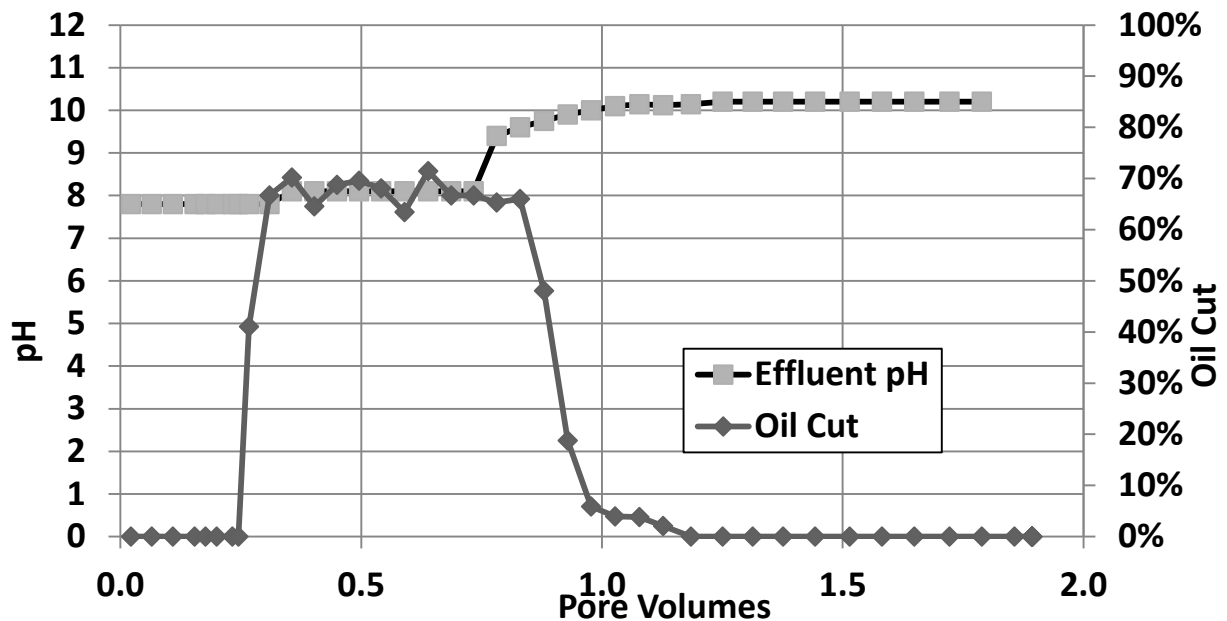
Figure 7.3.8: ACP-01 pH propagation

7.4 ACP-02 COREFLOOD

The success of displacing heavy oil at 100°C was encouraging for the ACP process. However, industry resistance to heating a reservoir is strong and understandable; even moderate heating could be a hard sell, although energy requirements are much more modest than for steam drive as the heat losses are much lower. This being the case, lowering the temperature of the experiments to find the limitations of the viscously-stable ACP flood was a primary objective of the study. A decrease in experimental temperature to 68°C was selected as the initial variable of interest in the ACP-02 coreflood.

The temperature change allowed for design changes in the coreflood. Higher permeability Bentheimer sandstone was selected as the core, despite issues with mineralogy, due to higher fluid viscosity. Epoxy-hardened cores were used in place of steel core-holders. Oil viscosity increased three fold, from 71 cP to 220 cP.

75

The ACP-02 coreflood was successful in recovering over 90% of tertiary recovery, but exhibited higher pressure drops than expected due to problems predicting shear rates in the core. This result clearly showed the practical viscosity limitation for viscously-stable ACP in heavy oils is above 220 cP, and below 68°C for the particular oil investigated. As polymer concentration was too high, the high pressure drop was somewhat welcome to researchers: it meant lower polymer concentrations can be used. Subsequent corefloods were designed with the more accurate shear rate information obtained from the coreflood.

ACP-02 Phase Behavior

The same formulation as ACP-01 was selected as the formulation of interest in ACP-02. The phase behavior plots didn't change appreciably with temperature from 100°C to 68°C; see the activity map in the ACP-01 phase behavior section.

ACP-02 Epoxy Core Procedure

As mentioned, a 1 foot long Bentheimer sandstone core was used in the ACP-02 flood. After cutting, the core was allowed to dry in an 85°C oven overnight; It was measured and weighed the next day. After measuring, it was fitted to 2" polycarbonate core end caps, which were fixed with 5-minute epoxy. The core itself was painted with 5-minute epoxy, to prevent the slow-setting epoxy from imbibing into the highly permeable rock. An acrylic shell was slipped around the core and held in place with silicone gel. The annular space between the core and the shell was filled with slow-setting Versamid 2-part epoxy and allowed to set up overnight. The next day communication to the core was established with five pressure taps, 2 on the end caps and 3 in the core face. Fittings were attached and the core was leak tested. Afterwards, it was evacuated like the cores in the stainless steel

core-holder, and was saturated with 20,000 ppm NaCl brine. A tracer test was done to confirm the porosity value calculated from the mass balance of saturating brine.

ACP-02 Core Properties

Like earlier corefloods, ACP-02 was initially brine-flooded to measure the brine permeability and to check the coreflood setup for issues. Oil was then forced into the core under high pressure to displace the wetting water phase; initial oil saturation was 82%. Unfiltered oil was used in the ACP-02 coreflood, as Bentheimer sandstone is permeable enough to prevent plugging. Waterflood was conducted at 68°C with 20,000 ppm NaCl brine containing 2,000 ppm sodium dithionite as a reducing agent. The particular lot of Bentheimer sandstone contains significant iron oxide, which can degrade polymer via the fenten-reaction mechanism (Levitt, Slaughter, Pope, & Jouenne, 2011). Maintaining a core ORP of <-500 mV and high pH ensures that the iron in the core will have very low solubility. The ORP of the injection fluids was -600 mV, but the core was never reduced to a value below -60 mV; this is probably because the dithionite solution is unstable at temperatures much above 60°C. To address this issue, the core temperature was lowered to 55°C, and 15 PV of dithionite brine was injected. The temperature was then raised to 68°C. The core ORP was approximately -120 mV, and the chemical slugs were injected. Tables 7.4.1 & 7.4.2 of essential core properties and flood performance are below.

Table 7.4.1: ACP-02 Core properties

Core ACP-2		
Outcrop	Bentheimer	
Mass	1150	g
Porosity	0.268	
Length	11.73	in
Diameter	1.85	in
Area	2.62	in^2
Temp	68	C
Brine Perm	2873	mD
PV	126	ml
S_{oi}	0.815	
S_{orw}	0.469	
k_{ro}	1.19	
k_{rw}	0.053	

Table 7.4.2: ACP-02 flood data by section

Section	ΔP_{Brine} (psi)	k_{Brine} (mD)	k_{oil} (mD)	k_{ro}	k_{wf} (mD)	k_{rw}
1	0.35	2690	2763	1.03	127	0.047
2	0.31	2930	3383	1.15	172	0.059
3	0.35	2690	3754	1.4	144	0.053
4	0.31	2949	3126	1.06	136	0.046
whole core	1.38	2670	3183	1.19	142	0.053

ACP-02 Coreflood Design

The most important difference in design of ACP-02 is the mobility requirement. The oil is now much more viscous than in previous floods, and is in higher permeability rock with lower shear rate.
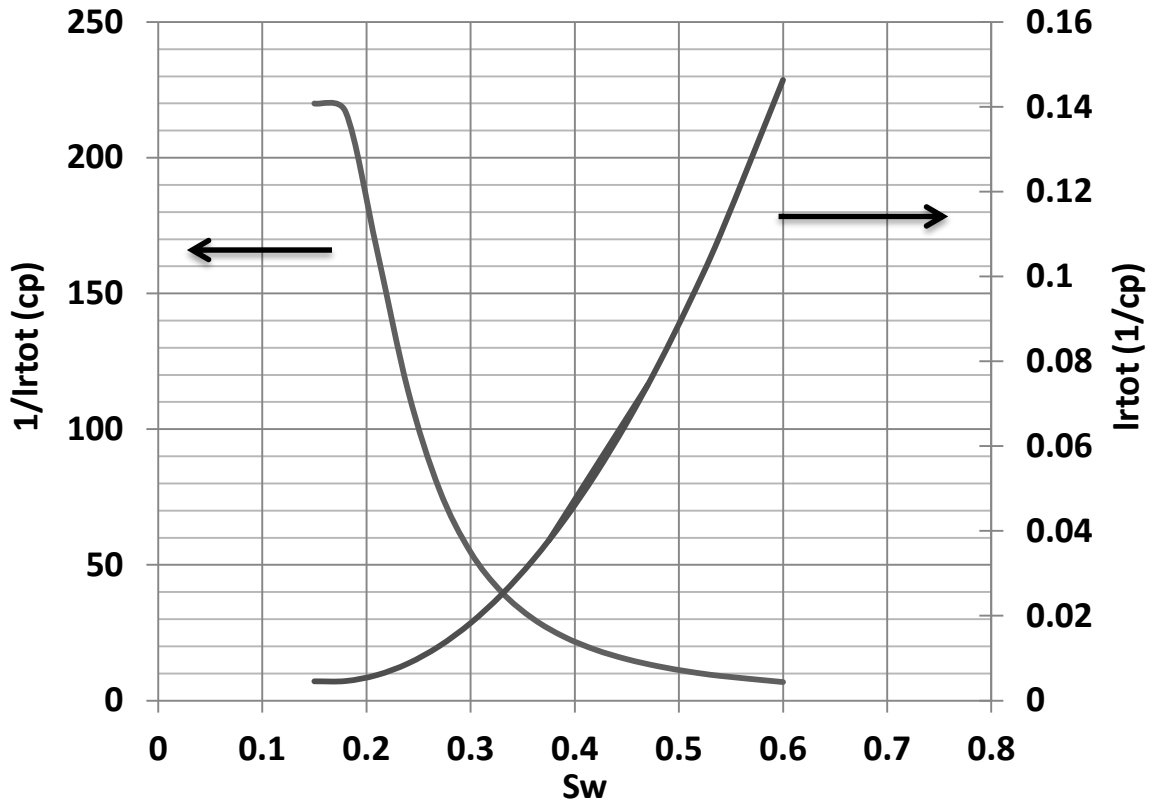
Figure 7.4.1: ACP-02 mobility control requirements

Based on the mobility requirements a viscosity of 250 cP for the slug and drive was determined to be sufficient at the estimated shear rate in the core, about 4 sec^{-1}. The following slugs were made based on the salinity gradient requirements and the mobility requirements.

Table 7.4.3: ACP-02 ACP slug and PD drive composition

Slug Component	ACP Slug	Polymer Drive
PV injected	0.25	2
[HPAM 3630s] ppm	6,000	6,000
[Cosolvent], wt.%	1% IBA-5EO	---
ppm Na_2CO_3	**10,000**	**5,000**
TDS ppm	**10,000**	**5,000**
Frontal velocity ft/day	1.08	1.08
Viscosity at 5.6/s & 68°C, cP	**205**	**291**
Filtration Ratio F.R.	1.01	1.04
pH	11.5	11.4
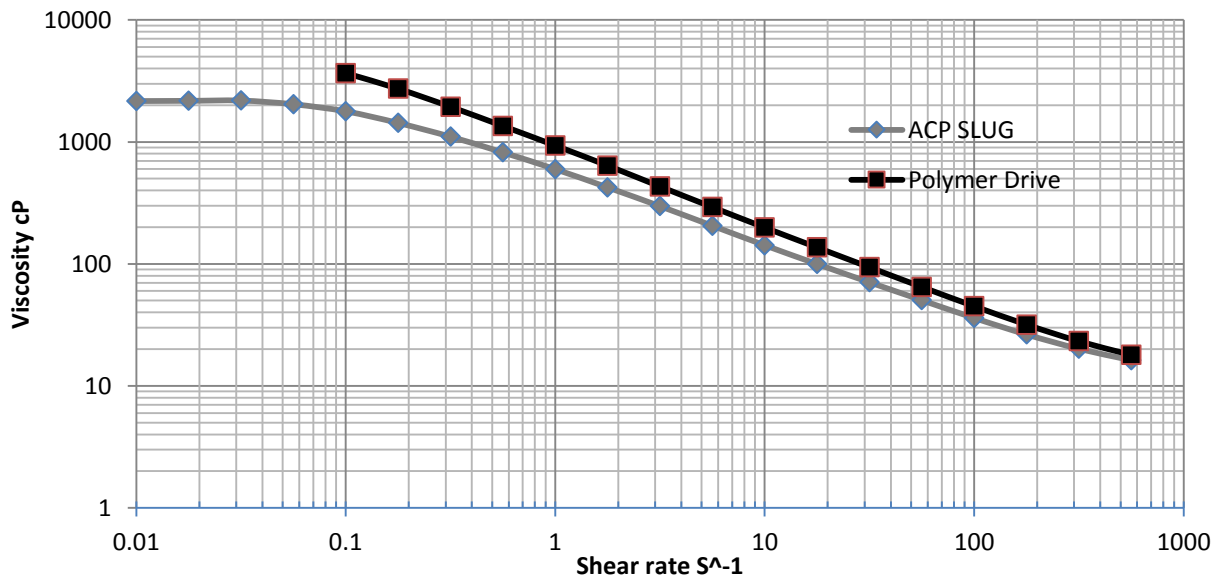
Figure 7.4.2: ACP-02 slug and drive viscosity

The high polymer concentration was based on an incorrect design assumption, that the shear rate in the core would be around 4-5 sec^{-1}. This was determined by the shear rate equation with the parameters in table 7.4.4:

Table 7.4.4: ACP-02 shear equation parameters

Frontal Advance Rate (ft/day)	**1.08**
Porosity (decimal)	**0.26**
Absolute Permeability (mD)	**2700**
End-Point Water Relative Permeability	**0.95**
Sorw (decimal)	**0.45**
n (power law exponent)	**0.45**
C (shear correction factor)	**3**

The final in-situ shear rate with these parameters is 5.6^{sec-1}, however the true correction factor was closer to 1.5, rather than 3, and the shear rate closer to 2.0 sec^{-1}. See section 7.5 for details.

ACP-02 Chemical Flood

The ACP-02 ACO flood was successful at recovering tertiary oil; within 1.2 PV 93.6% of oil was recovered, and 80% oil recovery was seen by the time emulsion broke through at 0.85 PV. Final oil saturation in the core is 2.92%.
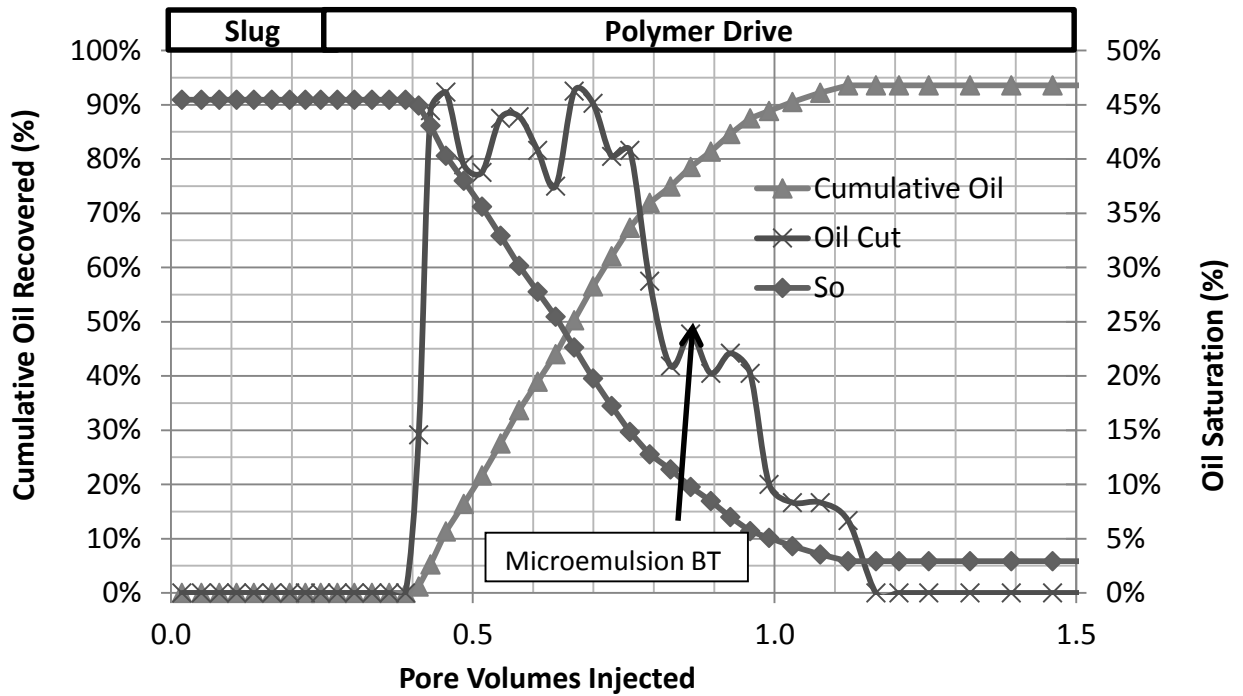
Figure 7.4.3: ACP-02 Oil Recovery

The more viscous oil resulted in a very high oil bank cut, ~85% oil, as expected from fractional-flow theory. The flood, despite its excess mobility control, took slightly more injection to produce oil than the Berea ASP and ACP sandstone floods at 100°C. Pressure drops for the flood follow in figure 7.4.4.
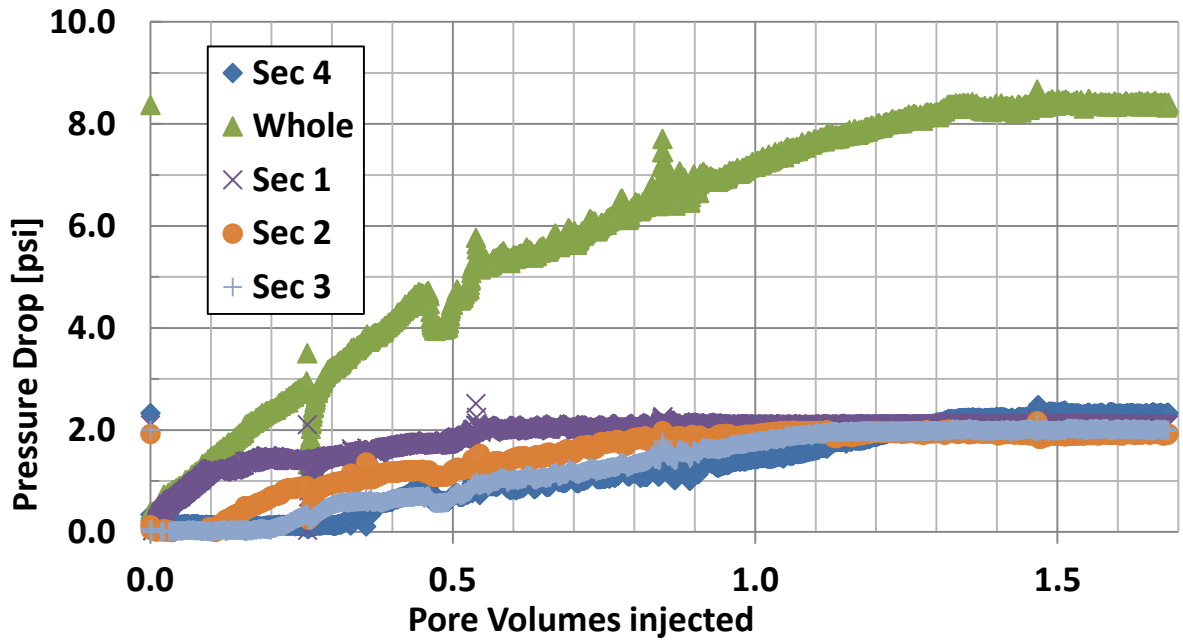
Figure 7.4.4: ACP-02 pressure drop data

The final pressure drop of 8.5 PSI/ft is unrealistically high for a field application of ACP technology, and was addressed in later ACP floods. The apparent viscosity in the core, assuming no permeability reduction, 8.5 psi pressure drop and 2700 mD permeability is ~650 cP, far higher than required as shown by the relative mobility curves above.

Table 7.4.5: ACP-02 Chemical flood relative permeability and permeability reduction factor

Section	ACP Flood Perm (mD)	dP (psi)	Perm reduction factor
1	2491	2.1	1.080
2	2612	2.0	1.122
3	2616	2.0	1.028
4	2245	2.2	1.314
overall	2578	8.3	1.074

ACP-02 Effluent Analysis

Recovery vs. pH follows.
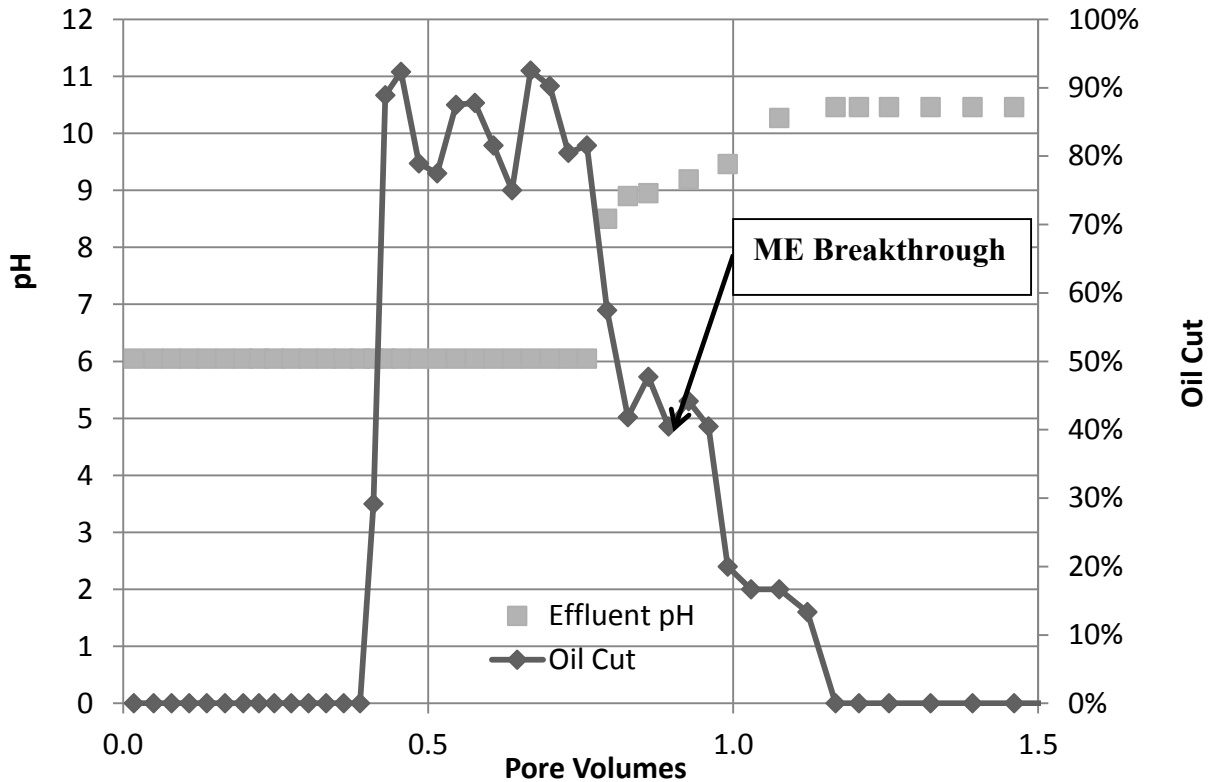
Figure 7.4.5: ACP-02 Coreflood oil recovery

ACP-02 Discussion

Pessimistic estimate of shear rate in the ACP-02 coreflood led to a design with an excess of polymer. Part of the logic behind the high polymer concentration was a fear that unreduced ferric (Fe^{3+}) iron would be present and could degrade the polymer, adversely impacting the mobility control. After effluent analysis showed no obvious degradation in the polymer, it was decided to learn more about the effect of mobility control on following experiment.

7.5 CALCULATING CORE SHEAR RATES

Shear rate is an important parameter in flood design, and estimating it properly depends on good understanding of the rock being used as well as experience. The equivalent shear rate was calculated using the equation:

$$\gamma_{eq} = \frac{4uC}{\sqrt{8\phi k k_{rw}S_w}}\left(\frac{3n+1}{4n}\right)^{\frac{n}{n-1}}$$

Where γ_{eq} is the equivalent shear rate(1/s), u is q/A in (cm/s), ϕ is the porosity, k is the brine permeability (cm^2), k_{rw} is the relative permeability to water, S_w is the water saturation in the core, and n is the polymer power-law exponent. When using the equation, unit consistency is important; all lengths should be in cm and time in seconds. The C parameter is the shear correction factor in the equation. The assumption for the coreflood design was a C-factor of 2.5-3, leading to an in-situ final shear rate of about 5.5 sec^{-1}; if this shear rate were in-situ, the polymer viscosity in the designed slugs would have been appropriate. The shear rate was overestimated, however, due to the C factor estimate being too high. A better value for C is about 1.3 in the Bentheimer cores, the determination of which is defined below.

To determine the value of C, it was necessary to measure the rheology of a polymer solution both in a rheometer and in a rock core at several shear rates. First the bulk rheometer data for the polymer drive in an ACP flood were plotted.
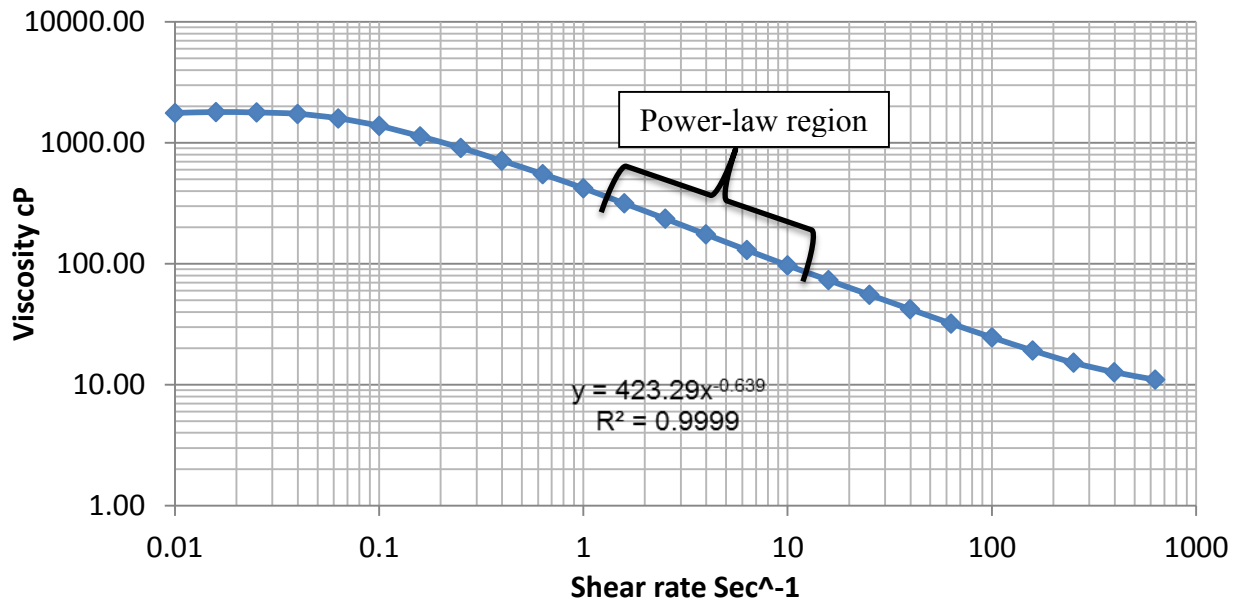
Figure 7.5.1: ACP-04 bulk polymer drive rheology

From the bulk rheometer data, the power law relationship from the power-law region, shown above ($y = K_c x^b$, here $y = 423.29x^{-0.639}$) was calculated. The exponent, n, is $1-b$, while K_c is the bulk viscosity at 1sec^{-1}, assuming the power-law relationship held at 1 sec^{-1}. This isn't always true, and oftentimes extrapolation is needed, though in the above figure 7.5.1, 1 sec^{-1} is still within the power law region.

After completion of a coreflood with ~100% recovery (ACP-04), the polymer solution was pumped through the core at different rates to obtain a more accurate C factor for Bentheimer sandstone. From the pressure drops recorded, and the flow rate, an apparent viscosity was calculated via Darcy's law.

Table 7.5.1: ACP-04 raw data from polymer flood

Frontal Advance (ft/day)	Flow rate (ml/min)	dP (PSI)	Flux (cm/sec)	Apparent shear rate (sec^{-1})	Apparent Visc (cP)
1.04	0.100	4.50	8.761E-05	1.234	330.054
2.59	0.250	6.64	2.182E-04	3.072	194.805
5.19	0.500	9.40	4.372E-04	6.157	137.889
10.37	1.000	14.50	8.736E-04	12.301	106.351

The apparent shear rate is calculated from an uncorrected shear rate equation, i.e. where the C-factor C=1.

$$7.5.1 \quad \gamma_{eq} = \frac{4u}{\sqrt{8\phi k k_{rw} S_w}} \left(\frac{3n+1}{4n}\right)^{\frac{n}{n-1}}$$

The apparent viscosity was plotted vs. apparent shear rate, and determined if it was power-law or not. The below data are appropriately shear-thinning.
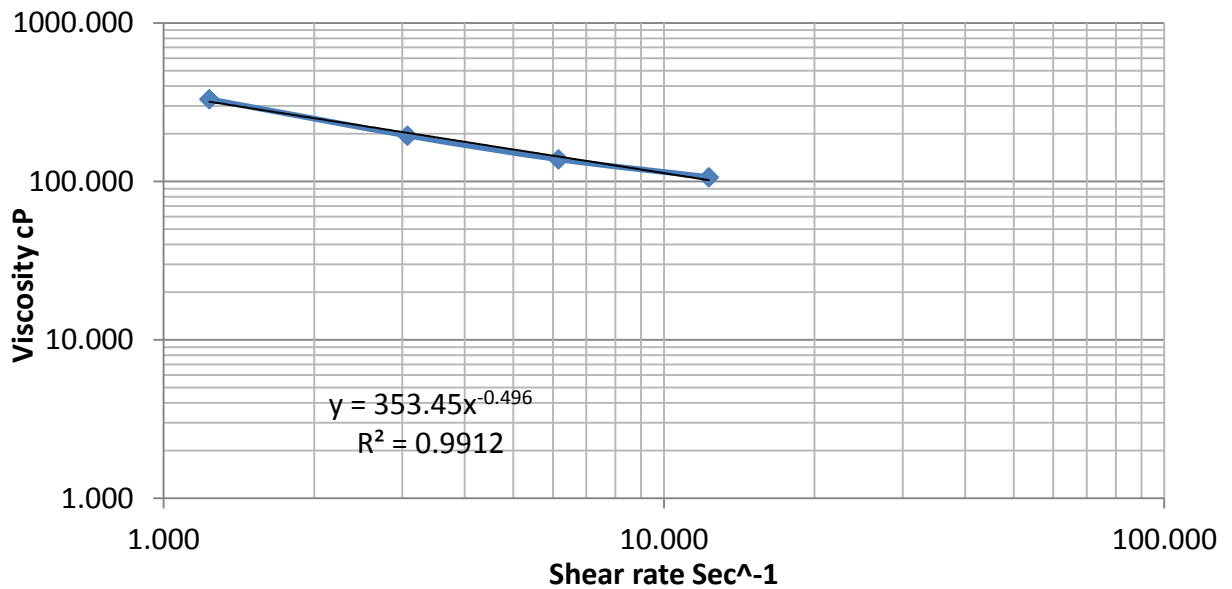
Figure 7.5.2: ACP-04 apparent shear rate vs. apparent viscosity, during ACP-04 polymer drive flood

The points in the power-law regime were plotted on a log-log graph. The parameters for the coreflood apparent viscosity vs. shear rate were recorded, again where $y = K_v x^b$. The parameter $K*$ was then be determined by:

7.5.2 $$K* = \frac{K_{core}}{K_{Viscometer}}$$

$K*$ will always be < 1, as the polymer's viscosity will always be higher in a rheometer than a core at an *apparent* shear rate in the core. Once the K* parameter was obtained, it was transformed to the C-factor via:

7.5.3 $$C = [K*]^{\frac{1}{n-1}}$$

Once the C-factor was calculated, the earlier-obtained data was corrected for shear rate in the equivalent shear-rate column. The C factor for this Bentheimer flood was C = 1.67

Table 7.5.2: ACP-04 core viscosity data with corrected, equivalent shear rate

Frontal Advance (ft/day)	Flow rate (ml/min)	dP (PSI)	Flux (cm/sec)	Apparent shear rate (sec^{-1})	Apparent Visc (cP)	Equivalent Shear Rate (sec^{-1})
1.04	0.100	4.50	8.761E-05	1.234	330.054	2.061
2.59	0.250	6.64	2.182E-04	3.072	194.805	5.134
5.19	0.500	9.40	4.372E-04	6.157	137.889	10.288
10.37	1.000	14.50	8.736E-04	12.301	106.351	20.555

Once the true C factor was accounted for, the core viscosity data and the rheometer viscosity data collapsed as expected.
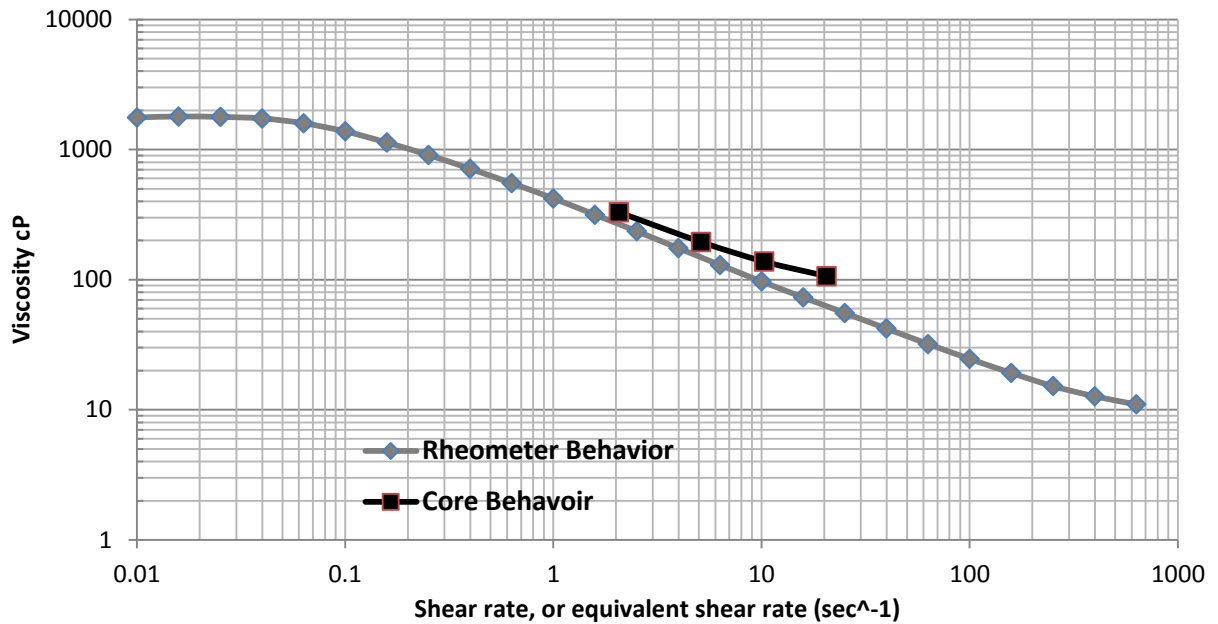
Figure 7.5.3: ACP-04 Polymer viscosity in rheometer and in core, demonstrating power
of correct C-factor

The core data show excellent agreement with the bulk rheometer at low shear rates. Higher shear rates show increasing apparent viscosity, a phenomenon understood to involve polymer shear-thickening (Delshad et. al., 2008. Obtaining a correct C-factor was a helpful in designing later corefloods, as apparent polymer viscosity could be better estimated.

7.6 ACP-03 COREFLOOD

The ACP-03 coreflood was identical in design to ACP-02, except in terms of polymer concentration. The impact on tertiary oil recovery of reducing polymer viscosity was expected to be negative, but reducing the concentration of polymer from an unrealistic 6000 ppm was an optimization priority.

ACP-03 was largely successful in oil recovery terms; it produced 80.3% of tertiary oil within 1.2 PV of injection. Though significantly lower than the preceding ACP-02 flood, which recovered 93.6% of tertiary oil, the significant decrease in polymer concentration probably explains this lower recovery factor. The flood was quite successful in reducing pressure drop, and demonstrated concretely the impact of polymer concentration on ACP pressure drop in the viscously stable regime (as opposed to microemulsion viscosity, which can dominate in corefloods with less viscous oils).

ACP-03 Phase Behavior

Phase behavior in ACP-03 was unchanged from earlier floods. See ACP-01 phase behavior.

ACP-03 Core Properties

The core setup in ACP-03 was Bentheimer sandstone in an epoxy core, as in ACP-02. It was handled as in the ACP-02 coreflood, as the temperature, oil viscosity and chemical formulation were also the same as ACP-02. A tracer curve was generated to calculate the pore volume of the core, afterwards the core was flooded with reduced resident brine (1000 ppm dithionite; -650 mV) to calculate single phase permeability to brine. The temperature was raised to 86°C and the core was allowed to come to equilibrium overnight. The core was then oil flooded with surrogate crude S at 30 ft/day the next day to establish an initial oil saturation of 0.86. Resident brine was flooded through the core at

10ft/day until pressure drops were steady and oil cut low; S_{orw} was calculated to be 0.484. Waterflood brine was pumped into the 68°C oven from a vessel outside, which allowed the reduced brine to remain stable for a longer period. The brine was pumped through 2m of coiled overhead tubing to ensure it was heated to near-core temperature before injecting. ORP of the effluent brine after several pore volumes was < -60 mV, as in ACP-02. After establishing remaining-oil conditions, chemicals were injected. See tables 7.6.1 & 7.6.2.

Table 7.6.1: ACP-03 Core properties

Core ACP-3		
Outcrop	Bentheimer	
Mass	1068.9	g
Porosity	0.268	
Length	11.73	in
Diameter	1.85	in
Area	2.62	in^2
Temp	68	C
Brine Perm	2675	mD
PV	126	ml
S_{oi}	0.860	
S_{orw}	0.469	
k_{ro}	1.19	
k_{rw}	0.053	

Table 7.6.2: ACP-03 flood data by section

Section	ΔP_{Brine} (psi)	k_{Brine} (mD)	k_{oil} (mD)	k_{ro}	k_{wf} (mD)	k_{rw}
1	0.36	2450	2573	1.050	107	0.044
2	0.33	2669	3150	1.180	146	0.055
3	0.36	2450	3495	1.427	122	0.05
4	0.35	2379	2911	1.223	115	0.048
Whole	1.38	2675	3005	1.123	120	0.045

ACP-03 Coreflood Design

After the success in the ACP-02 coreflood, the decision to reduce chemical use was a logical step. Though 6000 ppm polymer ACP slug and drive showed good performance in terms of recovery, the high viscosity led to excess mobility control in the flood and pressure drops which would be unsustainable in the field environment (~8.3 psi/ft). A final polymer concentration of 3000 ppm was chosen, as it significantly decreased polymer without strongly impacting the stable displacement seen in ACP-02. Mobility requirements, slug compositions and viscosity are shown below in Figure 7.6.1.
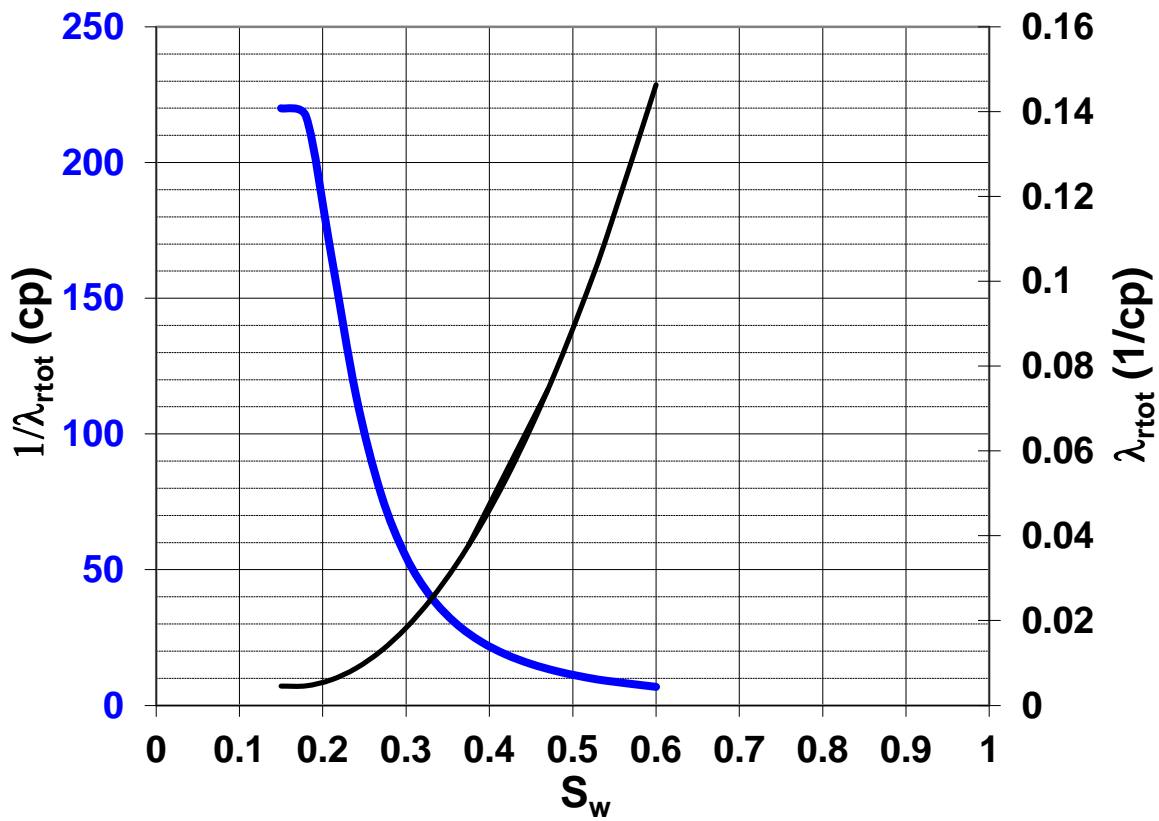
Figure 7.6.1: ACP-03 mobility control requirements

For a viscously-stable displacement to occur, the inverse of total mobility of the chemical slugs needs to exceed 225 cP. The more accurate information about shear rate in the core, predicted from earlier Bentheimer floods, allowed for more accurate prediction of the polymer viscosity in-situ. The following slugs in table 7.6.3 were made based on the salinity gradient requirements and the mobility requirements.

Table 7.6.3: ACP-03 ACP slug and PD drive composition

Slug Component	ACP Slug	Polymer Drive
PV injected	0.25	2
[HPAM 3630s] ppm	**3,000**	**3,000**
[Cosolvent], wt.%	1% IBA-5EO	---
Na$_2$CO$_3$ ppm	10,000	5,000
TDS ppm	10,000	5,000
Frontal velocity ft/day	1.08	1.08
Viscosity at 5.6/s & 68°C, cP	**98**	**140**
Viscosity at 1.77/s & 68°C, cP	**185**	**289**
Filtration Ratio F.R.	1.01	1.04
pH	11.5	11.4
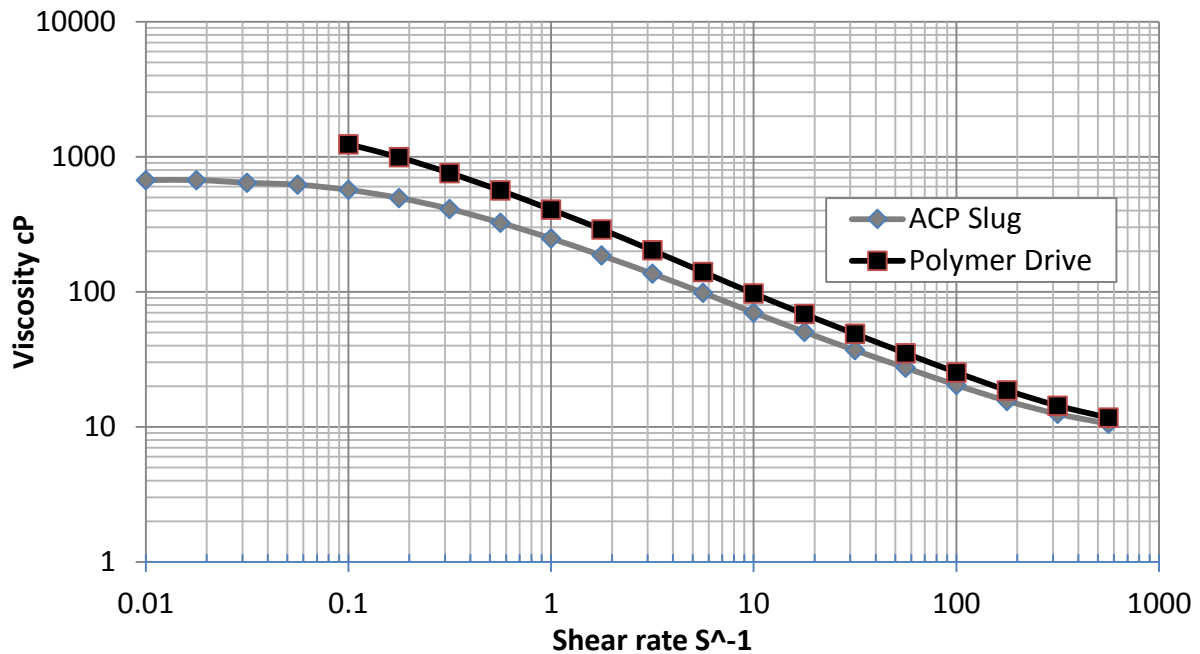
Figure 7.6.2: ACP-03 slug and drive viscosity

The viscosity curves in Figure 7.6.2 show that the ACP slug will be slightly viscously unstable (if the core final shear rate was approximately 1.8-2 sec^{-1} as predicted by the revised Canella C-factor), while the PD will be viscously stable. This prediction was validated in the results of ACP-03.

Results ACP-03

The ACP-03 coreflood oil recovery plots are below. They show evidence of viscous instability in the ever decreasing oil cut after oil breakthrough, unlike the long, steady plateau in the earlier tests. Tertiary oil recovery was lower (80.5%) than earlier floods, and took slightly longer to achieve (~1.2 PV). The tail-off was relatively short, implying that the flood was close to viscous-stability, and was well swept by the more viscous polymer drive. Microemulsion breakthrough was significantly earlier in ACP-03 (0.63 PV) than

ACP-02 (0.86 PV), further evidence of viscous fingering present in the core. Residual oil saturation was 9.52%. See Figure 7.6.3
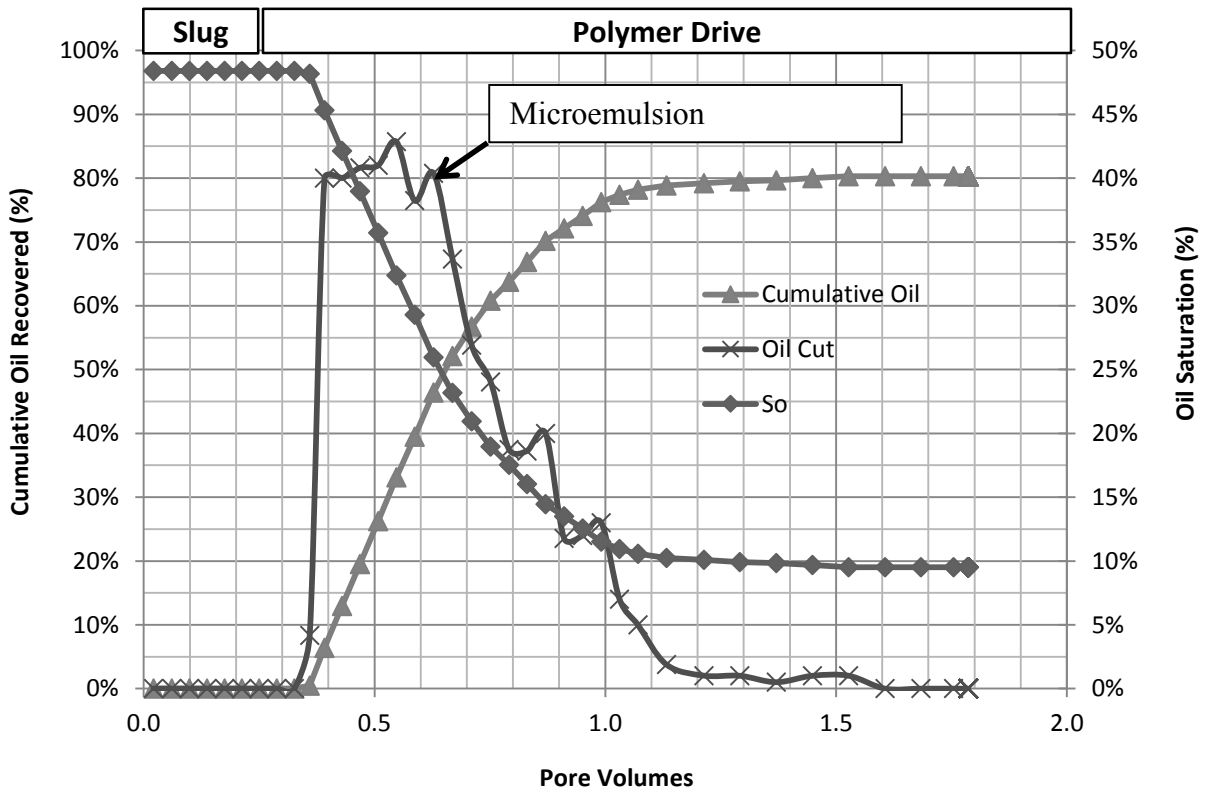
Figure 7.6.3: ACP-03 oil recovery

An overlay of the ACP-02 oil recovery vs. the ACP-03 curve is instructive (Figure 7.6.4). It shows the relative positions of the emulsion break-through and oil bank, and demonstrates the effect of mobility control on recovery; with lower mobility (high displacing viscosity) we see higher oil banks for longer periods, resulting in higher recovery factors, at the expense of high pressure drop and chemical concentration.
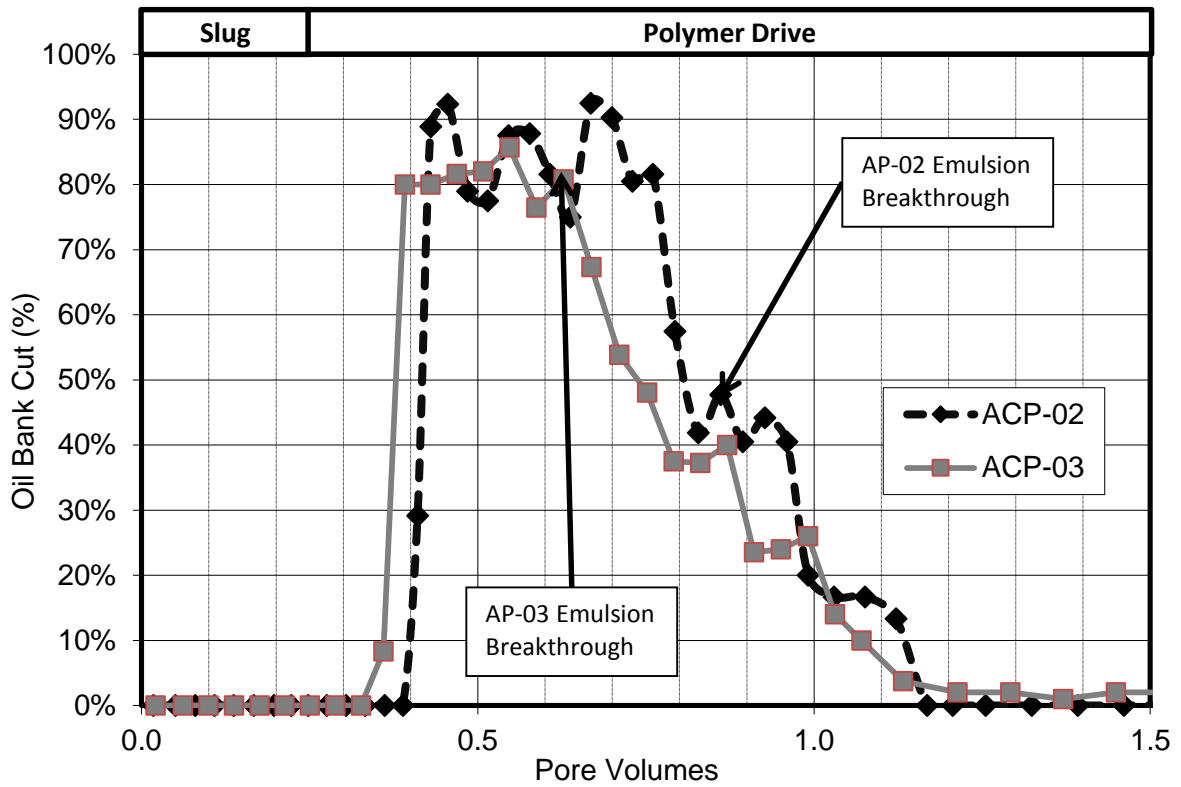
Figure 7.6.4: Overlay of ACP-02 and 03 corefloods

Pressure drop in the core was moderate at ~3.5 PSI/ft at steady state; this value may be sufficiently low to implement in field tests (Figure 7.6.5). The pressure curves show a slight spike in each section, representing the viscous oil bank, followed by the less viscous ACP slug. The more viscous polymer drive then displaces the ACP slug and oil bank, and pressure drop increases as a consequence.
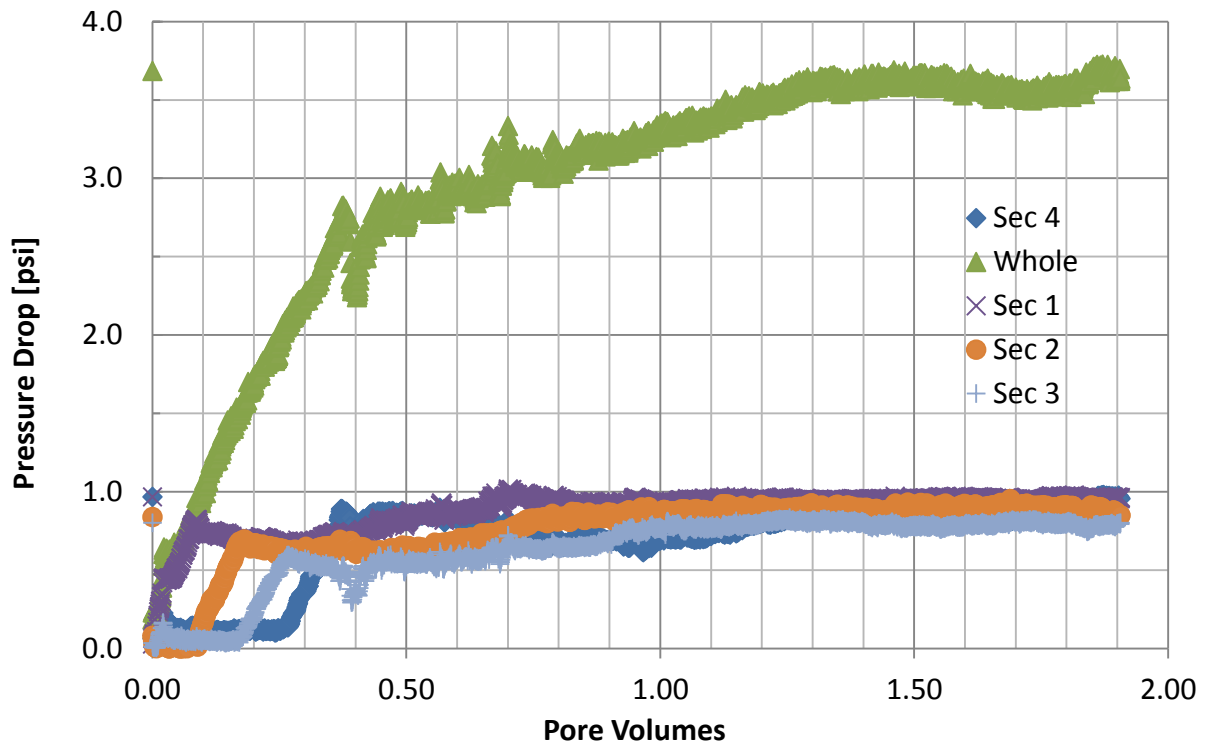
Figure 7.6.5: ACP-03 pressure drop data

A final shear rate of 2.37 sec^{-1} was obtained from using a C-factor = 2. This corresponds to a polymer drive viscosity in the core at endpoint of 226 cP. Slight permeability reduction was experienced. Polymer was not degraded by the core, despite the potential presence of unreduced iron compounds.

Effluent Analysis

Salinity and pH were measured in the ACP-03 effluent. Both showed early breakthrough characteristic of the viscous instability. This is likely a combination of difficulty in reading the dark emulsion with a refractometer; the antagonistic effects of

lower salinity with the salinity gradient, while increasing dissolved oil in the microemulsion contribute to this difficulty.
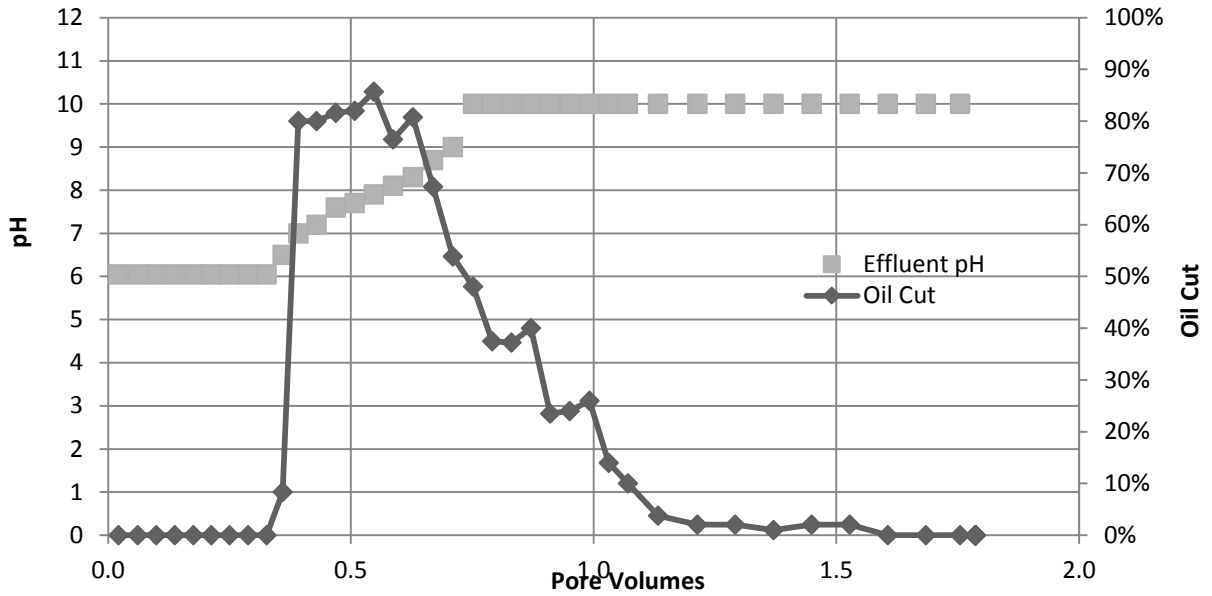
Figure 7.6.6: ACP-03 pH with injected volume. Propagation with oil bank is very tight.
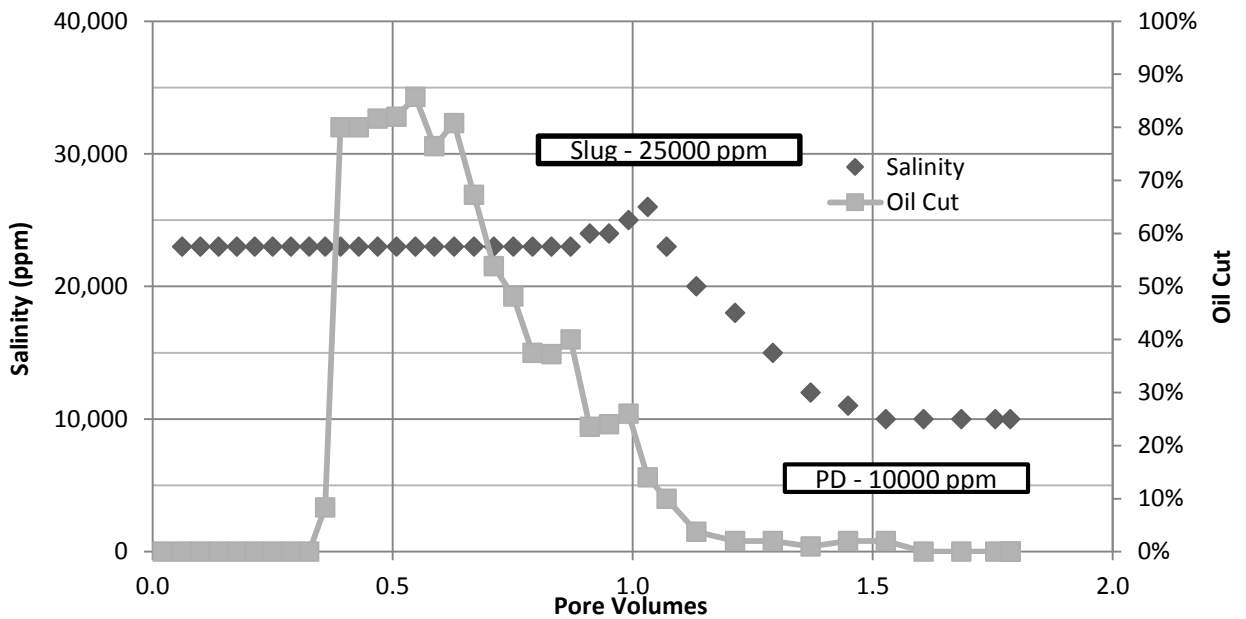
Figure 7.6.7: ACP-03 salinity propagation in core shows slight retardation.

98

7.7 ACP-04 Coreflood

ACP corefloods 1-3 proved quite successful at removing oil from high permeability Bentheimer sandstone. They demonstrated the successful implementation of applying robust design from ASP technology in ACP flooding, showed the impact of mobility control and temperature on pressure drop and oil recovery, and improved understanding of shear rate in the cores of interest. The floods, however, still required significant increase in reservoir temperature to be successfully implemented; even achieving 68°C is a tall order when reservoir temperature is 20-25°C. In order to hopefully minimize cost and demonstrate limitations of the new process, a flood was designed for 50°C environment. This corresponds to an oil viscosity of 970 cP, which researchers assumed would be outside the acceptable operating envelopes for the flood.

Good design practices developed at UT, however, allowed researchers to fulfill necessary requirements for a practical application of the technology. The ACP-04 flood showed high tertiary oil recovery (>95%) at reasonable pressure drop (4.4 PSI/ft), with moderate chemical concentration (<4100 ppm HPAM). That the phase behavior and salinity gradient remain virtually unchanged from 100°C to 50°C speaks volumes to the robustness of the process: in a heating scheme where temperature varies significantly in a reservoir, ACP shows special promise in the system investigated.

ACP-04 Phase Behavior

The phase behavior of the ACP-1 (1% IBA-5EO in Na_2CO_3) formulation for crude S changes very little with temperature from 100°C to 50°C; Optimum salinity remains the same at 10% oil, and increases only slightly (0.25% or less) in the 30 and 50% oil scans. The area of ultralow IFT seems to expand slightly, with good properties in the type 1 region (Figure 7.7.1).
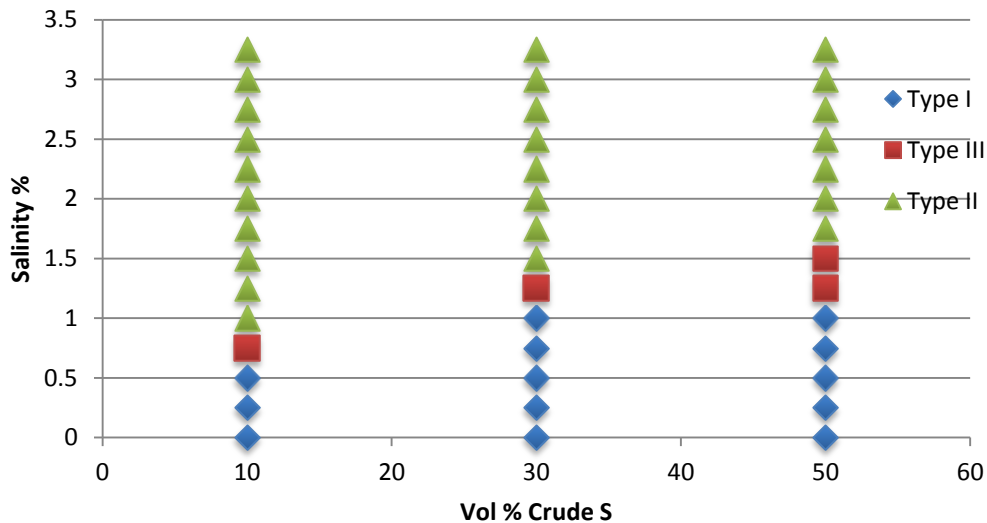
Figure 7.7.1: ACP-04 activity diagram

It was determined from the phase behavior chart above that the same salinity gradient can be implemented at 50°C as at 100°C and 68°C.

ACP-04 Core Properties

The ACP-04 core was Bentheimer sandstone in an epoxy mold, as in ACP-02 and 03. After calculating the pore volume in the core, a brine flood was performed to calculate the single phase permeability. Brine composition was 20,000 ppm NaCl with 1,000 ppm sodium dithionite to maintain reduction. Sodium bicarbonate wasn't present, so the core's reduced state was lost after some time. Core setup was largely the same as in earlier floods, with the exception of dithionite brine handling methods; as it is stable at 50°C, the dithionite brine was kept in the oven at all times and showed no signs of degradation. Crude oil S (970 cP) was injected at a constant pressure of 100 psi; oil relative permeability was

very high, calculated to be 1.3. This high oil relative permeability was an important factor in the successful implementation of the flood; it lowered pressure drop and required chemical concentration of polymer. Initial oil saturation was calculated to be 87.5%, the highest of any flood to this point, probably due to the high viscosity of the oil.

After the core was saturated with oil, waterflood commenced. Waterflood brine was 15,000 ppm NaCl, with 4,000 ppm Na_2CO_3 and 1,000 ppm $Na_2S_2O_4$ (dithionite) present as a buffer and reducing agent, respectively. ORP of the injection brine was <-600 mV, and pH was balanced to 7.6. Oil saturation was reduced to 0.59 after 2.5 PV of throughput. ACP slug and polymer drive were injected at 0.5 ft/day (unlike earlier floods at 1.0 ft/day); the decreased rate lowered pressure drop and decreased chemical requirements. Core properties are in Figs 7.7.1 & 7.7.2.

Table 7.7.1: Core properties ACP-04

Core ACP-04		
Outcrop	Bentheimer	
Mass	1139.6	g
Porosity	0.231	
Length	11.65	in
Diameter	1.94	in
Area	2.90	in^2
Temp	50	°C
Brine Perm	2505	mD
PV	130	ml
S_{oi}	0.875	
S_{orw}	0.59	
k_{ro}	1.33	
k_{rw}	0.024	

Table 7.7.2: ACP-04 flood parameters

Section	ΔP_{Brine} (psi)	k_{Brine} (mD)	k_{oil} (mD)	k_{ro}	k_{wf} (mD)	k_{rw}
1	0.85	2071	2572	1.24	88	0.043
2	0.6	2930	3959	1.35	64	0.022
3	0.7	2515	3954	1.57	54	0.022
4	0.62	2839	3559	1.25	48	0.017
Whole	2.77	2505	3361	1.33	60	0.024

The high oil relative permeability is an effect of increased oil viscosity (Downie & Crane, 1961). Lower k_{rw} is also seen than in prior floods; this is due to the much higher oil viscosity and concomitant decrease in sweep efficiency. To reduce this core to true S_{orw} would require much more throughput than was practical in the time constrained coreflood environment, a principle much more impactful in a reservoir.

ACP-04 Coreflood Design

Design of the 50°C ACP flood required a challenging balance of parameters; for the flood to be considered successful, pressure drop needed to be below 5 psi/ft, chemical concentration below 4500 ppm polymer, tertiary recovery over 80% oil in 1.25 PV or less and frontal advance rate of at least 0.50 ft/day. These criterion were met, but barely, and the flood result represents a near-practical limitation for stable ACP displacements of heavy oil in rocks like Bentheimer sandstone. The chemical slugs designed for the flood are described below in Table 7.7.3:

Table 7.7.3: ACP-04 Slug and drive composition

Slug Component	ACP Slug	Polymer Drive
PV injected	0.25	2
[HPAM 3630s] Ppm	**4,100**	**3,700**
[Cosolvent], wt.%	1% IBA-5EO	---
Na_2CO_3 ppm	**9,000**	5,000
Isoascorbic Acid	1,000	1,000
TDS ppm	10,000	5,000
Frontal velocity ft/day	**0.48**	**0.48**
Viscosity at 1.0/s & 68°C, cP	**673**	**663**
Filtration Ratio F.R.	1.07	1.01
pH	10.85	10.80

The salinity gradient design for the flood was essentially unchanged from earlier experiments. The low salinity in the ACP slug allowed for low polymer concentrations to be used, despite the fact the polymer was injected just below optimum salinity.
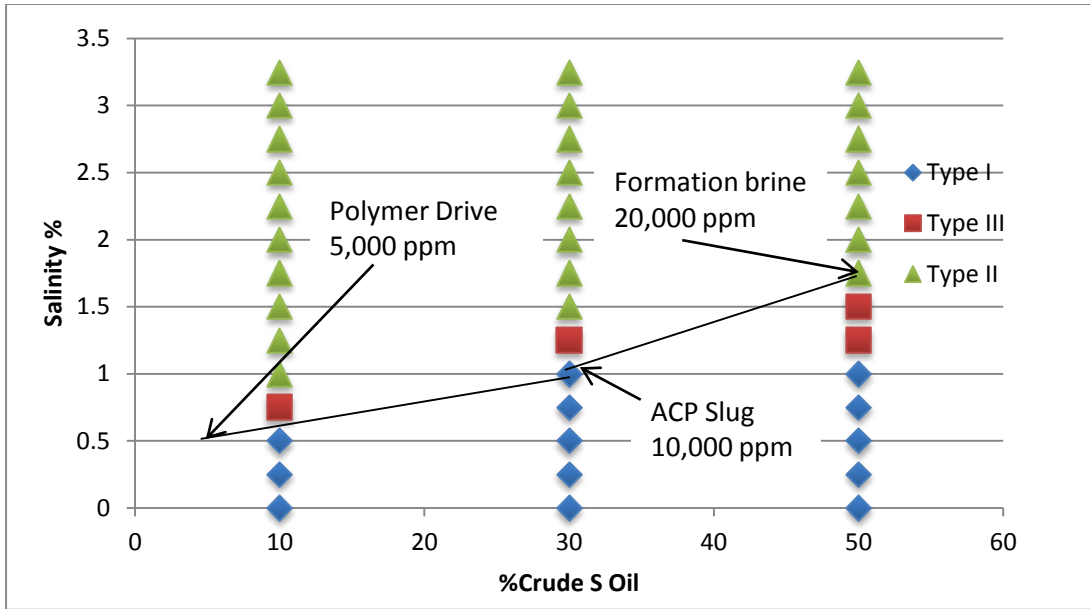
Figure 7.7.2: ACP-04 Salinity gradient design, 1% IBA-5EO @ 50C

Mobility curves show the total dominance of oil viscosity over relative permeability of water in the oil bank; the lowest mobility exists at the highest oil bank cut. Note the maximum mobility requirement (770 cP inverse) is substantially below the oil viscosity of 970 cP; this is a function of the high oil relative permeability of 1.3. Without this effect, pressure drop would have increased by about 25% in a stable flood, and chemical concentrations would need to be higher.
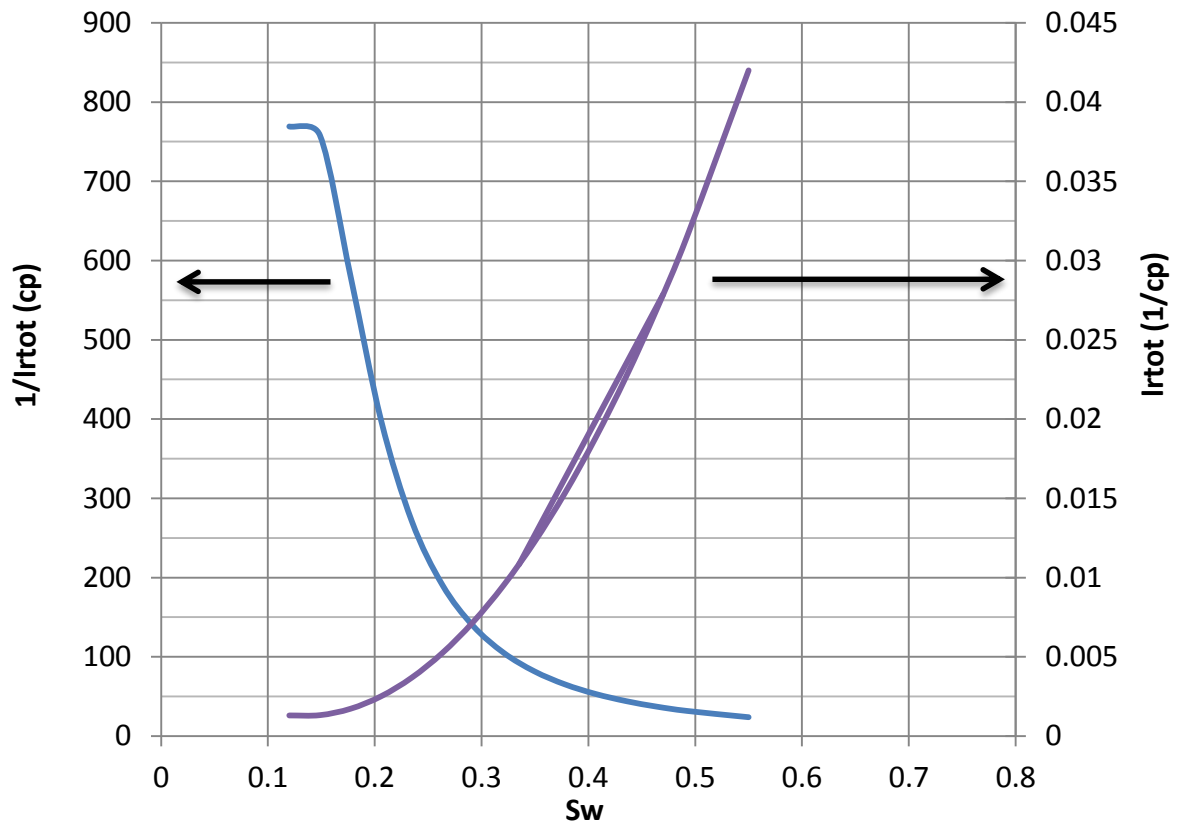
Figure 7.7.3: ACP-04 Mobility curves

Table 7.7.4: ACP-04 Mobility parameters

k_{rw}°	0.021	
k_{ro}°	1.3	
n_w	2	
n_o	2	
S_{wr}	0.12	
S_{or}	0.45	
$\mu_w =$	0.5	cP
$\mu_o =$	1000	cP

To overcome such challenging mobility requirements, the flood velocity was reduced to 0.5 ft/day, to take advantage of the extreme shear-thinning behavior of 3630s HPAM polymer. Curves for the design viscosity are below (Figure 7.7.3). Estimates of the shear rate in the core of 0.8 were determined from below parameters (Table 7.7.4).
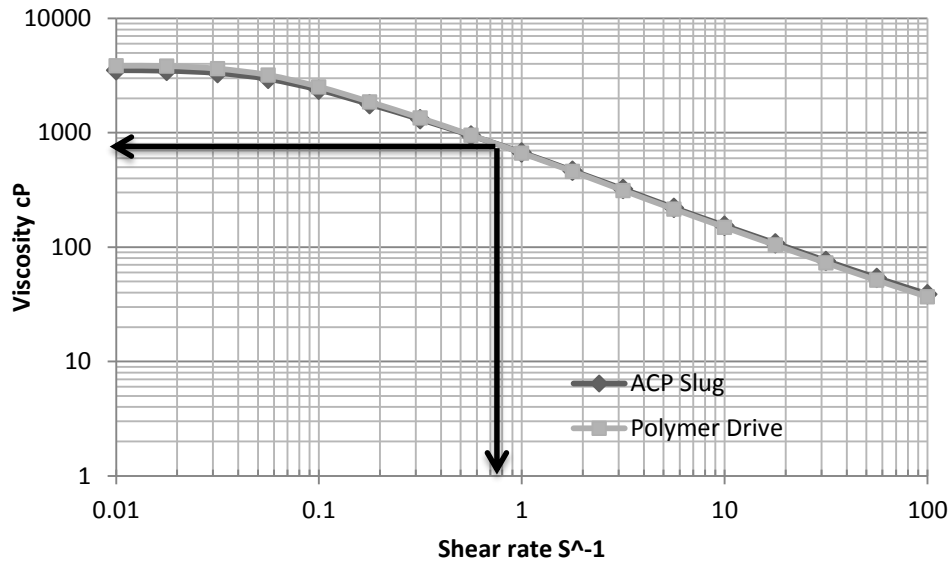
Figure 7.7.4: Viscosity curves for ACP-05 slug and drive. Arrow depicts final in-situ viscosity.

Table 7.7.4: ACP-05 Shear rate parameters

Frontal Advance Rate (ft/day)	0.48
Porosity (decimal)	0.24
Absolute Permeability (mD)	2500
End-Point Water Relative Permeability	0.95
Sorw (decimal)	0.6
n (power law term)	0.4
C (constant)	1.3
Final In-Situ Shear Rate (Sw = 1)	0.78

The flood was designed with very little safety factor in mobility, as seen above. This was due to the high pressure drop requirement and the assumption that if the flood were unstable, it would be only slightly so if polymer degradation weren't present.

Results ACP-04

The 50°C ACP-04 coreflood was successful in fulfilling required criterion. The tertiary oil recovery was 95.2%, with a S_{ORC} = 3 %. Oil bank was present very early, at 0.25 PV, due to the high initial oil saturation. The high oil viscosity contributed to a very wide and consistent oil bank cut, ~ 87% oil. The first evidence of Type II microemulsion was found at 0.86 PV, with a clear TIII-TI emulsion formed at 1 PV. Oil recovery was 87% at 0.86 PV when the emulsion broke through. Oil cut decreased rapidly and showed very little tail-off with time (Figure 7.7.4).
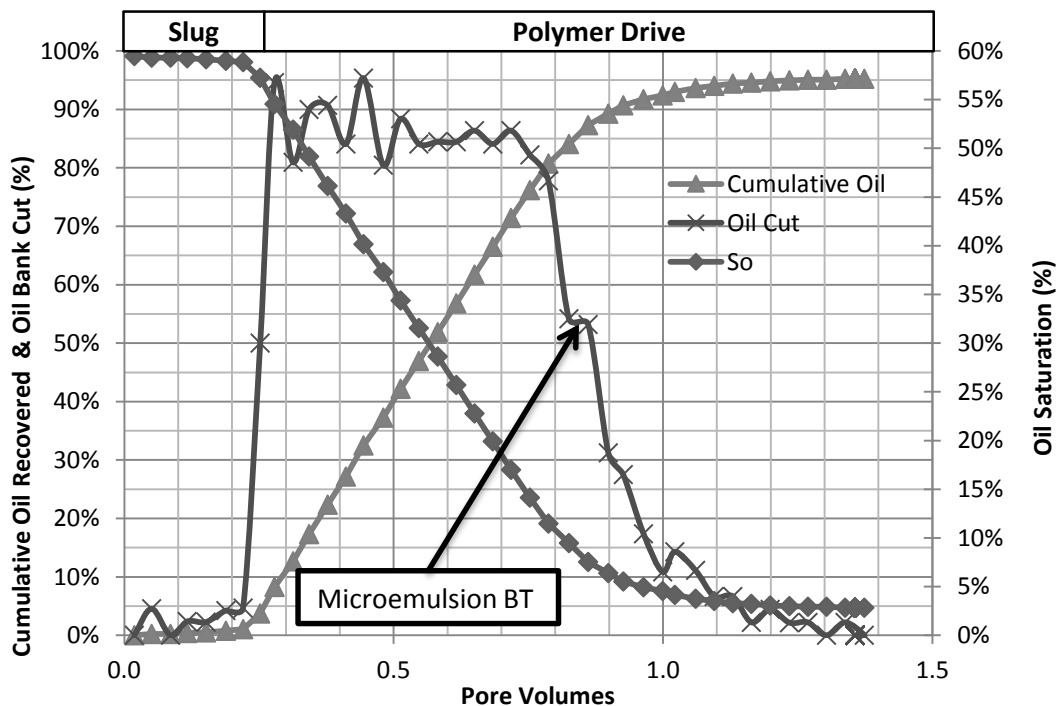
Figure 7.7.5: ACP-04 Oil recovery

The pressure drop data below show very tight design specifications resulted in a stable flood with virtually no excess mobility control. Pressure drop in each section was just over 1 PSI, and total steady state pressure drop was approximately 4.4 PSI/ft (Figure 7.7.5). Note the pressure peak corresponding to the oil bank is virtually identical in height to the steady state pressure drop.
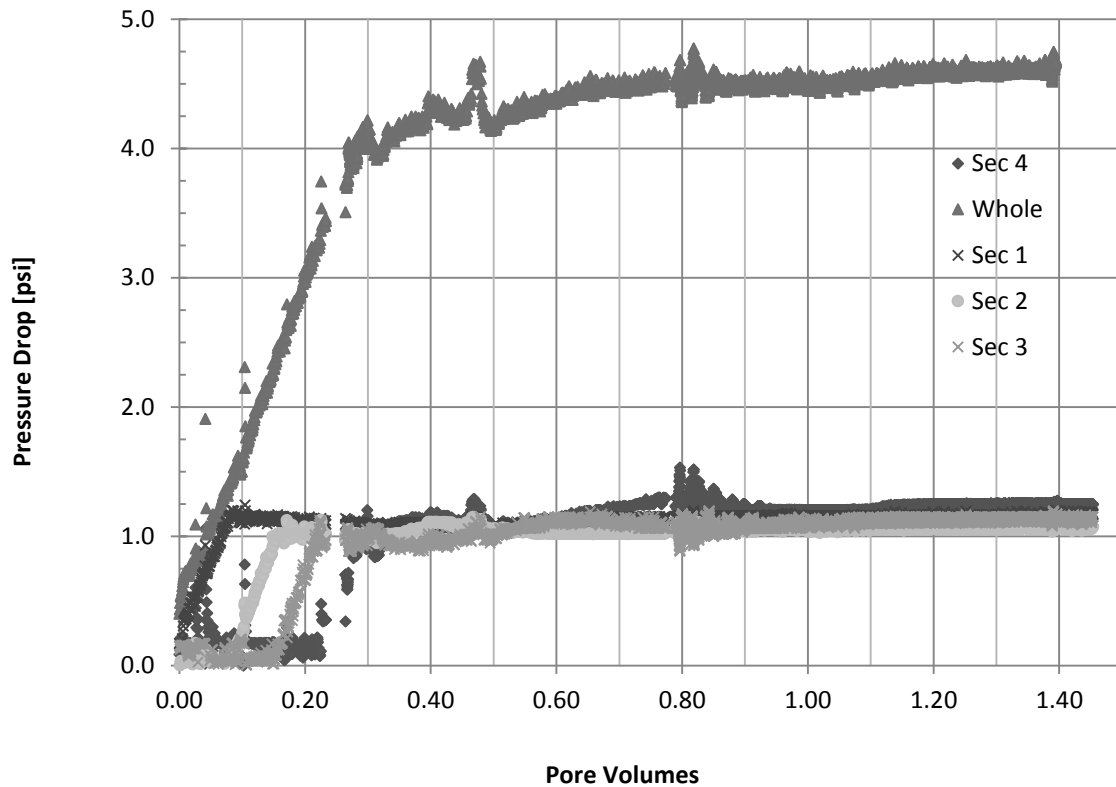
Figure 7.7.6: ACP-04 Pressure drop data

Effluent analysis (Figures 7.7.6 & 7.7.7) was as expected: salinity propagated correctly in the core as pH and TDS. The spike and subsequent decline of TDS is due to solubilized oil in the microemulsion. Polymer was assumed not to have been degraded based on apparent viscosity in the core.

Figure 7.7.7: ACP-04 pH propagation

Figure 7.7.8: ACP-04 Salinity propagation

109

7.8 ACP-05 COREFLOOD

To further explore the limitations of using ACP flooding to recover heavy oils, a coreflood was executed at room temperature with the same crude S, where viscosity = 4800 cP. The coreflood showed poor recovery tertiary recovery at 1 PV injection (60%) and unsustainable peak pressure drops (17 PSI/ft). Viscous stability was impractical to achieve at the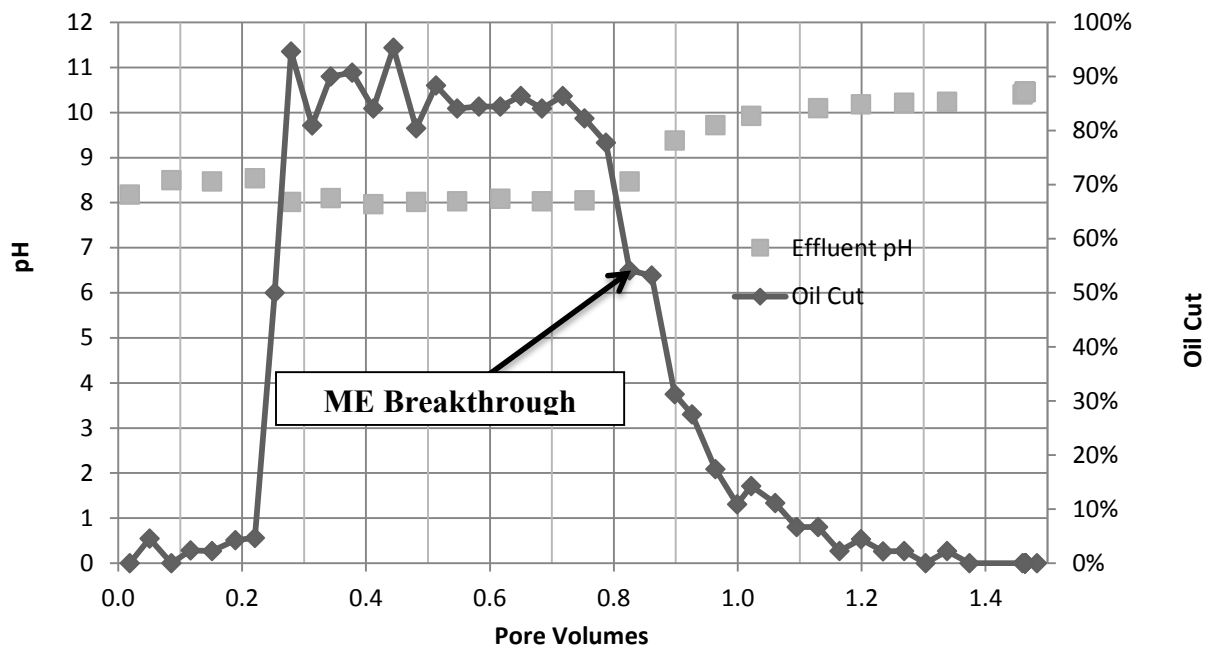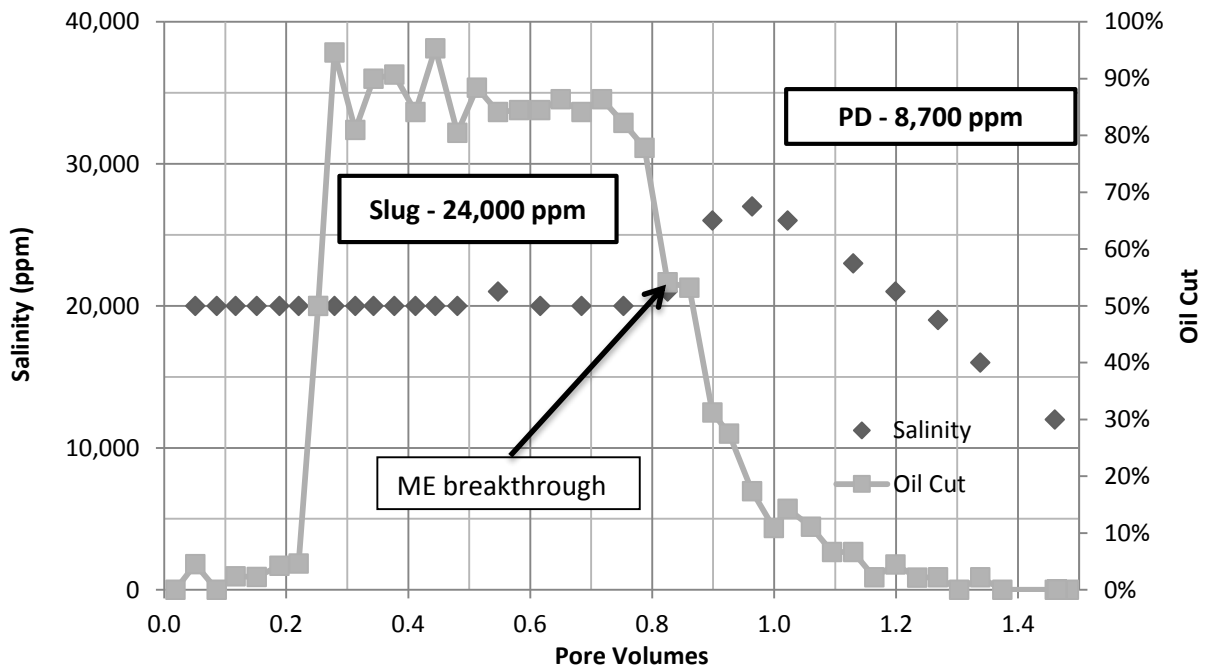 flood conditions, so the slug and drive composition were as in the above ACP-03 flood, resulting in a mobility ratio ~ 5; after 3 PV of injection, the flood still produced some oil. Final tertiary recovery was >90% at 3 PV, speaking to the effectiveness of the low IFT displacement measurement.

There were two major contributions to understanding cemented by the ACP-05 flood. The first is phase behavior at 25°C (room temperature) was very consistent with phase behavior up to 100°C; such behavior would be a major boon to an ACP flood in situ, and if it is general to heavy crude oils would provide a major boost in applicability. The second is the importance of adding alkali to the polymer drive. This has the dual advantage of protecting the polymer from degradation (recall iron was present in this core), and still can show IFT low enough for >90% displacement efficiency. The polymer drive effectively acts as an AP flood within the ACP flood; this fact could be very advantageous in a field study where viscous instability was expected.

ACP-05 Phase Behavior

Phase behavior of the ACP formulation with 1% IBA-5EO was encouraging; it is virtually the same as 50°C-100° phase behavior maps (Figure 7.8.1). This is very important in a hybrid thermal-chemical EOR scheme, as reservoir temperature would be far from uniform in the formation. If phase behavior were strongly affected by temperature, proper salinity gradient design would be very hard to achieve.

110
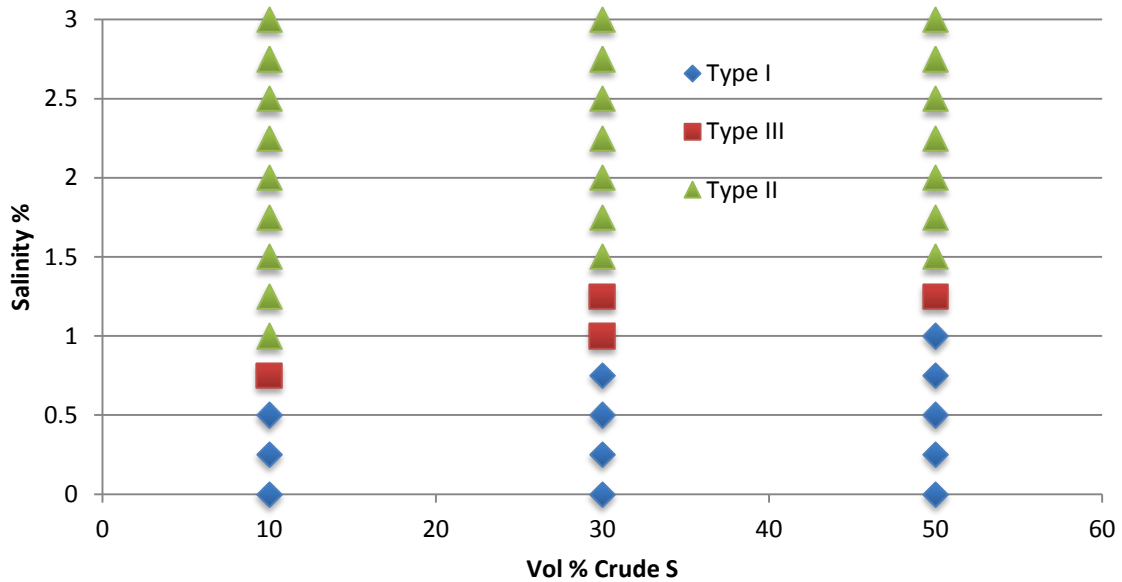
Figure 7.8.1: ACP-05 Activity map

In the scan, type III regions showed very nice ultra-low IFT emulsion characteristics, without excessive viscosity. The type I regions at lower salinity also showed low IFT, especially close to the type III region. The phase behaviors were challenging to interpret at room temperature due to the viscosity of the oil and the long equilibration times required, however the type III regions depicted above were clear.

ACP-05 Core Properties

Working with heavy oil at room temperature was challenging; at 4800 cP, oil flood and waterflood required high pressures and very low flow rate. All core handling was as ACP-05, without any oven heating required. Reduced brine saturated the core, and single-phase brine was used to establish residual saturation. To establish initial oil saturation,

crude S was injected at 100 PSI, resulting in S_{oi} = 88.9%. This very high oil saturation is likely near true residual water, and it is very little higher than the saturation from ACP-05 at 50°C despite increasing oil viscosity by a factor of 5. Section 1, which was lower permeability to begin with, was the only section where oil relative permeability was low, and probably experienced limited face plugging. The core was waterflooded with 20,000 ppm TDS reduced brine: 15,000 ppm NaCl, 1000 ppm dithionite and 4000 ppm $NaHCO_3$ (buffer). The viscosity of the oil posed a problem; the core was flooded at constant pressure of 100 psi initially to create injectivity for ~0.10 PV. This injectivity challenge is worth highlighting for field applications. Afterwards, the core was flooded at 0.1 ml/minute (1.1ft/day) for 10 hours, then at 1ml/minute (11ft/day) for 0.8 PV. Overall pressure drop was approximately 21 psi, leading to an overall Krw of 0.007. This extremely low value is a result of the high oil saturation remaining in the core and the viscosity of the oil. Initial oil saturation was 88.9%, and post-waterflood saturation was 64.5%. Relevant core properties are found in Tables 7.8.2 & 7.8.2.

Table 7.8.1: ACP-05 Core properties

Core ALK-01		
Outcrop	Bentheimer	
Mass	1147.5	g
Porosity	0.211	
Length	11.65	in
Diameter	1.96	in
Area	3.02	in^2
Temp	25	°C
Brine Perm	2369	mD
PV	121	ml
S_{oi}	0.889	
S_{orw}	0.625	
K_{ro}	1.33	
K_{rw}	0.007	
Oil Viscosity	4800	cP

Table 7.8.2: ACP-05 Coreflood parameters

Section	ΔP_{Brine} (psi)	k_{Brine} (mD)	k_{oil} (mD)	k_{ro}	k_{wf} (mD)	k_{rw}
1	0.35	2438	2490	1.02	35	0.014
2	0.32	2663	4039	1.51	19	0.007
3	0.25	3414	4772	1.4	14	0.004
4	0.45	1896	2647	1.4	11	0.006
Whole	1.44	2369	3156	1.33	16	0.007

ACP-05 Coreflood Design

The ACP-05 design was somewhat different than earlier corefloods. At room temperature, achieving viscous stability (~4800 cP in the core) was impractical with 3630 HPAM; not only would pressure drops be unacceptably high, but concentrations also would

be extreme (>6,000 ppm polymer). To allow for a direct comparison with another coreflood, and to maintain chemical concentrations at reasonable levels, the chemical slugs designed were the same as in ACP-04 (50° flood, 970 cP oil). Chemical slugs injected are below in Table 7.8.3:

Table 7.8.3: ACP-05 Chemical injection slug composition

Slug Component	ACP Slug	Polymer Drive
PV injected	0.25	2
[HPAM 3630s] Ppm	4,100	3,700
[Cosolvent], wt.%	1% IBA-5EO	---
Na_2CO_3 ppm	9,000	5,000
Isoascorbic Acid	1,000	1,000
TDS ppm	10,000	5,000
Frontal velocity ft/day	**0.50**	**0.50**
Viscosity 0.56 s^{-1}, 25 ºC	**1,295 cP**	**1,271**
Filtration Ratio F.R.	1.00	1.05
pH	10.20	10.40

The chemical slug design resulted in an in-situ mobility ratio of 4-5. This was expected from the design and is more practical in oils with viscosity > 1,000 cP.
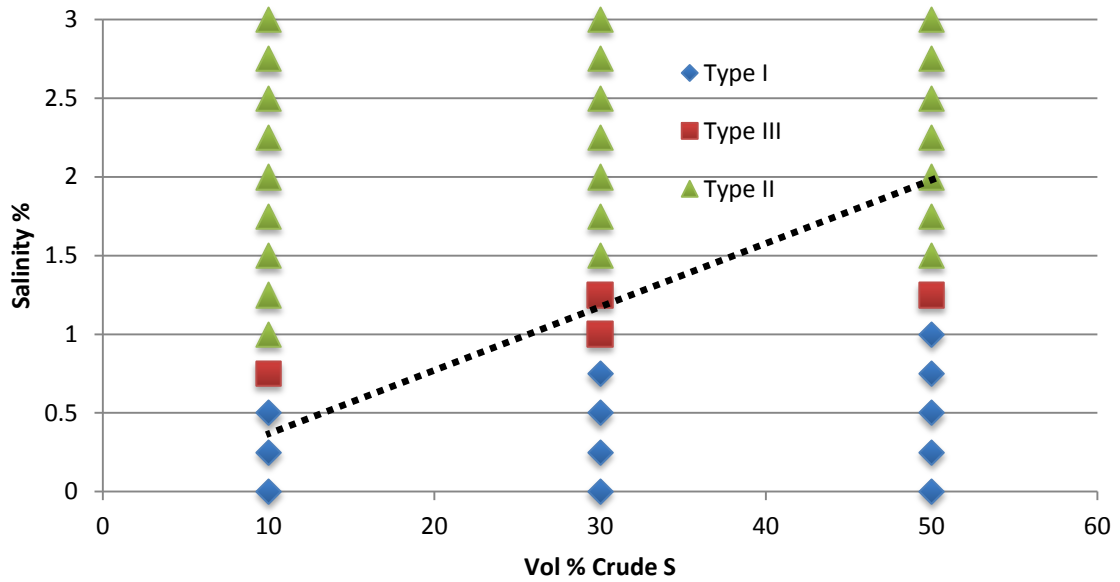
Figure 7.8.2: ACP-05 Salinity gradient and phase behavior.

The black dotted line represents the salinity gradient selected for the coreflood vs. the phase behavior of interest. The salinity gradient is virtually identical to all other ACP floods, even those at 100°C.
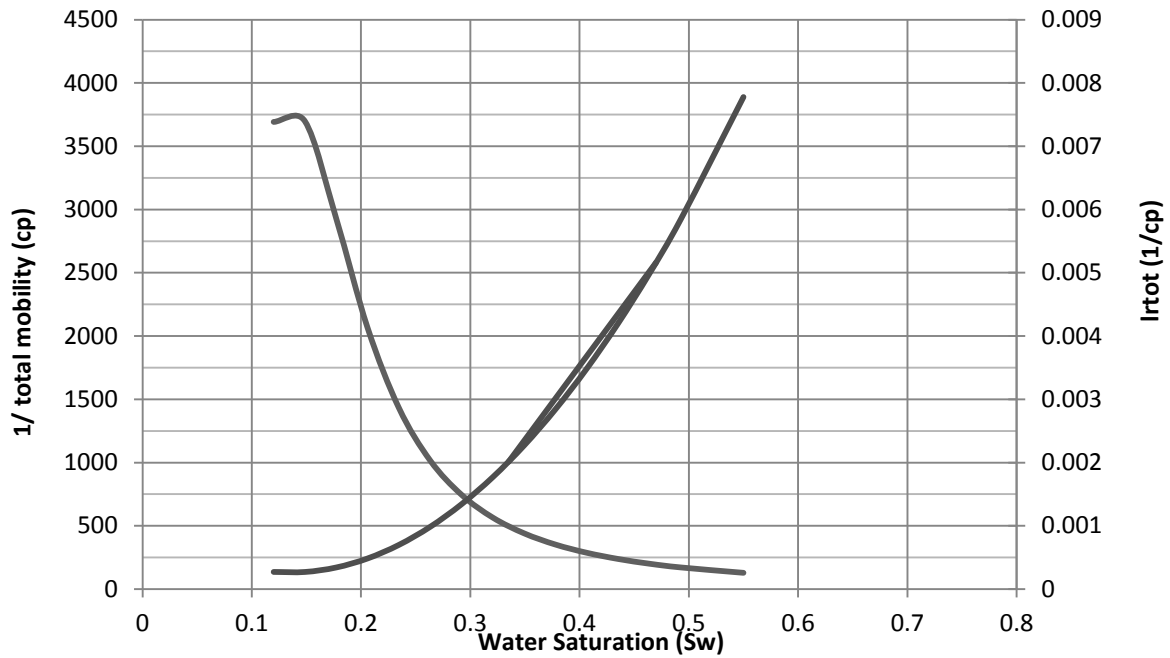
Figure 7.8.3: ACP-05 Mobility requirements

Table 7.8.4: ACP-05 Mobility control parameters in

k_{rw}°	0.007	
k_{ro}°	1.3	
n_w	2	
n_o	2	
S_{wr}	0.12	
S_{or}	0.45	
$\mu_w =$	0.9	cP
$\mu_o =$	4800	cP

Mobility control curves show the extreme viscosity required to displace the oil bank (Fig 7.8.3); as the oil saturation in the core was so high, this is a requirement for a significant portion of the injection cycle. Note that the water relative permeability is

116

virtually unnoticeable in this flood, despite the low relative permeability to water used in the calculation (0.007) Figure 7.8.4 and Table 7.8.5 detail slug & drive viscosity.
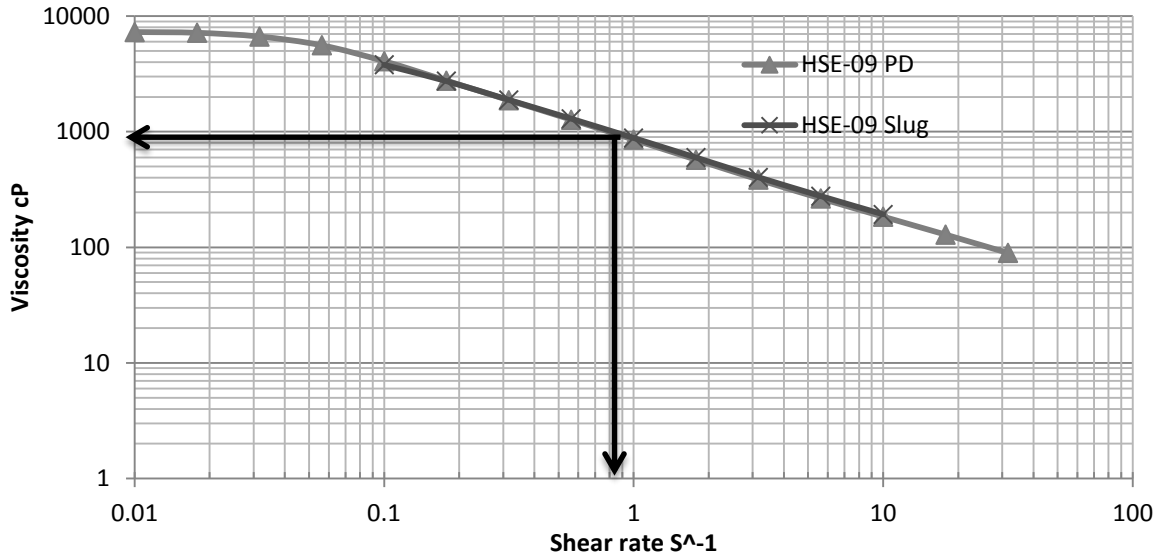
Figure 7.8.4: ACP-05 Slug and drive rheometery. Design rate and viscosity shown with arrows.

Table 7.8.5: ACP-05 Shear calculation parameters

Frontal Advance Rate (ft/day)	0.50
Porosity (decimal)	0.214
Absolute Permeability (mD)	2370
End-Point Water Relative Permeability	0.95
Sorw (decimal)	0.625
n (power law term)	0.38
C (constant)	1.36

Initial flood design assumed a shear rate correction factor C = 1.36, resulting in a shear rate of 0.86 and viscosity = 947 cP. Post-flood analysis showed this shear factor

assumption to be slightly on the low side, the calculated correction factor of C=1.57 in the core, results in a shear rate of 0.95 sec^{-1} and viscosity of about 850 cP.

ACP-05 Results

The HSE-09 coreflood was succesful in displacing oil, with a final recovery of ~95% tertiary recovery. The max oil cut (~85% oil) was high, but rapidly fell as the slug and drive broke through early, as expected from fractional flow theory. While the earlier successful ACP floods produced >90% recovery within 1 PV, the ACP-05 coreflood required 2 PV of throughput to achieve 90% recovery, with 4.15% S_{orc}. Though high oil cuts were initially achieved, and could prove promising in a field recovery, the pressure drop of the early flood was far greater than can be practially achieved in a reservoir. Microemulsion breakthrough occurred at 0.45 PV, as expected for a viscously-unstable flood. Maximum pressure drop occurred when the oil bank was at peak volume in the core, and was 17.5 PSI. This pressure would have been even higher but for a leak in the polymer drive column, which took some time to fix. Figure 7.8.5 shows ACP-05 oil recovery, while 7.8.6 shows ACP-04 vs. ACP-05.

The flood is an excellent example of the challenges in applying ACP flooding at low reservoir temperatureand how increasing the temperature even 25°C can lead to dramatic improvements in heavy oil recovery performance.
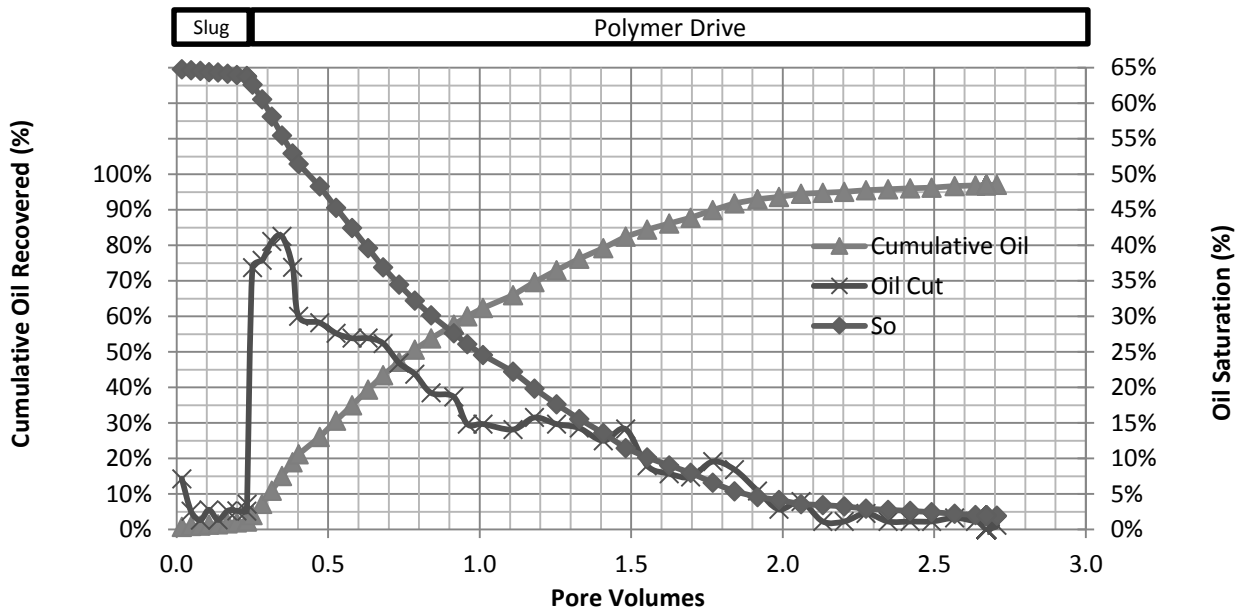
Figure 7.8.5: ACP-05 Oil recovery plot.
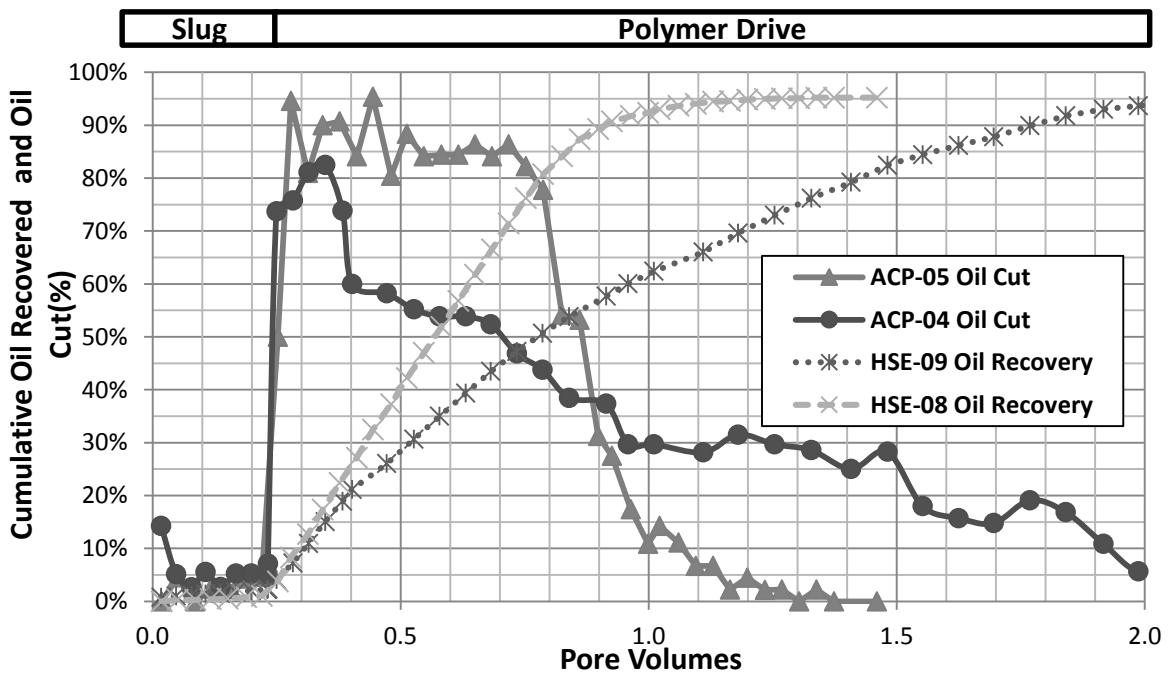
Figure 7.8.6: ACP-05 vs. ACP-04 oil cut and recovery.
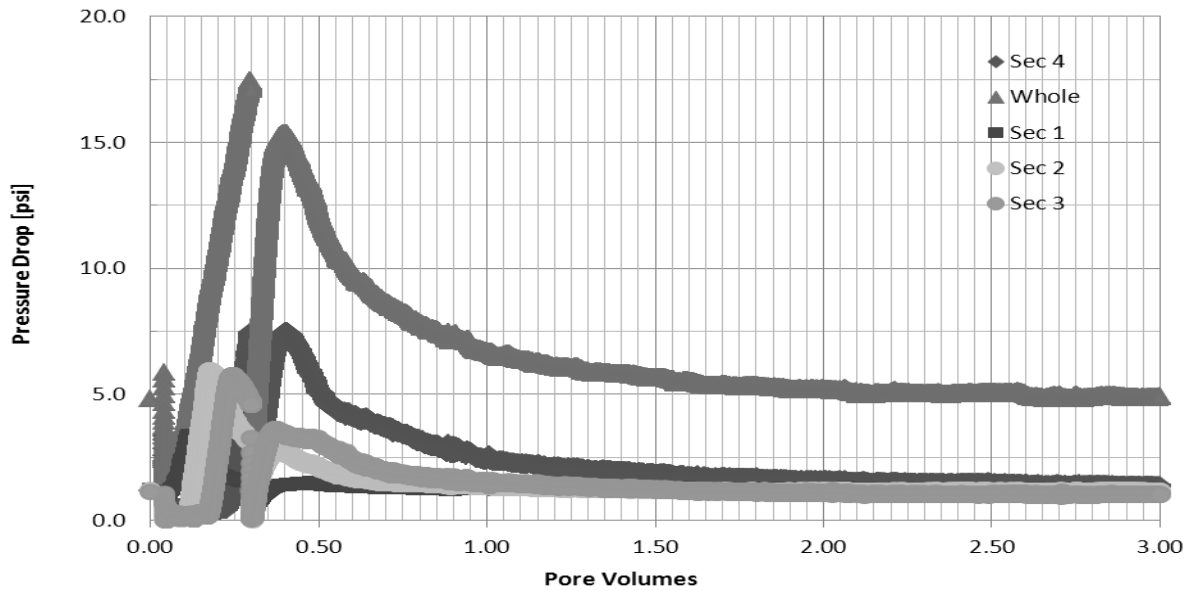
Figure 7.8.7: ACP-05 Pressure drop data

The above pressure data (Fig. 7.8.7) show the primary obstacle to displacing heavy oils at high viscosity: extreme pressure (17 psi/ft) is required to mobilize these fluids at reasonable rates. Most heavy oil production schemes involve some mitigation to this problem, either via heating with steam or water, or producing the unconsolidated formation itself as in CHOPS.

Table 7.8.6: Chemical flood performance

Section	ACP Flood Perm (mD)	dP (psi)	Perm reduction factor
1	2364	1.35	1.03
2	2897	1.1	0.92
3	2901	1.1	1.17
4	2659	1.2	0.70
overall	2501	5.0	0.93

120

The chemical flood performed approximately as expected in terms of viscosity at recovery. Post-calculation of core shear rates confirmed a C factor of 1.5, slighly higher than the 1.3 selected for the design of the flood. The shear rate in the core was calculated to be 0.93 sec^{-1}, which corresponds to a polymer viscosity of 850 cP. The pressure drops from the flood show an apparent viscosity of about 800 cP. Salinty and pH propogated with the chemical slug as expected, and showed early breakthrough characteristic of viscous instability (Figs 7.8.8 & 7.8.9).

Figure 7.8.8: ACP-05 pH propagation and oil cut vs. throughput.

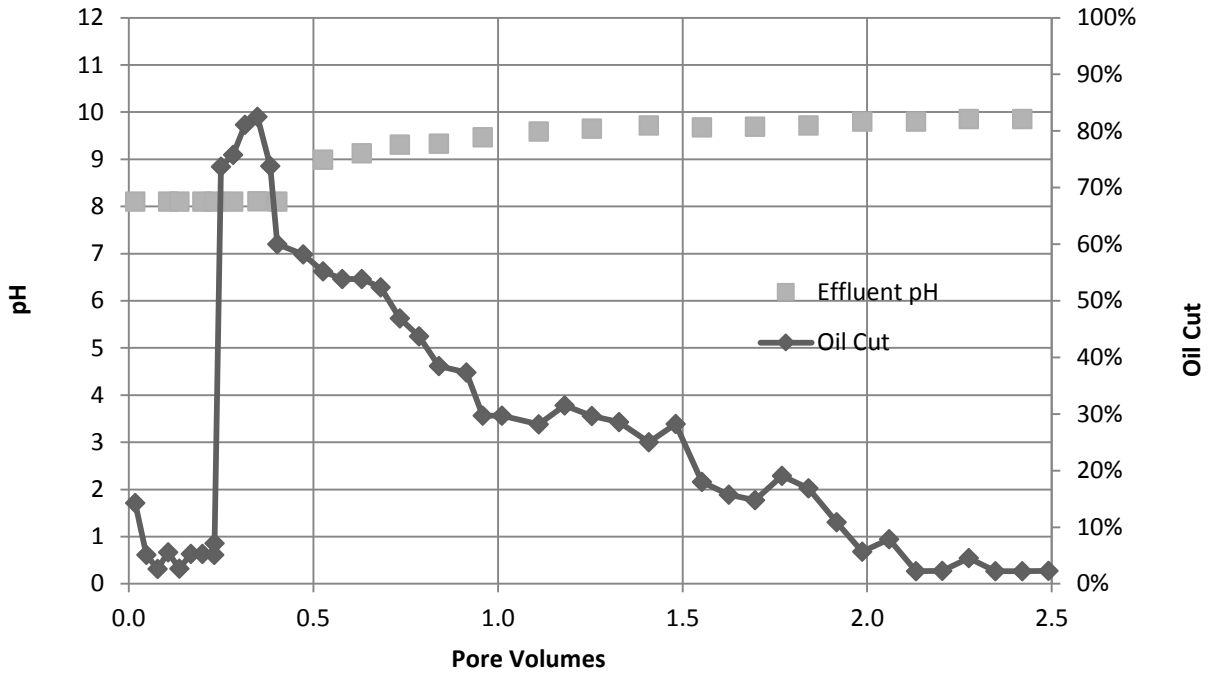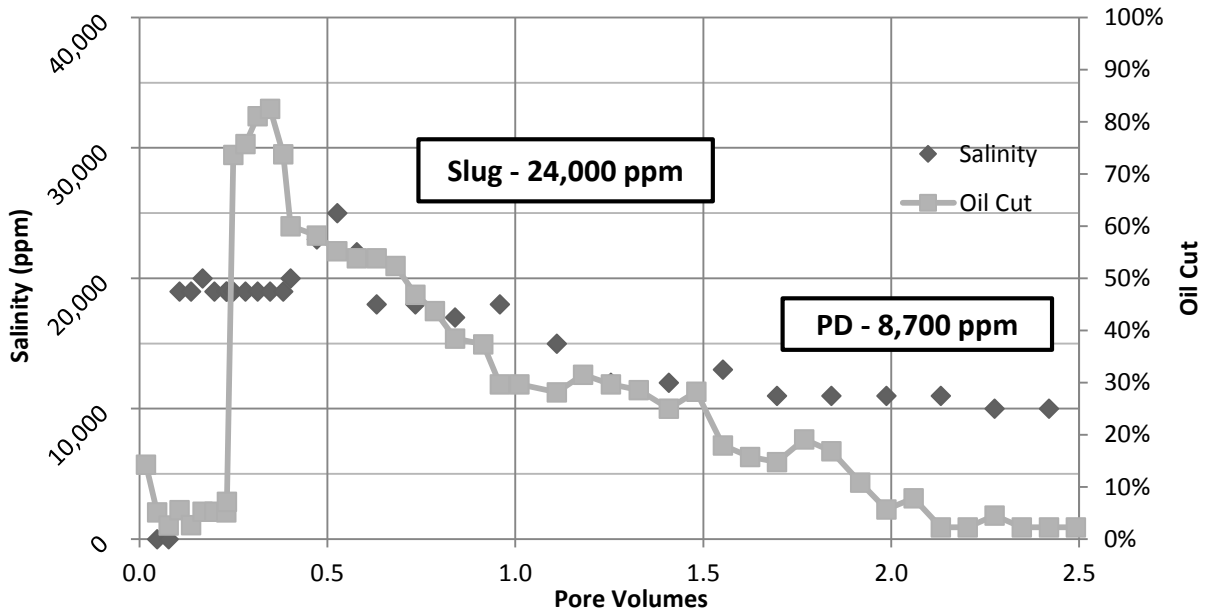Figure 7.8.9: ACP-05 Salinity propagation and oil cut

122

Chapter 8: Alkaline Floods

ACP flooding was demonstrated in 5 corefloods as an alternative to ASP flooding to recover heavy oils. Two corefloods were run at 68°C to demonstrate the advantages of ACP flooding vs. alkaline flooding, or alkaline-polymer (AP) flooding.

8.1 ALKALINE-POLYMER FLOOD AP-01

An AP coreflood was designed to show the various advantages and disadvantages of the AP flood vs. the new ACP alternative. The primary advantages of the ACP process over AP are completely customizable phase behavior through the use of cosolvents, and the reduction of the formation of viscous emulsions. Demonstration of the custom phase behavior principle is within the scope of this work, but the proof of issues with viscous emulsions requires further experimentation.

The AP-01 flood was carried out in Bentheimer sandstone at 68°C, confined by epoxy as in corefloods ACP-02 and 03. Viscous emulsions formed at this temperature without cosolvent, and were anticipated to cause lowered tertiary recovery and increased pressure drop profiles in the coreflood. This wasn't demonstrated in the flood however; AP-01 chemicals recovered 96.9% of the tertiary oil at a pressure drop of 4.5 PSI/ft This rather high pressure drop can be shown to be a direct result of the polymer viscosity and not an effect of a viscous emulsion; however the deleterious effects of such an emulsion in the field can be surmised from other experiences data.

AP Flood Phase Behavior

When alkali forms soaps from crude oils without the presence of cosolvent or surfactant, the resulting phase behavior system shows major hydrophobic character. The soaps generated are, after all, crude oil components, and only show suitable phase behavior

at very low salinity. A map of the alkali-only phase behavior with Crude S in Na_2CO_3 is shown below in Figure 8.1.1.
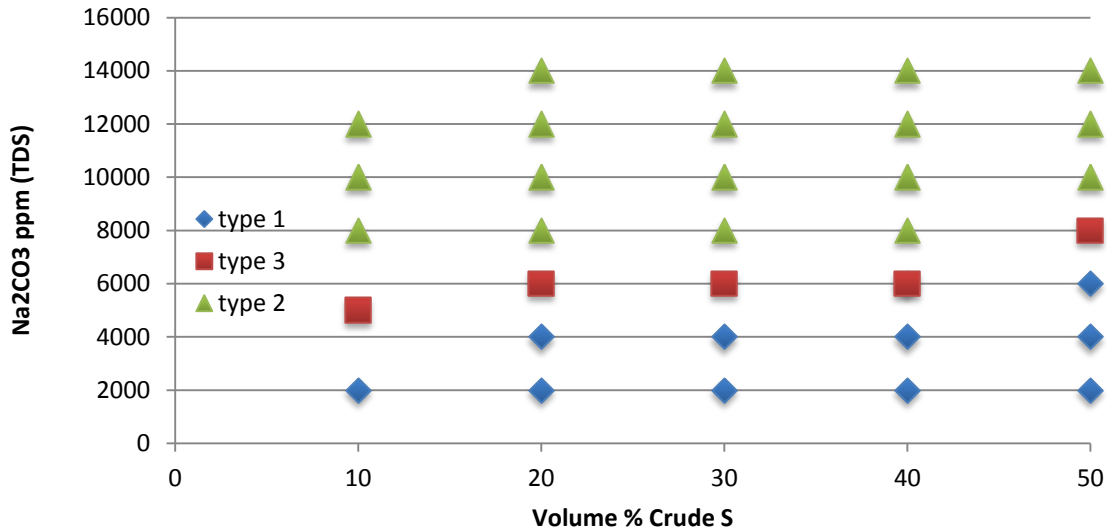
Figure 8.1.1: Alkali scan with crude S

The much lower salinity required for a successful AP flood is apparent immediately. In order to realize the major advantage of a salinity gradient, an injection slug needs approximately 6,000 ppm Na_2CO_3, and polymer only requires 2,500 ppm. Alkali consumption is one of the major problems with such low salinity. When alkali is consumed at high rates, it can seriously retard the formation of the low IFT oil bank. Though polymer in an AP flood would likely still be of benefit in terms of improved sweep, the resulting oil recovery would be below what was expected for a robust chemical flood. Alkali consumption would be an even greater problem if electrolytes other than Na_2CO_3 were required in the formulation; in such a case the effective alkali concentration would be even lower, and consumption issues exacerbated. The other major problem with extremely low injection salinity is issues with clays: when exposed to such fresh water, clay will swell

124

significantly and can dramatically reduce permeability in the rock (Zhou et. al, 1996). Such a reduction in permeability could be a major problem for a flood with viscous fluids like AP.

AP-01 Core Properties

The core in AP-01 flood was handled like the other epoxy core ACP floods at 68°C. Reduced brine with 20,000 ppm NaCl, 8,000 ppm $NaHCO_3$ (buffer) and 1000 ppm $Na_2S_2O_4$ (reducing agent) saturated the core and established pore volume. Afterwards, the same brine was injected to calculate single-phase brine permeability. Initial oil saturation with Crude S was established under 50 PSI injection pressure, and was subsequently waterflooded with the same brine as above. Brine pH was injected at 8.0 and ORP <-600 mV, and was produced after waterflood at pH 7.91 and ORP <-600 mV. S_{oi} was only 83.5%, due to the lower saturation pressure used in the flood; this was due to the potential of the core cracking under high pressure during oil flood from poor quality control during core construction. Waterflood was completed at 10.84 ft/day, and oil saturation after waterflood was 48.4%. Tables 8.1.1 & 8.1.2 detail relevant core properties.

Table 8.1.1: AP-01 Core Properties

Core AP-02		
Outcrop	Bentheimer	
Mass	1150	g
Porosity	0.238	
Length	11.67	in
Diameter	1.94	in
Area	2.90	in^2
Temp	68	°C
Brine Perm	2700	mD
PV	135	ml
S_{oi}	0.835	
S_{orw}	0.59	
k_{ro}	1.33	
k_{rw}	0.024	

Table 8.1.2: AP-01 Coreflood parameters

Section	ΔP_{Brine} (psi)	k_{Brine} (mD)	k_{oil} (mD)	k_{ro}	k_{wf} (mD)	k_{rw}
1	0.34	2728	1324	0.485	105	0.040
2	0.28	3212	3992	1.243	111	0.035
3	0.29	3072	3751	1.221	75	0.025
4	0.38	2441	3385	1.387	47	0.019
Whole	1.34	2700	2594	0.961	71	0.026

The low oil relative permeability in section 1 was likely due to face plugging in the section; the injection of the high-pressure waterflood seems to have resolved the issue. Plugging seemed likely based on photos of the core after completion of the flood. The later sections show the greater than unity relative permeability to oil characteristic of viscous oils.

AP-01 Coreflood Design

Design of the AP-01 coreflood depended on the core properties at the temperature of interest, which were similar to the ACP floods at 68°C, and the phase behavior of the AP formulations, which was quite different. Oil viscosity is 220 cP. The following slugs (Table 8.1.3) were selected as the appropriate for the AP-01 injection slug and drive.

Table 8.1.3: AP-01 Slug and drive. Bold shows differences from ACP-03 flood.

Slug Component	ACP Slug	Polymer Drive
PV injected	0.25	2
[HPAM 3630s] ppm	3,000	3,000
[Cosolvent], wt.%	---	---
Na_2CO_3 ppm	**6,000**	**2,500**
Isoascorbic Acid	1,000	1,000
TDS ppm	7,000	3,500
Frontal velocity ft/day	1.0	1.0
Viscosity at 2.51/s & 68°C, cP	**236**	**245**
Filtration Ratio F.R.	1.15	1.10
pH	10.40	10.40

The phase behavior shown above gave rise to the following salinity gradient.
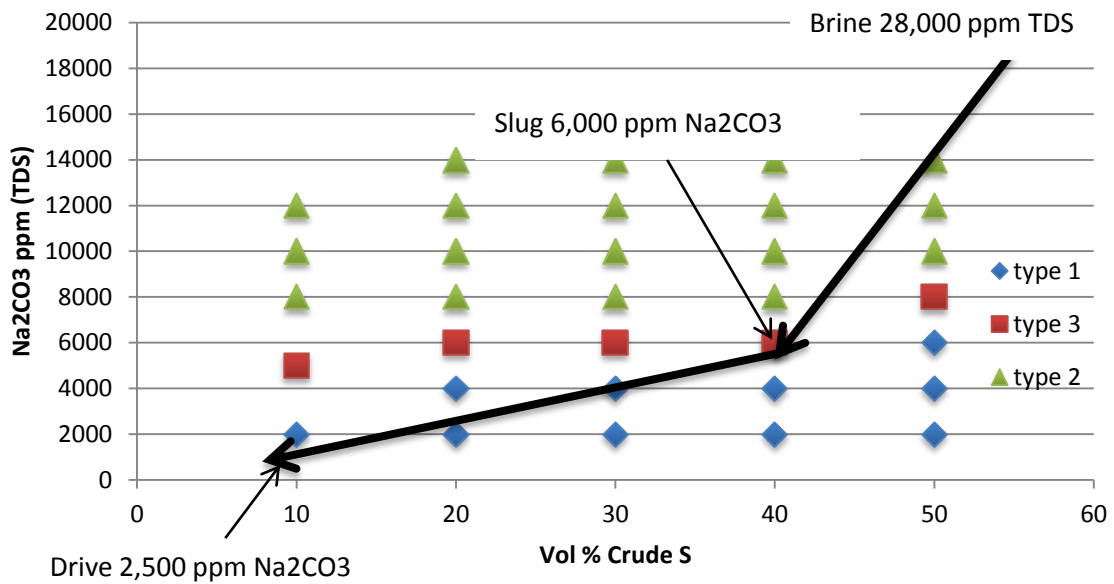
Figure 8.1.2: AP-01 Salinity gradient design

The positive effect of salinity gradient on the result of this flood is important to emphasize. The result of this AP flood was far better than many others in the literature (though the experiments weren't nearly identical); this was almost certainly due to the application of sophisticated best practices like the salinity gradient to the technology (Potts & Kuehne, 1988; Wu, Dong, & Shirif, 2011).

The mobility requirements for this flood were virtually identical to the ACP-03 flood, and a mobility curve is below.

Figure 8.1.3: AP-01 Mobility requirements

From the mobility curves (Fig 8.1.3), the slugs described above were determined to be appropriate from this viscosity profile and calculated in-situ shear rate. Viscosity of the chemicals in the core was designed to approach 280 cP, affording a good deal of excess mobility control if needed (Fig 8.1.4 & Table 8.1.4).
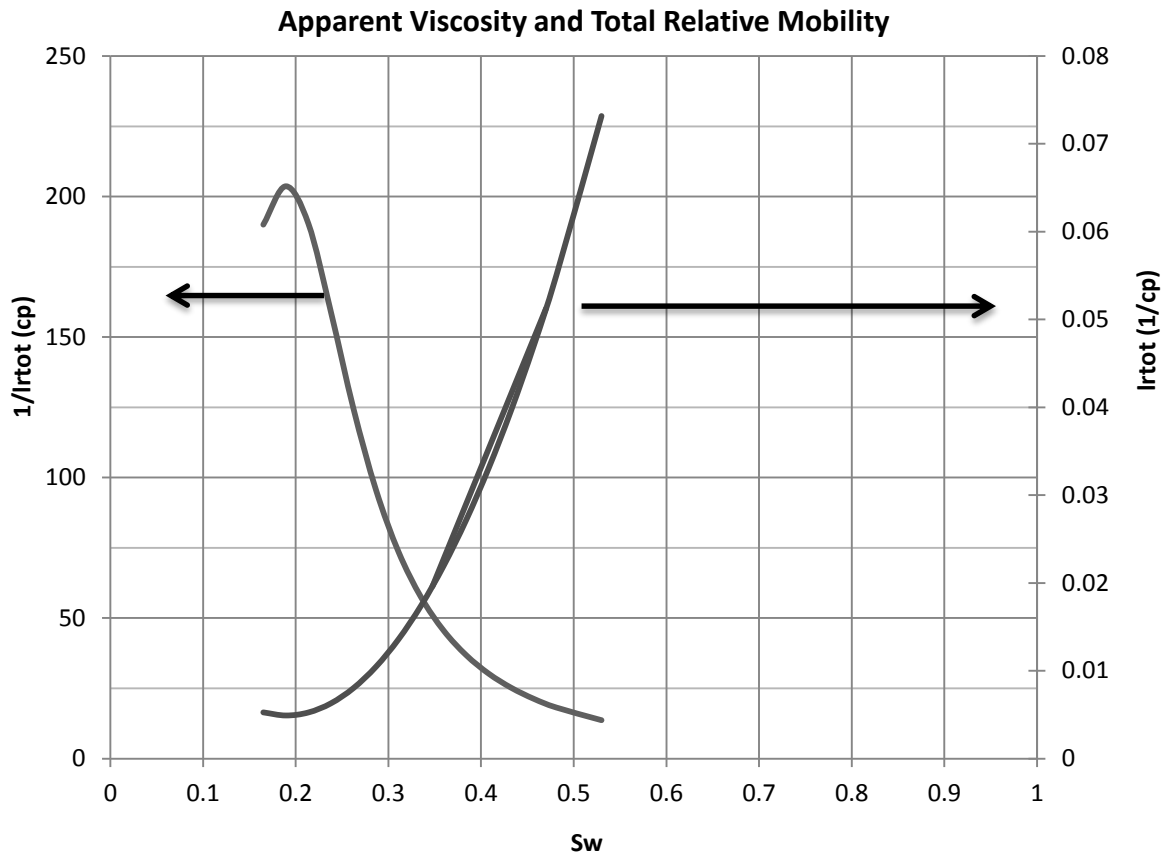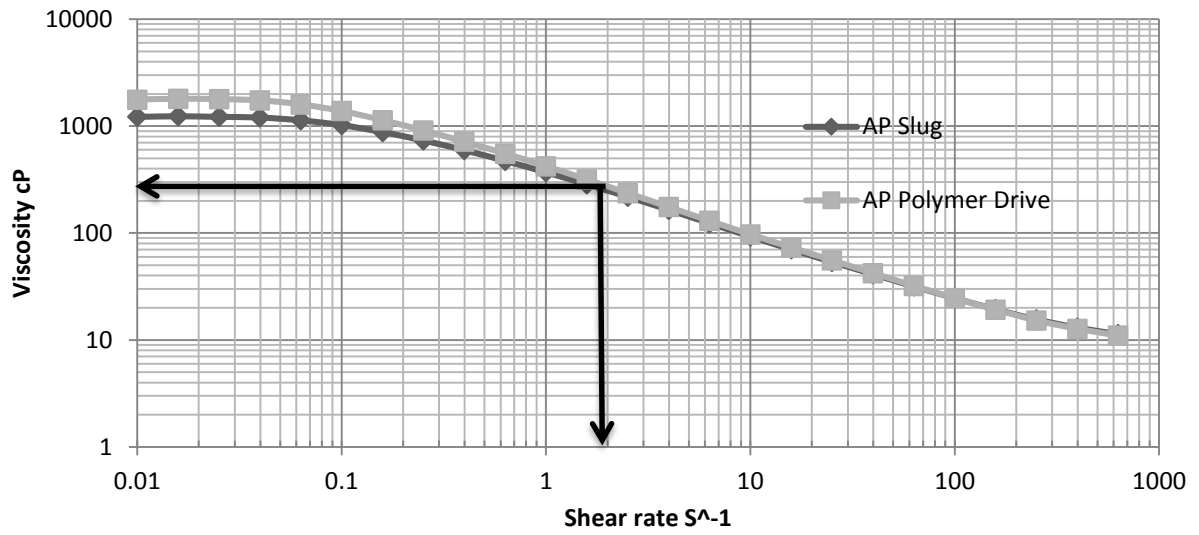
Figure 8.1.4: AP-02 Slug and drive viscosity

Table 8.1.4: AP-01 Shear rate calculation parameters.

Frontal Advance Rate (ft/day)	1
Porosity (decimal)	0.2388
Absolute Permeability (mD)	2700
End-Point Water Relative Perm	0.045
Sorw (decimal)	0.45
n (power law term)	0.45
C (constant)	1.6
Final In-Situ Shear Rate (Sw = 1)	1.92

The reason the flood was designed with excess mobility control to this extent involved the properties of the viscous emulsions seen in phase behavior studies of the AP formulation. Even emulsions with only 30% oil were as viscous as the surrogate crude S at low shear rate (Fig 8.1.5).

Figure 8.1.5: Viscosity of AP emulsion vs. ACP microemulsion. 30% vol. crude S.

The figure clearly shows the increase in viscosity for AP emulsions relative to ACP microemulsions. In the type I emulsion above, almost 1.5 orders of magnitude separate the emulsion from the ACP microemulsion; at low shear (<1 sec^{-1}) the type 1 emulsion is more visco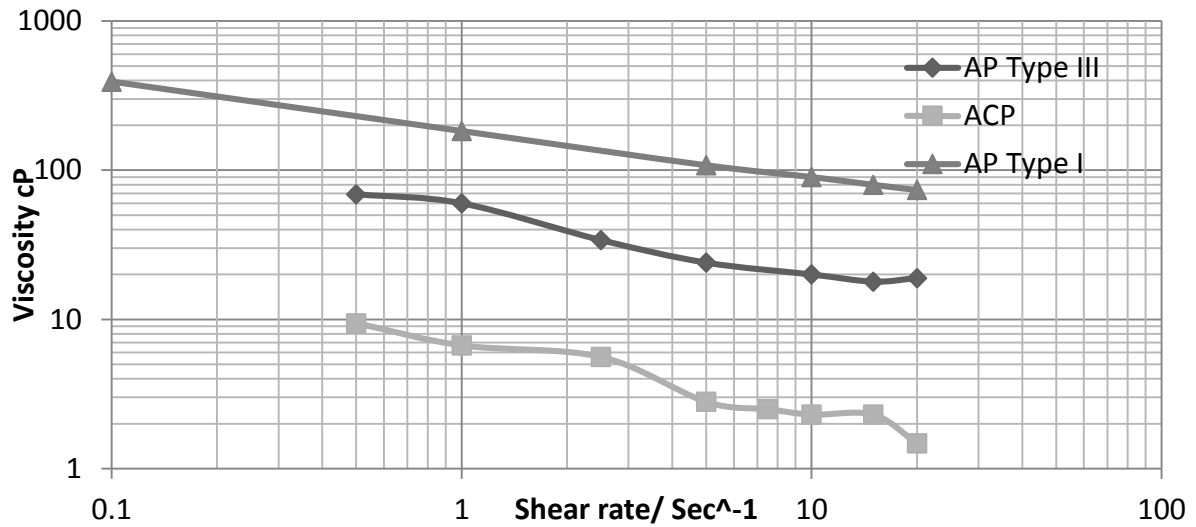us than the crude S viscosity. Though hard to estimate, it was supposed that an emulsion of much higher oil content (50-80% oil) could form in the AP-01 coreflood and show major negative impacts. This hypothesis wasn't demonstrated in the execution of the flood, and pressure drop was dominated by the polymer and not a viscous emulsion.

AP-02 Results

The AP-02 coreflood performed better than anticipated. It recovered almost 97% of tertiary oil, with a residual saturation of only 1.48% at a moderate 4.5 PSI/ft pressure drop. The excellent performance was due to solid mobility control and very favorable IFT properties, likely helped by the lack of cosolvent (which raises IFT). The application of best principles was also a major contributing factor to the success of the flood.

131

The absence of viscous emulsion formation was a major benefit to the flood, and has potential to allow for overly optimistic interpretation of the results. In a field environment, with major heterogeneity and very long residence times, the emulsions detailed in the design section could have negative impact on the flood, especially when they are >50% oil (as would likely be the case in a nearly unproduced heavy oil application).

The oil recovery plot (Fig 8.1.6) shows high oil cut averaging >80% oil, consistent between 0.3 and 0.7 PV. Type II emulsion is barely present at 0.82 PV, when 85% of tertiary oil had been produced. Final recovery of tertiary oil was 96.9% with $S_{orc} = 1.48\%$.
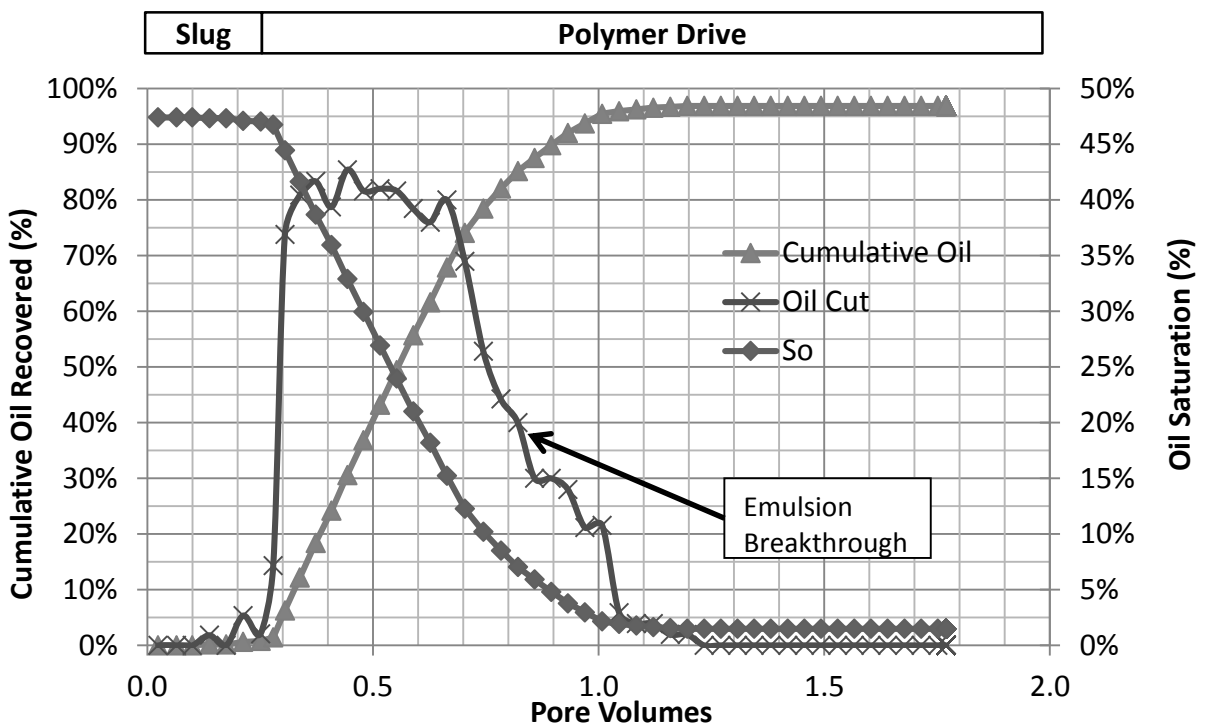
Figure 8.1.6: AP-02 Chemical flood oil recovery

Pressure drop was high but possibly field-applicable at a maximum 4.5 psi/ft (Fig. 8.1.7). The excess mobility control in the flood is clearly seen in the curves; pressure drop continually increases with polymer viscosity as the core is swept out and shear rate decreases as a consequence.
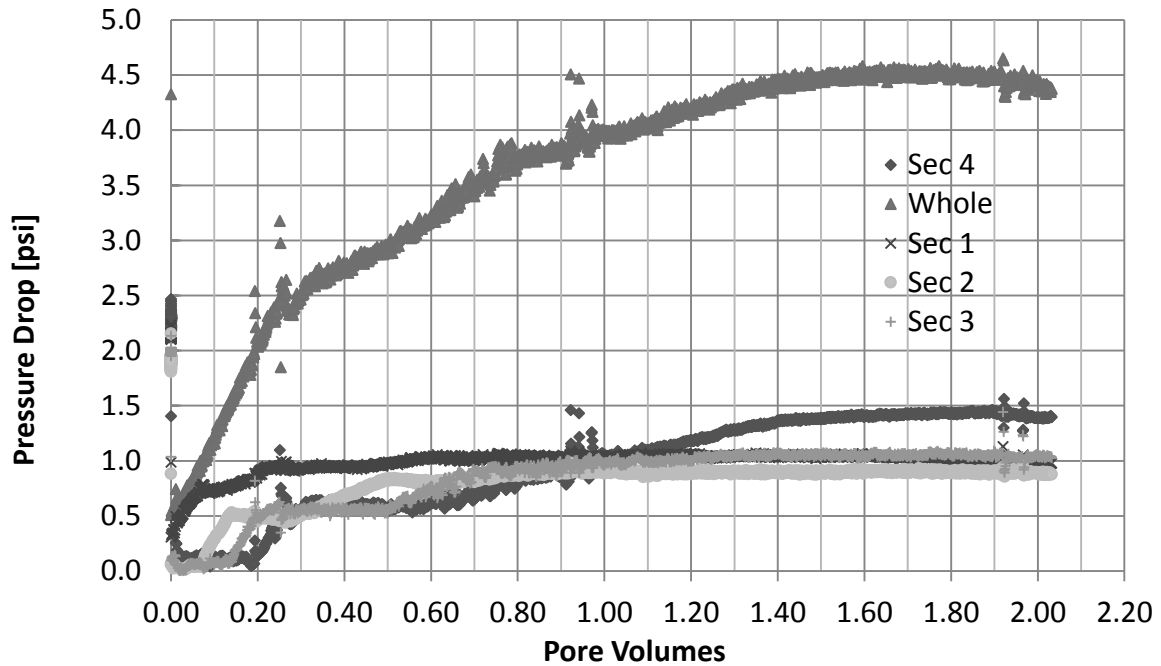
Figure 8.1.7: AP-01 Chemical flood pressure drop

Salinity and pH propagated with the slug as expected (Fig's 8.1.8 & 8.1.9).
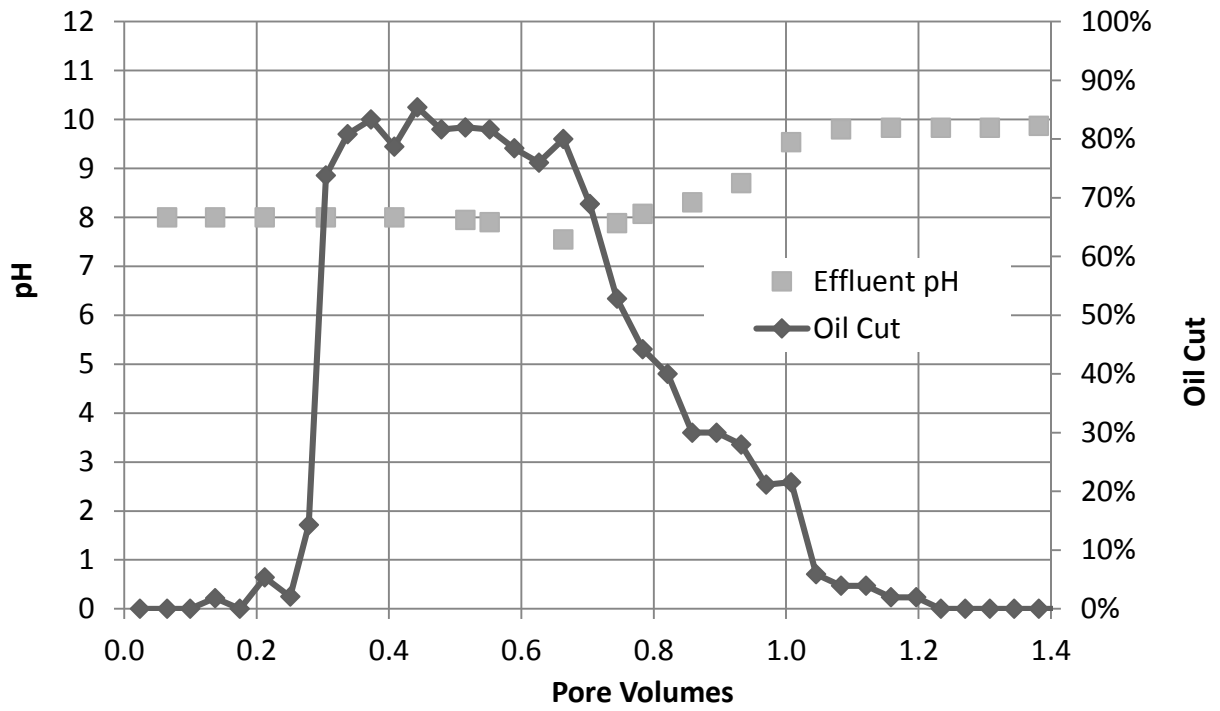
Figure 8.1.8: AP-01 pH propagation.
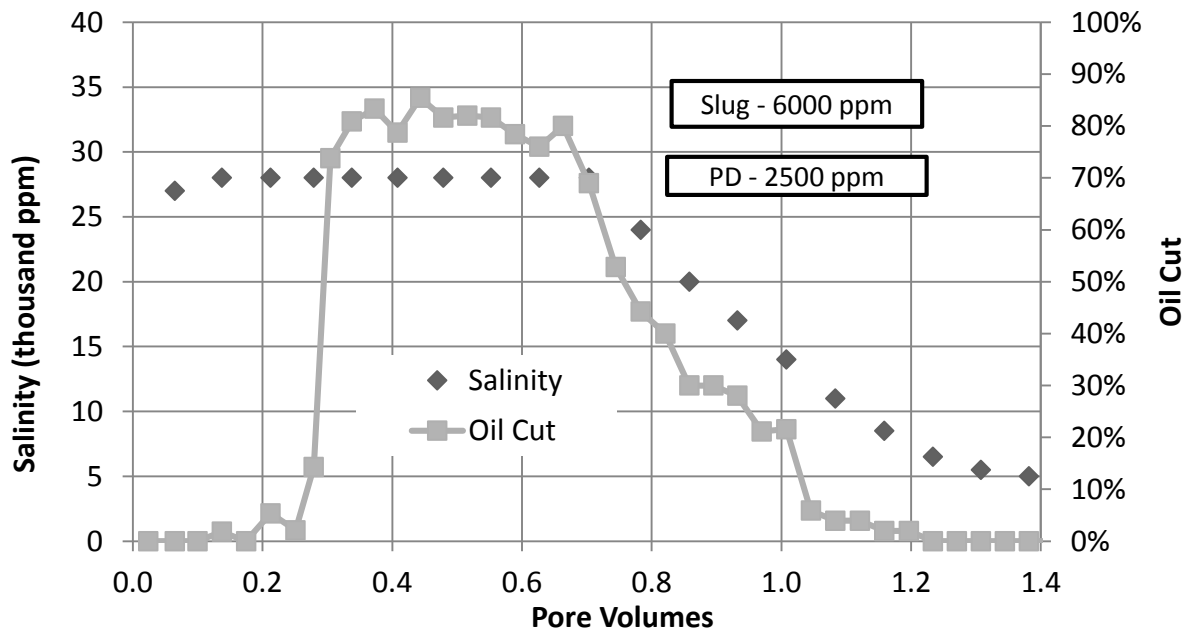
Figure 8.1.9: AP-01 Salinity propagation

The slug and drive were not degraded in the core as shown in below effluent rheology (Fig 8.1.10). The polymer protection package used, in combination with the high permeability rock, was enough to overcome the presence of iron minerals which could degrade polymer.
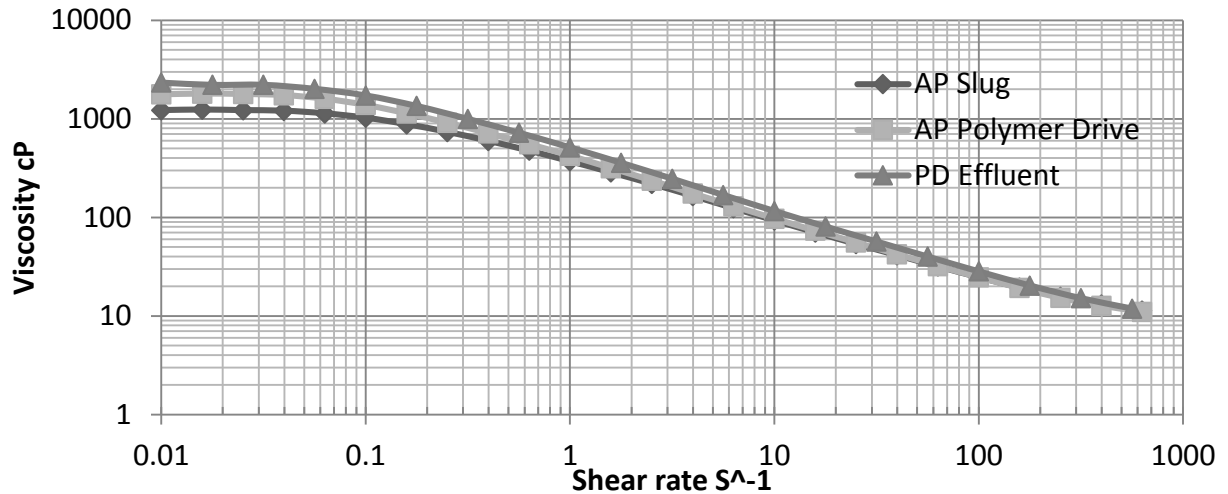
Figure 8.1.10: AP-01 Slug viscosity pre-injection and post-injection

8.2 ALKALI FLOOD ALK-01

Part of the reason the viscous emulsion was of little impact in AP-01 was the excess mobility control in the flood. To demonstrate the deleterious effects of viscous emulsion formation in a core, as well as show the definite need for polymer in an alkaline flood, the alkaline flood ALK-01 was designed and implemented. ALK-01, like AP-01, was a Bentheimer sandstone core in epoxy at 68°C.

The alkaline flood showed tertiary recovery of 40%, poor compared to the >90% recoveries in AP and ACP floods. This response is typical of chemical floods when inadequate mobility control is used; early emulsion breakthrough, very high emulsion production, low oil cut and poor overall oil recovery.

ALK-01 Core Properties

The ALK-01 epoxy core was Bentheimer sandstone, and was handled as in preceding corefloods. Reduced brine saturated the core, and single-phase brine was used to establish residual saturation. Oil was flooded to the core at 75 PSI & 68°C, resulting in S_{oi} = 81.4%. Oil flood seemed to cause some plugging in section 1 (see the relative permeability values below), which was alleviated by briefly flowing oil counter-current to remove plugs. Waterflood was completed at 68°C, and reduction of the core was incomplete (-270 mV) due to instability of dithionite at 68°C. So remaining was high after waterflood at 51.5% and krw low due to high oil viscosity and relatively little throughput (2.5 PV water) Tables 8.2.1 - 8.2.3 show relevant core properties.

Table 8.2.1: ALK-01 Brine composition

Brine Composition		
NaCl	10,000	ppm
NaHCO3	4,000	ppm
Dithionite	1,000	ppm
ORP	-600	mV
pH	7.13	

Table 8.2.2: ALK-01 Core Properties

Core ALK-01		
Outcrop	Bentheimer	
Mass	1058.2	g
Porosity	0.243	
Length	11.84	in
Diameter	1.94	in
Area	2.95	in^2
Temp	68	°C
Brine Perm	2666	mD
PV	125.5	ml
S_{oi}	0.814	
S_{orw}	0.515	
k_{ro}	1.13	
k_{rw}	0.026	
Oil Viscosity	220	cP

Table 8.2.3: ALK-01 Flood parameters

Section	ΔP_{Brine} (psi)	k_{Brine} (mD)	k_{oil} (mD)	k_{ro}	k_{wf} (mD)	k_{rw}
1	0.45	2171	1357	0.708	105	0.040
2	0.35	2707	3553	1.20	111	0.035
3	0.31	3056	4128	1.39	75	0.025
4	0.28	2830	3648	1.05	47	0.019
Whole	1.45	2666	2607	1.13	71	0.026

ALK-01 Coreflood Design

The ALK-01 coreflood design was based primarily on phase behavior. As polymer wasn't present, there was no concern about achieving mobility control, unlike all prior floods. Table 8.2.4 shows alkaline flood composition. Figure 8.2.1 details the identical salinity gradient from the AP-01 coreflood in Section 8.2

Table 8.2.4: ALK-01 Chemical slug detail

Slug Component	ALK Slug	Water Drive
PV injected	0.25	2
[HPAM 3630s] ppm	---	---
[Cosolvent], wt.%	---	---
Na_2CO_3 ppm	6,000	2,500
Isoascorbic Acid	1,000	1,000
TDS ppm	7,000	3,500
Frontal velocity ft/day	1.0	1.0
Viscosity at 2.51/s & 68°C, cP	**0.41**	**0.41**
Filtration Ratio F.R.	---	---
pH	10.90	10.88
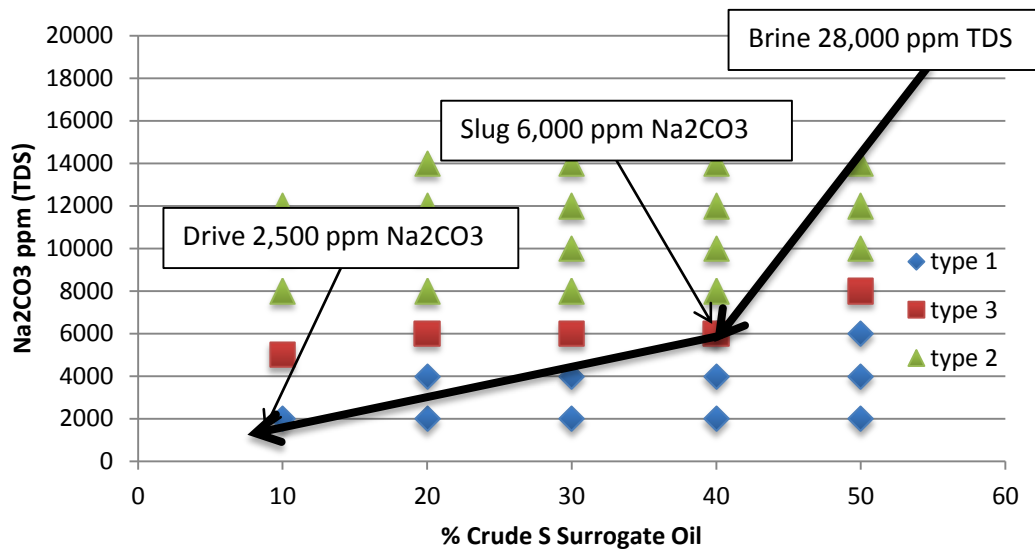
Figure 8.2.1: ALK-01 salinity gradient design

ALK-01 Results

The ALK-01 coreflood was largely a failure, and speaks to the importance of adequate mobility control and reducing formation of viscous emulsions. Tertiary recovery was 46% after 2.5 PV of alkaline brine were injected (Fig 8.2.2). The emulsions formed weren't as viscous as was considered possible in the flood design; since the flow paths were already established by the waterflood, the chemical flood simply bypassed the high oil saturation zones and swept little excess oil. Despite this fact, the pressure drop peaked at 1.7 PSI/ft. In the last section of the core, pressure drop spiked as high as 0.78 PSI/ft, which corresponds to an apparent oil/alkaline flood viscosity of 300 cP. This apparent viscosity is as high as in the AP-01 flood at steady state, despite the complete lack of polymer, and demonstrates problem effects of viscous emulsions. Maximum oil cut was

40%, and quickly tapered down. Very large volumes of emulsion were produced, which could be challenging to manage in a reservoir or surface facility.
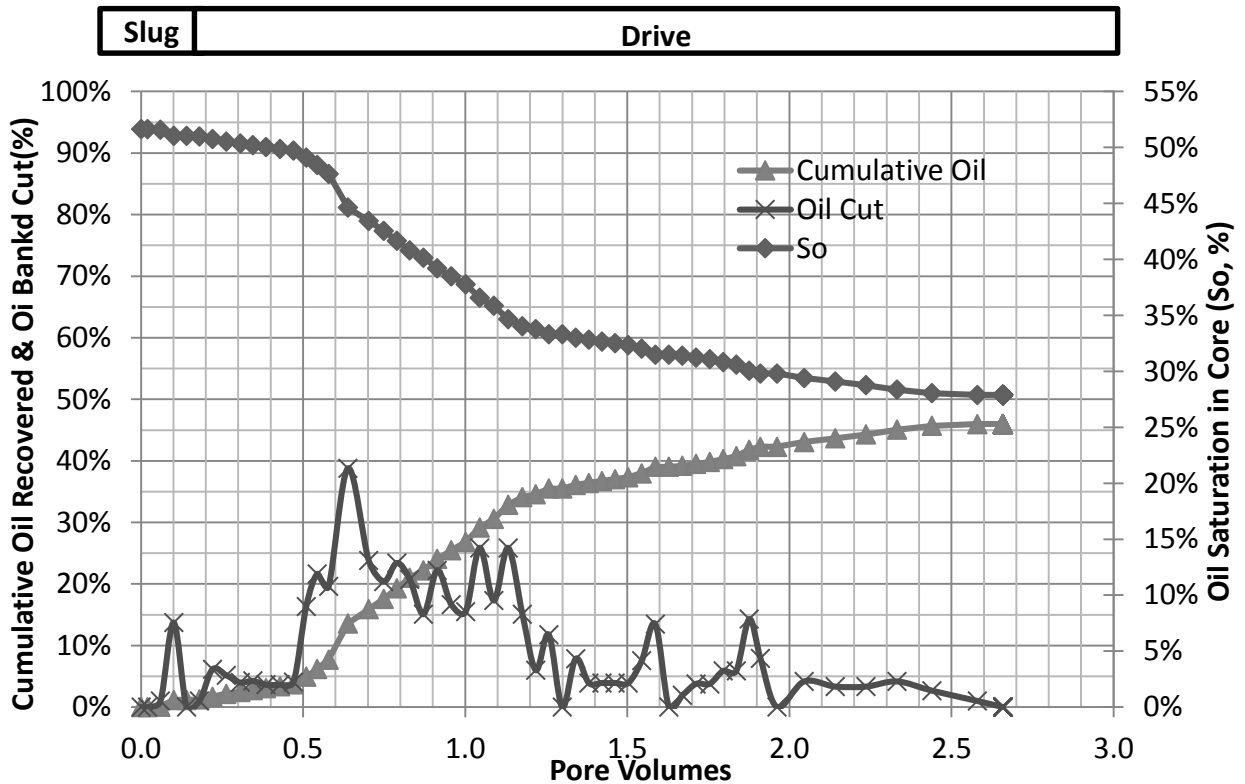
Figure 8.2.2: ALK-01 Oil Recovery

Pressure drops are high early in the flood (Fig 8.2.3), when a large oil bank is displaced by a viscous emulsion. They taper off and decrease and then show increase later in the flood. This may be due to mineral swelling, as the injected brine is very low salinity, but Bentheimer sandstone contains very little clay. It also seems that the low oil-content emulsions were still viscous even at the end of the flood. The pressure drop was dominated by the emulsion and oil bank propagation: in a viscous oil flood with higher residual oil saturation (likely in the field), emulsions could be yet much more viscous and damaging.

Figure 8.2.3: ALK-01 flood pressure data

The flood matches well with Koval's theory of miscible, viscously-unstable displacements. Parameters used in the match are shown in Table 8.2.5.

Table 8.2.5: ALK-01 Koval parameters

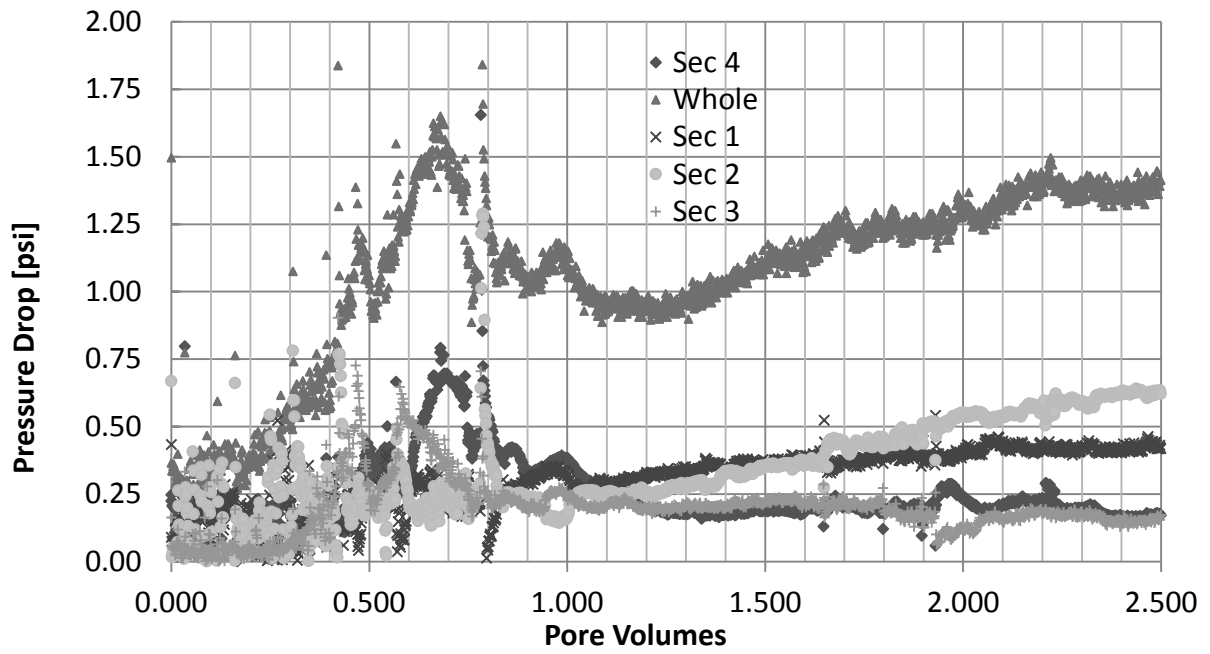| Parameter	Description	Value	Units/Source
μO	Oil viscosity used in viscosity ratio	220	cP
μS	Alkaline slug viscosity.	0.41	cP
E	Koval viscosity ratio.	11.4	Calculated
Vdp	Dykstra-Parsons coefficient. (Homogenous)	0.3	
H	Heterogeneity factor	2.09	Calculated
F	Gravity Factor	1	
K	Koval factor for calculating swept with throughput. K = H*F*E	24.0	1/PV
Vpvbt	Breakthrough of solvent in PV, Vpvbt = 1/K	0.04	PV
So	Initial oil saturation	0.81	
So	Oil saturation start of flood	0.51	
Sor	Residual oil saturation in flood of interest	0.05	

The match of oil tertiary oil recovery in Koval vs. the flood is seen below. The initial mismatch is due to the formation of an oil bank, as the flood was in tertiary mode. The oil bank production quickly brings the flood recovery in line with the simple Koval model, and matches it for at least 2.5 PV. A more sophisticated Koval model can capture this effect.
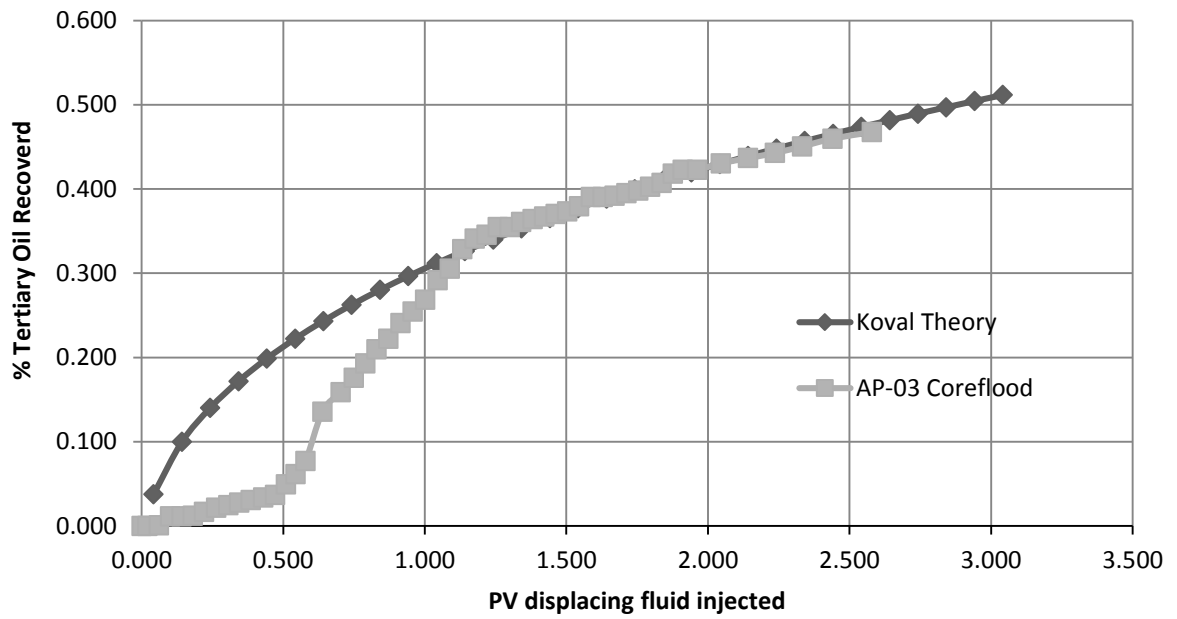
Figure 8.2.4: ALK-01 recovery and theoretical Koval match

Chapter 9: Summary and Conclusions

This research produced several important conclusions relevant to chemical EOR, heavy oil EOR and hybrid thermal chemical EOR.

9.1 ACP TECHNOLOGY

Based on the experimental results of this study, the new ACP flooding process shows major advantages relative to other chemical floods for the recovery of heavy oils. It is cheaper, simpler and more robust than surfactant-based processes, while having no disadvantage in terms of oil recovery. It shows much more favorable oil recovery characteristics than alkaline-only flooding, and its customizable phase behavior allow for more flexibility in design than in cosolvent-free AP (alkaline-polymer) flooding.

9.2 HEAVY OILS AND ACP

Heavy oils are extremely abundant, particularly in the western hemisphere, and will represent a major portion of the future energy portfolio of the world. The difficulties in producing them are well documented, and any improved or new technology in heavy oil EOR has potential to see widespread application in the field.

Chemical EOR has already been demonstrated in several heavy oil fields, with encouraging results; Application of the advantageous ACP process could prove a major breakthrough in Heavy Oil EOR. The heavy oils themselves are extremely well suited for ACP technology, as they typically contain high concentrations of soap-forming fractions. However there are major limitations in all EOR types in extremely viscous oils where injection and production rates are very low, and heavy oil ACP is no exception. At viscosity/permeability ratio >3 cP/mD, corefloods show excessive pressure drop and high chemical concentration; in addition to viscous instability and production rates.

9.3 THERMAL-CHEMICAL EOR HYBRID

The major potential for heavy oil production using ACP chemical flooding (suitable chemistry, abundance, good formations) justified the evaluation of strategies for overcoming the limitations of oil viscosity common to heavy oil reservoirs. Addition of thermal energy was shown in experiments to have potential to reduce or eliminate many problems associated with using EOR to produce heavy oil. .

Fundamentally, heating the reservoir decreases oil viscosity. Heavy oil viscosity decreases dramatically with temperature: an increase of 20°C can reduce oil viscosity an order of magnitude. Such a reduction in viscosity would have immediate positive impact on injection and production rates in the reservoir, but has other benefits as well. Heating the reservoir can lower the chemical concentration required to displace the heavy oil bank, while also dramatically improving sweep and tertiary recovery. Another significant finding showed the ACP phase behavior of two heavy oils to be largely stable with temperature. In a heated reservoir with a temperature gradient present, an ACP flood which functions well over the entire range of temperatures encountered is critically important.

The thermal-chemical EOR hybrids were demonstrated in corefloods, and showed major promise at viscosity/permeability ratio as high as 3 cP/md. While a room temperature ACP coreflood showed excessive pressure drop, poor tertiary recovery and viscous instability, a moderate increase of 25°C allowed for reasonable pressure drop, 95% tertiary recovery within 1 PV of injection and viscous stability. This highlights the underlying motivation for hybrid-thermal-chemical EOR: moderate temperature increase leads to major improvements in recovery.

Although these experimental laboratory results are extremely encouraging, there is of course a need for additional research to more fully develop the use of ACP flooding to

recover heavy oil. Some of this research is already underway at the University of Texas. For example, the use of electrical preheating is being studied. Specific applications will also require ACP core floods using reservoir cores and fluids. There is also the potential to discover even better cosolvents to use for ACP floods with particular heavy oils. Finally, additional lab experiments using heavy oils with an even higher viscosity than studied in this research should be done to explore the limits of the technology.

Symbols List

cP is centipoise, a measurement of viscosity. It is $1/100^{th}$ of a poise. Units are 0.01 g * cm^-1 * S^-1

D is depth

g is the gravitational constant

GOR is gas-oil ratio, often expressed in standard cubic feet/stock tank barrel (SCF/STB)

HLB is hydrophile - lipophile balance. This term refers to the balance of affinity of the

head and tail groups in surfactants for aqueous and oleic phases, respectively.

k is Permeability (millidarcy, 1 mD = $10^{-5}cm^2$)

$\bar{k}$ is the single phase permeability (usually defined with respect to brine)

$\bar{\bar{k}}\cdot$ is the permeability tensor

k_{rf} is the relative permeability of the fluid

M_f is the mobility of the fluid

M_s is mobility ratio of the shock front

N_t is the trapping number

O/W is an Oil-in-Water emulsion

S_{oi} is initial oil saturation

S_{orw} is residual oil saturation to water

v_l is the volume of oil or water solubilized in the microemulsion

v_s is the volume of surfactant

WOR is Water Oil Ratio

Greek Symbols

μ_f is the viscosity of the fluid

k is Permeability Tensor

Φ is Potential gradient

γ is Interfacial tension (dynes/cm)

ρ is fluid density

WORKS CITED

Abe, M., Schechter, D., Wade, R., Weerasooriya, U., & Yiv, S. (1986). Microemulsion Formation with Branched Tail Polyoxyethelene Sulfonate Surfactants. *Journal of Colloid and Interface Science*, 342-356.

Adkins, S., Liyanage, P., Mudiyanselage, T., Arachchilage, G., Weerasooriya, U., & Pope, G. (2010). A New Process for Manufacturing and Stabilizing High-Performance EOR Surfacants at Low Cost for High-Temperature, High-Salinity Oil Reservoirs. *SPE IOR Symposium* (p. SPE 129923). Tulsa, OK: Society of Petroleum Engineers.

Alberta Energy Ministry. (2009). *Talk About SAGD*. Retrieved 12 12, 2012, from http://www.energy.gov.ab.ca/OilSands/pdfs/FS_SAGD.pdf

Alvarado, V. (2010). Enhanced Oil Recovery: An Update Review. *Energies*, 1529-1575.

Arhuoma, M. Y., Dong, M., & Idem, R. (2009). Determination of Increase in Pressure Drop and Oil Recovery Associated with Alkaline Flooding for Heavy Oil Reservoirs. *Canadian International Petroleum Conference*.

Asomaning, S. (1997). *Heat Exchanger Fouling by Petroleum Asphaltenes.* University of British Columbia.

Bourrel, M., & Schechter, R. (1988). *Microemulsions and Related Systems* (5 ed.). (M. Bourell, Ed.) New York, NY: Marcel Dekker.

Buckley, J. S., & Fan, T. (2007). Crude Oil/Brine Interfacial Tensions. *Petrophysics*, 175-185.

Burk, J. (1987). Comparision of Sodium Carbonate, Sodium Hydroxide, and Sodium Orthosilicate for EOR. *Society of Petroleum Engineers, 2*(1), 9-16.

Cayias, J., Schechter, R., & Wade, W. H. (1976). Modeling Crude Oils for Low Interfacial Tension. *Society of Petroleum Engineers* , 351-357.

Closmann, P., & Seba, R. (1990). A correlation of viscosity and molecular weight. *Journal of Candadian Petroleum Technology, 29*(4), 115-116.

Dake, L. (1978). *Fundamentals of Reservoir Engineering.* New Work City: Elsevier.

Delshad, M., Kim, D. H., Magbagbeola, O., Huh, C., Pope, G., & Tarahhom, F. (2008). Mechanistic Interpretation and Utilization of Viscoelastic Behavior of Polymer Solutions for Improved Polymer-Flood Efficiency. *SPE/DOE Symposium on Improved Oil Recovery.* Tulsa: SPE.

Deroo, G. (1979). *The Oil Sands Deposits of Alberta: Their Origin and Geochemical History.* Calgary, Alberta: Institute of Sedimentary an dPetroleum Geology.

Doll, T. (1988). *Performance Data Through 1987 of teh Isenhour Unit, Sublette County, Wyoming, Polymer-Augmented Alkaline Flood.* TIORCO . Casper, WY: Society of Petroleum Engineers.

Downie, J., & Crane, F. (1961). Effect of Viscosity on Relative Permeability. *SPE, 1*(2), 59-60.

Dusseault, M. (2001). *Comparing Venezuelan and Canadian Heavy Oil and Tar Sands.* Calgary: Canadian International Petroleum Conference.

Dusseault, M. (2002). *Emerging Technology for Economic Heavy Oil Development.* Waterloo, Ontario: Porous Media Research Institute, University of Waterloo.

Emery, L., Mungan, N., & R.W. (1970). Caustic Slug Injection in the Singleton Field. *Journal of Petroleum Engineering, 22*(12), 1569-1576.

Energy Information Agency. (2012). *Annual Energy Outlook 2012.* Washington D.C.: US Departement of Energy.

Falls, A., Thigpen, D., Nelson, R., Caiston, J., Laswon, J., Good, P. U., et al. (1994). A Field Test of Cosurfactant-Enhanced Alkaline Flooding. *Society of Petroleum Engineers*.

Fan, T., & Buckley, J. (2007). Acid Number Measurments Revisited. *SPE*, 496-500.

Flaaten, A., Nguyen, Q., Pope, G., & Zhang, J. (2009). A Systematic Approach to Low-Cost, High-Performance Chemical Flooding. *SPE Res Eval & Eng, 12*(5), 713-723.

Flaaten, A., Nguyen, Q., Pope, G., & Zhang, J. (2009). A Sytematic Laboratory Approach to Low-Cost, High-Performance Chemical Flooding. *Society of Petroleum Engineers*, 713-723.

Fu, X., & Mamora, D. (2010). Enhanced Oil Recovery of Viscous Oil by Injection of Water-in-Oil Emulsion Made with Used Engine Oil. *Improved Oil Recovery Symposium.* Tulsa, OK: SPE.

Fuhr, B., Holloway, L., & Reichert, C. (1986). Rapid Analytical Characterization of Residues from Heavy Oil and Bitumen Upgrading Processes. *The Journal of Canadian Petroleum Technology*.

Fustic, M. (2006). Reservoir and Bitumen Heterogeneity in Athabasca Oil Sands. (pp. 1-13). Calgary: CSPG-CSEG-CWLS Convention.

Graue, D. C., & Johnson, C. C. (1974). Field Trial of Caustic Flooding Process. *Journal of Petroleum Technology, 26*(12), 1353-1358.

Green, D., & Willhite, G. (1998). Enhanced Oil Recovery. Houston, TX: Society of Petroleum Engineers.

Healy, R. N., & Reed, R. L. (1974). Physicochemical Aspects of Microemulsion Flooding. *Society of Petroleum Engineering Journal*, 491-501.

Hirasaki, G. J., Miller, C. A., & Puerto, M. (2011). Recent Advances in Surfactant EOR. *SPE*, 889-907.

Hirasaki, G., van Domeselaar, H., & Nelson, R. (1983). Evaluation of the Salinity Gradient Concept in Surfactant Flooding. *SPE*, 486-499.

Jennings, H. Y. (1975). A Study of Caustic Solution-Crude Oil Interfacial Tensions. *SPE*, 197-202.

Johnson, J. (1976). Status of Caustic and Emulsion Methods. *Journal of Petroleum Technology, 28*(1), 85-92.

Kamath, J. e. (2001). Understanding Waterflood Residual Oil Saturation of Four Carbonate Rock Types. *SPE annual Technical Conference and Exhibition.* New Orleans, LA: Society of Petroleum Engineers.

Kulawardana, E., Koh, H., & Liyanage, P. (2012). *Rheology and Transport of Improved EOR Polymers under Harsh Reservoir Conditions.* Society of Petroleum Engineers.

Kumar, M. (2008). High-Mobility-Ratio-Waterflood Performance and Prediction; Challenges and New Insights. *SPE*, 186-196.

Lake, L. (1989). *Enhanced Oil Recovery.* Upper Saddle River, NJ: Prentice-Hall.

Leach, R. O., Wagner, O. R., Wood, H., & Harpke, C. F. (1962). A Laboratory and Field Study of Wettability Adjustment in Waterflooding. *J. Pet. Tech, 2*(25), 247-252.

Levitt. (2008). *Selection and Screening of Polymers for Enhanced-Oil Recovery.* Tulsa, OK: Society of Petroleum Engineers.

Levitt et. al., D. (2008). Identification of High-Performance EOR Surfactants. *SPE*.

Levitt, D. B., Slaughter, W., Pope, G. A., & Jouenne, S. (2011). The Effect of Redox Potential and Metal Solubility on Oxidative Polymer Degradation. *SPE Reservoir Evaluation and Engineering, June*, 287-298.

Lu et. al., J. (2012). *Novel Large-Hydrobe Alkoxy Carboxylate Surfactants for Enhanced Oil Recovery.* Tulsa: Society of Petroleum Engineer.

Lu, J., Pope, G., & Weerasooriya, U. (2013). Stability Investigation of Low-Tension Surfactant Floods. *Symposium on Oilfield Chemistry* (pp. 1-11). The Woodlands, TX: SPE 164090.

Lu, X. (2010). Application of Thermal Recovery and Waterflood to Heavy and Extra-heavy Oil Reservoirs: Analog Knowledge from More Than 120 Clastic Reservoirs. *CPS/SPE Internaional Oil & Gas Conference and Exhibition.* Beijing, China: SPE.

Mayer, E., Berg, R., Carmichael, J. D., & Weinbrandt, R. (1983). Alkaline Injection for Enhanced Oil Recovery - A status Report. *Society of Petroleum Engineers, 35*(1), 209-221.

Nelson, R., Lawson, J., Thigpen, D., & Stegemeier, G. (1984). Cosurfactant-Enhanced Alkaline Flooding. *SPE Enhanced Oil Recovery Symposium.* Tulsa, OK: SPE.

Nutting, P. (1925). Soda Process for Petroleum Recovery. *Oil and Gas Journal, 25*(45,76,150).

Parker, R. J., & Chung, E. S. (1986). Acid numbers of Saskatchewan heavy oils. *Journal of Canadian Petroleum Technology*, 72-75.

Pei, H. H., Zhang, G. C., Ge, J. J., Ding, L., Tang, M. G., & Zheng, Y. F. (2012). A Comparative Study of Alkaline Flooding and Alkaline/Surfactant Flooding for Zhuangxi Heavy Oil. *SPE Heavy Oil Conference Canada*.

Pope, G. A., Tsaur, K., Schechter, R. S., & Wang, B. (1982). The Effect of Several Polymers on the Phase Behavior of Micellar Fluids. *SPE*, 816-830.

Pope, G., & Nelson, R. (1978). A Chemical Flooding Compositional Simulator. *SPE Journal, 18*, 339-354.

Pope, G., Wu, W., Narayanaswamy, G., Delshad, M., Sharma, M., & Wang, P. (2000, April). Modeling Relative Permeability Effects in Gas-Condensate Reservoirs with a New Trapping Model. *SPE Reservoir Evaluation and Engineering, 3*(2), 171-178.

Potts, D., & Kuehne, D. (1988). Strategy for Alkaline/Polymer Flood Design With Berea and Reservoir-Rock Corefloods. *SPE Reservoir Engineering*, 1143-1152.

Sahni, V., Dean, R., Britton, C., Kim, D., Weerasooriya, U., & Pope, G. (2010). *The Role of Co-Solvents and Co-Surfactants in Making Chemical Floods Robust.* Tulsa, OK: IOR Symposium.

Salter, S. (1977). The Influence of Type and Amount of Alcohol on Surfactant-Oil-Brine Phase Behavior and Properties. *SPE.*

Scriven, L. (1976). Equilibrium bicontinuous structure. *Nature, 263*, 123-125.

Shandrygin, A., Dinariev, O., Mikhailov, D., Nukhaev, M., & Lutfullin, A. (2010). Enhancing Efficiency of Steam-Thermal Treatment of Formations With High-Viscosity Oil. *Russian Oil & Gas Technical Conferenceand Exhibition* (pp. 1-15). Moscow: SPE.

Solairaj et. al., S. (2012). *New Correlation to Predict the Optimum Surfactant Structure for EOR.* Society of Petroleum Engineers.

Stegemeier, G. (1977). Mechanisms of Entrapment and Mobilization of Oil in Porous Media. In D. Shah, & R. Schechter, *Improved Oil Recovery by Surfactant and Polymer Flooding* (pp. 55-91). New York City: Academic Press.

Subkow, P. (1942, July 7). *Process for the removal of Bitumen From Bituminous Deposits.* U.S. Patent No. 2,288,857.

Thom, W. (1926). Possible Natural Soda Drive in the Salt Creek Type of Pool, and Its Significance in Terms of Increased Oil Reserves. *The American Institute of Mining, Metallurgical and Petroleum Engineers Inc., G-26*(1), 210-217.

Walker, D., Britton, C., Kim, D. H., Dufour, S., Weerasooriya, U., & Pope, G. (2012). *The Impact of Microemulsion Viscosity on Oil Recovery.* Tulsa, OK: SPE IOR Symposium.

Winsor, P. (1954). Solvent Properties of Amphiphilic Compounds. London: Butterworths.

Wu, Y., Dong, M., & Shirif, E. (2011). Study of Alkaline/Polymer Flooding for Heavy-Oil Recovery Using Channeled Sandpacks. *SPE Reservoir Evaluation and Engineering*, 310-319.

Zaitou, A., & Potie, B. (1983). Limiting Conditions for the Use of Hydrolyzed Polyacrylamides in Brines Containing Divalent Ions. *International Symposium on Oilfield and Geothermal Chemistry* (pp. 1-18). Denver, CO: SPE.

Zhou, Z., Gunter, W. D., Kadatz, B., & Cameron, S. (1996). Effect Of Clay Swelling On Reservoir Quality. *Journal of Canadian Petroleum Technology, 35*(7), 18-23.